

1 2 9 0



UNIVERSIDADE DE  
**COIMBRA**

Elisabeth Steiner, BSc

**MACROFAUNA AS INDICATORS OF SOIL VARIABILITY IN  
OAK AND PINE FORESTS**

Master's Thesis in the International Masters of Applied Ecology

Supervised by Dr. Luís das Neves Kalchhauser Cunha and by Prof. Dr. José Paulo Sousa  
Submitted to the Department of Life Sciences at the Faculty of Science and Technology at the  
University of Coimbra

Julho de 2025



## **Declaration of Independence**

I hereby declare that this thesis was independently written and organised by me and has not been submitted previously, in whole or in part, for the purpose of obtaining any other academic degree.

The research presented herein was conducted within the framework of the EU Horizon Europe BENCHMARKS project (Grant Agreement No. 101091010; <https://soilhealthbenchmarks.eu/>), through a collaboration between the University of Coimbra and project consortium partners. The site description, sampling design, and macrofauna sampling were developed in close collaboration with Prof. Titia Muller (Wageningen University). Soil sampling, along with associated chemical and physical measurements, was conducted as part of the project's collaborative fieldwork efforts involving institutional partners. I was personally responsible for all remaining laboratory procedures and for conducting the data analysis.

Vienna, 31 July 2025

## Acknowledgements

I would like to express my deepest gratitude to those who have supported and guided me throughout the development of this thesis.

First and foremost, I am sincerely thankful to Dr. Luís das Neves Kalchhauser Cunha, my supervisor, for his constant guidance, scientific insight, and unwavering support during the course of this work. His dedication and constructive feedback were fundamental to the progress of this project.

I am also grateful to Prof. Dr. José Paulo Sousa, my co-supervisor and program coordinator, for his valuable advice, encouragement, and for facilitating the academic environment that made this work possible. His leadership and commitment to research excellence have been truly inspiring.

A heartfelt and very special thank you goes to MSc Luisa Fraga, who was so much more than a lab technician. Her dedication, patience, and kindness made a profound impact on this journey. She was not only a key collaborator during the lab work but also a true friend, always ready to offer help, guidance, and a listening ear. Her support extended far beyond the laboratory, including being our daily “taxi driver,” ensuring we got to and from the lab safely and on time. Her generosity, good humor, and constant encouragement were essential pillars throughout this entire experience, and I am deeply grateful for everything she has done.

I would also like to acknowledge the entire Engel Lab for the collaborative spirit, stimulating discussions, and the supportive atmosphere. Working alongside such a dedicated and skilled group was an enriching experience.

Special thanks to EU Horizon Europe BENCHMARKS project in collaboration with the University of Coimbra, for the opportunity to carry out this project within the framework of such an important initiative. Their support and resources were essential to the successful completion of this thesis.

Last but not least, I am profoundly grateful to my mother, for her unwavering love, emotional support, and financial assistance throughout my academic journey. Her belief in me has been a constant source of strength and motivation.

To all of you, thank you.

## **Abstract**

Soil macrofauna play a critical role in ecosystem functioning and are increasingly recognized as potential bioindicators of soil health. However, their integration into standardized soil monitoring frameworks remains limited. This study, conducted within the EU Horizon Europe BENCHMARKS project, investigates the spatial variability of soil macrofauna communities in two contrasting forest systems oak (*Quercus pyrenaica*) and pine (*Pinus pinaster*) forests in Sabugal, Portugal. Using a combination of traditional morphological identification and COI metabarcoding, the research compares two sampling designs k-means clustering and random sampling against the standardized LUCAS protocol to evaluate their efficiency in capturing biodiversity and environmental heterogeneity.

Results revealed that sampling strategy effectiveness varied with ecosystem complexity. In the structurally heterogeneous oak forest, the k-means approach captured greater species richness, higher sample coverage, and more consistent community composition than random sampling. Conversely, in the more homogeneous pine forest, random sampling performed better, indicating that the spatial structure of the environment should guide sampling strategy selection. Soil chemical analyses supported these findings, showing significantly higher variability in pH, phosphate, and exchangeable cations in oak sites compared to pine.

A methodological comparison of morphological and molecular data highlighted the strengths and limitations of each approach. Morphology provided reliable abundance data for well-characterized taxa, while metabarcoding detected a broader taxonomic spectrum, including cryptic and juvenile forms.

These findings underscore the importance of aligning sampling design with ecosystem structure and advocate for the integration of molecular tools to enhance biodiversity detection in soil health assessments. The study contributes valuable insights toward refining soil monitoring strategies under the EU Soil Strategy and supports the use of macrofauna as effective biological indicators in forest ecosystems.

**Keywords**, Biodiversity Monitoring, Bioindicators Metabarcoding, Soil Health, Sampling Design, Soil Macrofauna

## **Resumo**

A macrofauna do solo desempenha um papel fundamental no funcionamento do ecossistema e é cada vez mais reconhecida como um potencial bioindicador da saúde do solo. No entanto, a sua integração em estruturas padronizadas de monitorização do solo continua a ser limitada. Este estudo, realizado no âmbito do projeto BENCHMARKS da UE Horizon Europe, investiga a variabilidade espacial das comunidades de macrofauna do solo em dois sistemas florestais contrastantes: florestas de carvalho (*Quercus pyrenaica*) e pinheiro (*Pinus pinaster*) no Sabugal, Portugal. Utilizando uma combinação de identificação morfológica tradicional e com técnicas de “metabarcoding” do gene COI, esta investigação compara duas tipologias de amostragem, agrupamento “k-means” e amostragem aleatória, assim como com o protocolo LUCAS, para avaliar a sua eficiência na captura da biodiversidade e da heterogeneidade ambiental.

Os resultados revelaram que a eficácia da estratégia de amostragem variou com a complexidade do ecossistema. Na floresta de carvalhos estruturalmente heterogénea, a abordagem “k-means” capturou uma maior riqueza de espécies, uma maior cobertura da amostra e uma composição da comunidade mais consistente do que a amostragem aleatória. Por outro lado, na floresta de pinheiros mais homogénea, a amostragem aleatória teve um melhor desempenho, indicando que a estrutura espacial do ambiente deve orientar a seleção da estratégia de amostragem. As análises químicas do solo apoiaram estas conclusões, mostrando uma variabilidade significativamente maior no pH, fosfato e catiões permutáveis nos locais com carvalhos em comparação com os pinheiros.

Uma comparação metodológica dos dados morfológicos e moleculares destacou os pontos fortes e as limitações de cada abordagem. A morfologia forneceu dados confiáveis de abundância para taxas bem caracterizadas, enquanto o “metabarcoding” detetou um espectro taxonómico mais amplo, incluindo formas crípticas e juvenis. Embora a abundância relativa de leitura (RRA) do “metabarcoding” não refletisse diretamente as contagens morfológicas, os dados RRA normalizados mostraram correlações estatisticamente significativas, apoiando a sua aplicabilidade semiquantitativa.

Essas descobertas ressaltam a importância de alinhar o projeto de amostragem com a estrutura do ecossistema e defendem a integração de ferramentas moleculares para melhorar a deteção da biodiversidade nas avaliações da saúde do solo. O estudo contribui com registos valiosos para refinar as estratégias de monitorização do solo sob a Estratégia do Solo da UE

e apoia o uso de membros da macrofauna como indicadores biológicos eficazes em ecossistemas florestais.

**Palavras-chave:** Macrofauna do Solo, Bioindicadores, Monitorização da Biodiversidade, Metabarcoding, Saúde do Solo, Desenho de Amostragem

## **Table of Content**

<b>Declaration of Independence</b>	<b>1</b>
<b>Acknowledgements</b>	<b>2</b>
<b>Abstract</b>	<b>3</b>
<b>1 Introduction</b>	<b>1</b>
1.1 Soil Biodiversity	1
1.2 The Importance of Soil Biodiversity in Forest Systems	2
1.3 Soil Health	3
1.4 Soil Health Assessment	5
1.5 Knowledge Gaps, Research Challenges and Perspectives	7
1.6 Thesis Aims and Objectives	11
<b>2 Materials and Methods</b>	<b>12</b>
2.1 Study Sites	12
2.2 Sampling Design	14
2.3 Taxonomic Identification	17
2.3.1 Morphological Identification	17
2.3.2 Molecular Identification and Metabarcoding Pipeline	17
2.4 Statistical Analysis	25
2.4.1 Comparative Performance of Sampling Strategies	25
2.4.2 Biodiversity Assessment	27
2.4.3 Analysis of Environmental and Spatial Drivers	29
2.4.4 Taxonomic Response to Environmental and Spatial Variability	31
2.4.5 Comparative Analysis of Morphological and Molecular Data	32
<b>3 Results</b>	<b>33</b>
3.1 Comparative Performance of Sampling Strategies	33
3.2 Biodiversity Assessment	41
3.3 Analysis of Chemical Soil Parameters	51
3.4 Linking Community Structure to Chemical Soil Parameters	56
3.5 Community Response to Environmental and Spatial Variability	69
3.6 Investigating Taxonomic Indicator Response to Soil Variability	71
3.7 Comparative Analysis of Morphological and Molecular Data	71
<b>4 Discussion</b>	<b>74</b>
4.1 Evaluating the Performance of Spatial Sampling Strategies	74
4.2 Community Composition Shaped by Forest Type and Turnover Patterns	75
4.3 Soil Chemistry as a Filter of Community Structure	77
4.4 Spatial Structure vs. Environmental Filtering in Community Assembly	78
4.5 Identifying Bioindicator Taxa for Soil Health Monitoring	80
<b>5 Conclusion</b>	<b>81</b>
<b>6 Future Research Directions and Recommendations</b>	<b>82</b>
<b>References</b>	<b>84</b>
<b>Appendix</b>	<b>90</b>

# 1 Introduction

## 1.1 Soil Biodiversity

Beneath our feet lies a world teeming with life, harboring an immense diversity of microorganisms, including bacteria, archaea, fungi to a wide range of soil fauna. The soil ecosystem is one of the most species-rich habitats on the planet estimated to host approximately 25% of the Earth's described terrestrial biodiversity (Guerra et al., 2021; Wolters, 2001) with an even greater proportion of species likely remaining undiscovered (Decaëns et al., 2006).

Soil biodiversity, in its broadest sense, encompasses the variety of life belowground, from genes to species and their communities, and the ecological complexes of which they are part (FAO, 2020). It reflects the abundance, diversity, and organization of life within soils, along with the crucial ecological roles these organisms perform (Bispo et al., 2009; Creamer et al., 2022). This intricate web of life operates across a range of spatial scales, from interactions within microhabitats (e.g., rhizosphere, soil aggregates) to community dynamics across broader landscapes (FAO, 2020; van der Putten et al., 2010). Moreover, playing a crucial role in regulating important soil processes delivering ecosystem functions that provide long-term ecosystem stability and offer both human and planetary well-being (Bardgett & Van Der Putten, 2014; Wall et al., 2015)

However, soil biota continues to be one of the least understood components of global biodiversity and is still facing major drawbacks when it comes to taxonomic knowledge, ecology and distribution patterns of species when compared to other groups like higher plants and vertebrates (Briones, 2014; Cameron et al., 2018; Pulleman et al., 2012).

Soil animals, organisms that depend on soil for their entire life cycle or a critical stage of it (Orgiazzi et al., 2016; Pulleman et al., 2012), are commonly classified by body size (Figure 1), taxonomic group, or functional role (Coleman et al., 2024; Pulleman et al., 2012). Size-based classification, widely adopted according to FAO (2020), Jeffery et al. (2010), and Swift et al. (1979), divides soil fauna into four classes. Microbes and Microfauna are <0.1 mm. Mesofauna range from 0.1 mm to 2 mm. Macrofauna consist of organisms ranging in size from 2 mm – 20 mm, among which invertebrates represent a vast majority of major taxa within soil communities worldwide (Decaëns et al., 2006). Lastly, Megafauna, defined as organisms larger than 20mm, predominantly comprising vertebrate species.

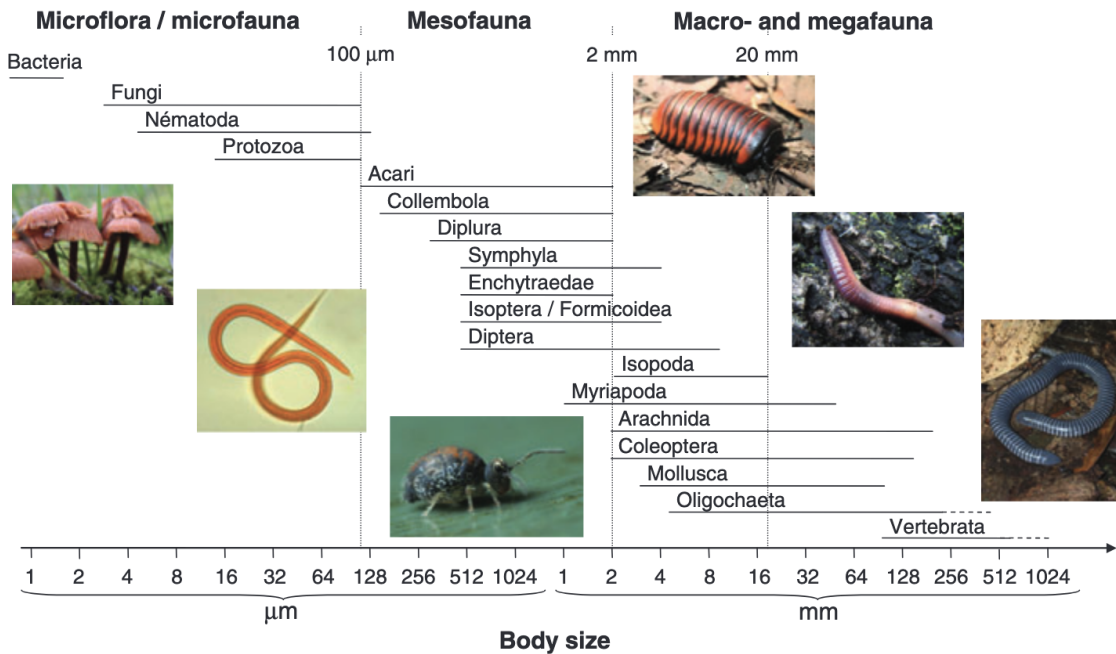


Figure 1: Representation of the main taxonomic groups of soil organisms on a body-size basis (from Decaëns et al., 2006, after Swift et al., 1979).

While size-based classification of soil organisms is practical, it offers a limited understanding of their functional roles because organisms within the same size category can have diverse physiological capabilities, and their significance in soil processes can vary (Briones, 2014; Kibblewhite et al., 2008; Pulleman et al., 2012). Categorizing organisms into functional assemblages based on their primary roles (Bardgett & Van Der Putten, 2014; Coleman et al., 2024), such as 'chemical engineers', 'biological regulators', and 'ecosystem engineers', better captures their ecological contributions (Kibblewhite et al., 2008; van der Putten et al., 2010). These groups function across varied spatio-temporal scales (Briones, 2014). Functional classifications are simplifications, as many organisms perform multiple roles, and their interactions are often dynamic (Creamer et al., 2022).

## 1.2 The Importance of Soil Biodiversity in Forest Systems

Forests are vital for global ecological stability, offering ecosystem services like carbon sequestration, climate regulation, and biodiversity preservation (Nadrowski et al., 2010). While aboveground biomass often dominates perceptions, forest ecosystem function and resilience are intrinsically linked to biological diversity (Brokerhoff et al., 2017). Evidence suggests that biodiversity, from genetic to landscape levels, supports key ecosystem functions like biomass production and nutrient cycling (Schweitzer et al., 2012).

Different forest types, such as coniferous forest or deciduous forest stands, create soil environments that differ due to variation in litter quality, pH, and nutrient cycling (Amori et al., 2021). Macroinvertebrate communities are dependent on underlying site conditions like soil texture (Wenglein et al., 2024), management practices (Korobushkin et al., 2025) and recovery from past disturbances (Vasconcellos et al., 2013) . Consequently, soil macrofauna serves a sensitive indicator for spatial habitat variation and management impacts (Korobushkin et al., 2025; Mamabolo et al., 2024; Vasconcellos et al., 2013). . Understanding the diversity and functional roles of soil macrofauna is not only of ecological interest, but also increasingly relevant to sustainable forest management and soil conservation. As ecosystem engineers, macrofauna contribute critically to organic matter decomposition, soil structure formation, and nutrient cycling, processes that support soil resilience and productivity (Brown et al., 2018). Yet despite their importance, these organisms remain largely underrepresented in most soil monitoring frameworks, particularly in ecologically complex systems like forests (Prescott, 2024).

Addressing this gap calls for robust methodologies that integrate both biological and abiotic indicators while accounting for spatial and temporal variability. In the following sections, I have examined current approaches to soil health assessment, highlight the emerging relevance of biological indicators such as macrofauna, and discuss the limitations of existing monitoring systems.

### 1.3 Soil Health

The critical importance of soil biodiversity in maintaining ecosystem resilience directly informs the concept of soil health (Lehmann et al., 2020; Wall et al., 2015). Soil health is defined as the continued capacity of soil to function as a living system within ecosystem and land use boundaries, that sustains productivity, maintains environmental quality, and contributes to planetary health over time (Bünemann et al., 2018; E. et al, 2022). This concept moves beyond viewing soil as an inert medium, recognizing it as a dynamic system where the interplay of physical, chemical, and biological properties determines its overall functionality and resilience against threats (Smith et al., 2024; Stolte et al., 2016).

The functionality of healthy soil provides a wide array of benefits through soil functions and ecosystem services (European Environment Agency., 2023). Soil functions are the inherent processes that underpin the delivery of ecosystem services such as the direct benefits that human societies receive from nature, which span all categories from supporting to provisioning and regulating services (Bünemann et al., 2018).

Soil animals, in particular, are significant contributors. Through their activities in specific zones of influence, or 'functional domains', they directly regulate key soil processes (Lavelle et al., 2006). The ecosystem services resulting from these functions, for example habitat provision, food production, and climate regulation, manifest at scales far greater than the individual organisms themselves (Brussaard, 2012; Wall et al., 2015). This underscores the conclusion that without the vital contributions of the entire soil biota, terrestrial ecosystems could face rapid collapse (Bardgett & Van Der Putten, 2014).

The ecosystem services delivered by healthy soils are increasingly jeopardized by a range of defined soil threats which are processes that damage the soil and its functional properties (European Environment Agency., 2023; Stolte et al., 2016). Major threats to European soils were identified nearly two decades ago and include erosion, organic matter decline, contamination, sealing, compaction, loss of biodiversity, and salinization (Bünemann et al., 2018; European Commission, 2002). The cumulative impact of these threats impairs soil functioning and diminishes the provision of essential services (FAO, 2015).

The scale of this problem is alarming. Recent assessments from the EUSO Soil Degradation Dashboard indicate that over 60% of EU soils are unhealthy, with most affected by multiple degradation processes. Loss of soil biodiversity is the most prevalent single issue, affecting 33% of EU land, followed by water erosion (19%) and the loss of soil organic carbon (14%) (Broothaerts et al., 2024).

The decline in soil health has direct implications for human well-being. This principle is captured by the 'One Health' concept, which recognizes that the health of humans, animals, and the environment are closely linked and interdependent, necessitating interdisciplinary collaboration ensuring a sustainable future (OHHLEP et al., 2022). Combined pressures as described by Smith et al , 2024 lead to major soil degradation (FAO, 2015), resulting in a negative cascade that ultimately harms human health (Wall et al., 2015). As a result, two major risks emerge: increased prevalence of soil-borne pests and pathogens due to the loss of natural antagonists, and reduced availability of clean water, air, and nutritious food (Wall et al., 2015).

This emphasizes that soil health is not just an environmental concern but a critical public health priority. This perspective is embedded in the EU Soil Strategy for 2030, which recognizes soils as fundamental to food systems and biodiversity and sets the goal of achieving healthy soils across the EU by 2050 (European Commission, 2021). To support this, a 2023 proposal introduced a legally binding Soil Health Law aimed at establishing a

unified monitoring framework with clear criteria to assess soil conditions, directly linking soil status to human and environmental health (European Commission, 2023). Such frameworks are underpinned by large-scale data initiatives like the Land Use/Cover Area Frame Survey (LUCAS). This EU-wide survey collects harmonized land use and cover data through a stratified random sampling design, with a subset of points including topsoil samples for chemical and physical analyses and recently involving biological parameters via e-DNA (Tóth et al., 2013). By providing standardized indicators across countries, LUCAS has played a central role in supporting evidence-based environmental and agricultural policymaking at the continental scale (Orgiazzi et al., 2018).

## 1.4 Soil Health Assessment

The main goal of soil health assessment is to evaluate the soil's ability to perform essential functions and provide ecosystem services, supporting policy, sustainable land management, and conservation efforts (Bünemann et al., 2018; Lehmann et al., 2020). Traditionally, assessments, often termed 'soil quality', focused on chemical and physical properties related to agricultural productivity, with limited emphasis on biological aspects (Lehmann et al., 2020). However, growing recognition of soil as a dynamic living system, where physical, chemical, and biological components interact (Creamer et al., 2022; Rinot et al., 2019) (Creamer et al., 2022; Rinot et al., 2019), has shifted this perspective. There is now a strong push to incorporate biological indicators to better address sustainability challenges such as biodiversity loss, climate change, and public health (Griffiths et al., 2016; Karlen et al., 2019; Lehmann et al., 2020).

Soil health indicators are measurable attributes that reflect a soil's capacity to perform essential functions (Bünemann et al., 2018; European Environment Agency, 2023). These indicators are typically grouped into three categories, physical, chemical, and biological (Lehmann et al., 2020), and are used either to highlight soil risks ( threat indicators) or to assess soil functions and their related ecosystem services (European Environment Agency, 2023). Effective indicators should be relevant to soil functions, sensitive to meaningful changes, cost-effective, timely, and informative for land management decisions (Bünemann et al., 2018; Rinot et al., 2019). They must also be reliable, reproducible, and broadly applicable (Broothaerts et al., 2024). However, not all meet these standards or are fully developed, though many still hold value for soil assessment (Lehmann et al., 2020).

Common chemical indicators include soil organic carbon (or organic matter) content and pH, available phosphorus and potassium, and total nitrogen. Physical indicators often encompass

water storage metrics and bulk density (Bünemann et al., 2018). Biological indicators are often limited to general metrics such as microbial biomass, soil respiration, or earthworm density (Bünemann et al., 2018). While most assessment schemes aim to include at least one from each category, biological indicators remain widely underrepresented despite their recognized importance in understanding soil functioning and resilience.

By providing standardized indicators across countries, the Land Use/Cover Area Frame Survey (LUCAS) has played a central role in supporting evidence-based environmental and agricultural policymaking at the continental scale (Orgiazzi et al., 2018). However, while LUCAS provides valuable baseline data, it presents several methodological and operational limitations that challenge its suitability for nuanced soil health assessments. One primary concern is spatial granularity: with sampling points typically spaced around 18 km apart, LUCAS lacks the resolution needed to capture fine-scale heterogeneity, particularly in ecologically diverse or fragmented landscapes such as forest ecosystems (Ballabio et al., 2016; Broothaerts et al., 2024). This reduces its utility for site-specific management or for detecting local patterns in biodiversity, especially among highly variable biological communities like soil macrofauna. A further limitation is its restricted biological scope. While chemical and physical parameters are routinely measured, biological indicators, critical for assessing soil ecosystem function, are largely absent or underdeveloped in LUCAS (Pulleman et al., 2012; Bünemann et al., 2018). Without integrating fauna or microbial data, LUCAS cannot adequately reflect the dynamic biological processes that underpin soil health. Operational challenges also exist around data harmonization. Despite standardized protocols, variations in implementation across member states, such as differences in technician training, equipment calibration, and seasonal sampling windows, can introduce bias and affect comparability (Orgiazzi et al., 2018; FAO, 2020). Moreover, as biological indicators are increasingly integrated into soil monitoring frameworks, the demand for taxonomic expertise imposes an additional training burden, particularly in regions where such expertise is limited (Löbl, et al., 2023). Lastly, LUCAS data represent static snapshots of soil conditions, typically collected at a single point in time. This limits the ability to monitor temporal processes such as seasonal faunal dynamics, post-disturbance recovery, or gradual trends in biodiversity decline, all of which are essential for adaptive soil management and early warning systems (Creamer et al., 2022; Lehmann et al., 2020). Given these constraints, there is a clear need for complementary, fine-scale approaches that can enrich and validate large-scale datasets like LUCAS. Integrating biological indicators and capturing spatial variability, particularly in underrepresented or ecologically sensitive systems such as forests,

is crucial to strengthen the scientific basis for operational soil health monitoring under the EU Soil Strategy.

## 1.5 Knowledge Gaps, Research Challenges and Perspectives

### *Methodological Barriers in Macrofaunal Assessment*

Despite their vital role in ecosystem functioning, biological indicators, especially those related to soil fauna, remain underrepresented in standardized soil health assessments (Pulleman et al., 2012). Büinemann et al. (2018) reported that 40% of proposed minimum datasets excluded biological indicators entirely. When included, assessments often rely on broad metrics like microbial biomass or earthworm density, neglecting other crucial macrofauna groups.

This exclusion stems from persistent research gaps. First, the definition of "soil macrofauna" lacks consistency; classification is often based on taxonomy rather than size, leading to incomparable datasets (Gongalsky, 2021). Second, traditional approaches, reliant on morphological identification, are time-consuming, labor-intensive, and increasingly constrained by a shortage of taxonomic experts (Watts et al., 2019). These methods are especially challenged by hyperdiverse or cryptic species, immature life stages, and damaged specimens, leading to potential misidentification or failure to identify specimens at all (Elbrecht et al., 2019; Young & Hebert, 2022). Third, standardized sampling methods are lacking, and commonly used extraction techniques frequently overlook small-bodied insects and organisms in their early larval stages, despite their important functional roles (Gongalsky, 2021). Lastly, combined with the natural variability of faunal communities and the absence of reference baselines, these issues complicate result interpretation and limit inclusion in soil models (Pulleman et al., 2012; Büinemann et al., 2018; Lehmann et al., 2020).

Addressing these challenges through standardized definitions, improved sampling methods, and advanced tools such as DNA metabarcoding and stable isotope probing will be essential. Integrating these approaches with long-term field studies can strengthen our understanding of biodiversity-function relationships and support the development of predictive, evidence-based tools for sustainable soil management (Büinemann et al., 2018; Creamer et al., 2022; Lehmann et al., 2020).

### *The Challenge of Linking Biodiversity to Function*

While it is well-established that ecosystem processes depend more on the structural and functional diversity of soil communities than on taxonomic richness alone (Pulleman et al., 2012) deciphering these links remains particularly complex for soil macrofauna. One major reason is the ontogenetic plasticity of many soil organisms their functional roles often shift over the course of their life cycle (Brussaard, 2012). For instance, detritivorous larvae may become predatory adults, altering their contribution to nutrient cycling, prey regulation, or bioturbation. As Gongalsky (2021) emphasizes, the failure to account for these ontogenetic stages for example, by lumping larvae and adults in the same analysis can lead to biased estimates of biomass and an incomplete understanding of ecological function.

In this context, biomass and abundance are not merely proxies for population size, but can serve as quantitative indicators of ecosystem influence. Abundance reflects how widespread and dominant a species or group is within a given soil system, while biomass integrates both presence and body size, offering a more ecologically meaningful metric when assessing contributions to ecosystem processes such as organic matter decomposition, nutrient mineralization, or physical soil structuring (Brussaard, 2012; Lavelle et al., 2006). For example, earthworms may be less diverse than arthropods in a given site, yet their biomass often far exceeds that of other macrofauna, making them disproportionately important to processes such as soil aggregation and nutrient turnover. Moreover, functional redundancy and complementarity, which are key drivers of ecosystem resilience, cannot be inferred solely from taxonomic lists. Instead, assessing patterns in abundance and biomass across functional groups can reveal shifts in community structure and soil functioning in response to environmental gradients, land use, or pollution (Bardgett & van der Putten, 2014). Unlike presence-absence data, abundance and biomass allow for density-dependent interpretations, helping identify whether a group is rare but functionally critical, or abundant but ecologically redundant.

This complexity is further compounded by the multiscale factors that shape macrofaunal distributions, ranging from broad biogeographic patterns to fine-scale variation in soil properties such as pH, organic matter content, and moisture (Brussaard, 2012). As a result, effectively linking biodiversity to ecosystem function in soil systems requires a multidimensional and hierarchical approach. This should incorporate not only functional traits, biomass, and abundance, but also structural indicators such as species evenness, dominance, and spatial turnover (beta diversity). To fully capture the variability and

ecological relevance of soil communities, measurements should be conducted at the individual, population, and community levels, spanning multiple organizational and spatial scales. Including both compositional and structural diversity metrics is essential for revealing how soil biodiversity contributes to key ecosystem functions such as nutrient cycling, bioturbation, and decomposition. Emphasizing these integrated response variables enables a transition from descriptive inventories to a mechanistic understanding of soil health and its biotic drivers.

### *Assessing Environmental Variability and the Challenge of Spatial Heterogeneity*

Understanding the spatial distribution of soil organisms is essential for conserving biodiversity and for the development of effective soil health strategies (Wall et al., 2015; Lehmann et al., 2020). Despite significant efforts, even well-studied taxa such as earthworms remain under-documented in terms of distribution, abundance, and ecological function. Soil biodiversity is inherently heterogeneous, shaped by complex interactions among trophic networks, land use history, soil texture, and microclimatic factors (Decaëns et al., 2006). This heterogeneity complicates the use of biological indicators for soil health assessments as their interpretation is highly context-dependent and may vary across scales and ecosystems (Bünemann et al., 2018).

Emerging high-throughput monitoring tools including laboratory spectroscopy, remote sensing, and sensor networks offer new opportunities for detecting and mapping soil biotic and abiotic variability at meaningful spatial resolutions (Lehmann et al., 2020). These innovations support the BENCHMARKS EU project (<https://soilhealthbenchmarks.eu>) goal of harmonizing soil health assessment across Europe by enabling stratified, site-specific management recommendations. A refined understanding of spatial patterns in macrofaunal communities will directly inform the design of scalable sampling protocols and help validate indicators across land-use types and pedoclimatic zones, ensuring they are both reliable and operational at multiple scales. Therefore, employing a targeted sampling approach that strategically captures environmental heterogeneity across multiple spatial scales is essential for accurately characterizing macrofaunal assemblages (Brus et al., 2011; Decaëns, 2010). Such an approach enables researchers to disentangle biotic responses from underlying abiotic variability, uncover meaningful ecological patterns, and strengthen the role of macrofauna as reliable bioindicators for forest soil health assessment (Lavelle et al., 2006; Rousseau et al., 2013).

## *Opportunities and Challenges of Molecular Approaches in Soil Macrofauna Monitoring*

DNA metabarcoding has emerged as a powerful tool to advance soil biodiversity monitoring, offering high-resolution identification of soil macrofauna from bulk or environmental DNA. By targeting standardized markers like the mitochondrial cytochrome c oxidase subunit I (COI) gene and leveraging high-throughput sequencing technologies, metabarcoding enables efficient detection of diverse taxa, including morphologically cryptic, juvenile, or fragmented individuals (Hebert, et al., 2003; Taberlet et al., 2012). This approach is particularly valuable in soil ecosystems, where traditional morphological identification is time-consuming and taxonomically constrained (Keck et al., 2023; Goulpeau et al., 2025).

However, the method faces several key limitations. A major concern is the non-quantitative nature of PCR-based amplification, as biases in primer affinity, mitochondrial copy number variation, and DNA extraction efficiency can obscure the relationship between sequencing reads and actual biomass or abundance (Elbrecht & Leese, 2015). In a recent study, Dornellas et al. (in prep./2025) addressed this issue by comparing COI read abundance with morphologically identified and abundance counted soil macrofauna. When applying taxon-specific corrections and normalization, the study found moderate to strong correlations between read counts and abundance, indicating that semi-quantitative inference might be possible under optimized conditions. Another challenge is the limited taxonomic resolution due to gaps in COI reference databases, particularly for soil invertebrates in underrepresented regions such as Iberia (Orgiazzi et al., 2015; Porter & Hajibabaei, 2020;). Dornellas et al., 2023, mitigated this by integrating local morpho-taxonomic data to validate barcode assignments and flag potential misidentifications. This approach not only enhanced identification accuracy but also emphasized the need to develop regionally adapted, curated reference datasets to improve assignment reliability, a long well-known documented issue (Hogg & Hebert, 2004).

Despite these challenges, the potential benefits are considerable. Beyond taxonomic inventories, metabarcoding data can inform community composition, beta diversity, and, when paired with biomass proxies, functional trait distributions (Shelton et al., 2023; Hajibabaei et al., 2019). These metrics are essential for understanding how soil communities respond to land use, management interventions, and ecological restoration.

In summary, COI-based metabarcoding offers a scalable, reproducible, and taxonomically rich method for assessing soil macrofauna communities. While challenges remain, particularly regarding quantification and database completeness, recent research suggests that

integrated molecular and morphological approaches, combined with protocol refinement and reference expansion, can overcome many current limitations. Moving forward, emphasis should shift from purely taxonomic assessments toward quantitative and functional ecological indicators, aligning molecular methods with emerging soil health monitoring frameworks at regional and continental scales.

## 1.6 Thesis Aims and Objectives

The overall goal in this study is to assess the spatial variability of soil macrofauna communities and their relationship to environmental factors in oak and pine forest ecosystems, thereby evaluating their potential as bioindicators for soil health monitoring within the BENCHMARKS project framework . Within this, several specific objectives were developed, focusing on the technical side but also on the ecological background:

- Evaluate sampling strategies (k-means clustering vs. random sampling) for their efficiency in capturing macrofauna and environmental variability in forest soils and contrast it with the current approach used by LUCAS initiative at European level. Within this framework, it is expected that k-means sampling strategy captures higher variability in the macrofauna richness and environmental parameters compared to random or LUCAS-based sampling.
- Compare the macrofauna community composition between pine and oak forests in terms of richness, abundance, and taxonomic structure. It is hypothesised that oak and pine forests support significantly different macrofauna communities due to their distinct soil chemistry, vegetation structure and management schemes.
- Analyse the relationship between soil macrofauna communities and chemical soil properties (e.g., pH, TOC, TN, base cations) across forest types and associated management schemes. It is hypothesised that macrofauna community structure is significantly influenced by key environmental variables, particularly pH and organic matter content (e.g., TOC, TN), with differing predictors between forest types.
- Determine the influence of spatial structure and environmental filters on macrofauna community composition within each forest type. It is hypothesised that Spatial distance explains a significant portion of community variation in oak forests (due to heterogeneous microenvironments), whereas in pine forests, community composition is more strongly structured by environmental variables.

- Identify candidate taxa with strong associations to environmental variables and/or spatial patterns for potential use as bioindicators of soil health. It is hypothesised that specific macroinvertebrate taxa (e.g., Araneae, Coleoptera, Isopoda and Gastropoda) are significantly associated with particular environmental gradients and can serve as reliable indicators of soil health status.
- Integrate molecular (metabarcoding) and morphological data to compare taxonomic resolution, sampling completeness, and reliability of biodiversity assessment methods. It is hypothesised that DNA metabarcoding identifies a greater number of taxonomic units than morphological identification alone, although some rare or functionally important taxa may only be detected morphologically.

## 2 Materials and Methods

This thesis was conducted within the framework of the EU Horizon Europe BENCHMARKS project – Soil health: Building a European network for the monitoring and assessment of healthy soils (Grant Agreement No. 101091010; <https://soilhealthbenchmarks.eu/>), and is based at one of the project’s designated case study sites. BENCHMARKS aims to validate and refine soil health indicators to assess the functional capacity of soils and inform strategies for sustainable soil management. The project focuses on developing a coordinated, multi-scale assessment framework for soil health, while establishing a pan-European network to advance soil research, support evidence-based policymaking, and promote resilient land use practices..

### 2.1 Study Sites

This research investigates the soil macrofauna invertebrate communities inhabiting two contrasting forest ecosystems: pine and oak stands. Both forests are located in Sabugal, Portugal, situated the Beira Interior plateau near Serra da Malcata in the District of Guarda (Figure 1A), and are subject to differing forest management practices. The region is characterized by a Warm-summer Mediterranean climate, featuring (Csb according to the Köppen classification; Köppen, 1936), characterized of dry, warm summers and wet, mild to cold winters with an average annual temperature of 10.7°C and precipitation levels around 1248 mm (CMS, 2018). The soil in these sites is classified as humic cambisol, exhibiting a

coarse, sandy loam texture and low cation exchange capacity, primarily derived from granitic parent material.

The Oak forest (Figure 1B) is a native forest composed of oak (*Quercus pyrenaica*), characterized by a broadleaved stand with mixed tree species diversity, managed using an uneven-aged high forest system. Vegetation management includes no harvest management, and biodiversity is maintained by avoiding intense management practices. Carbon and nutrient management involve the use of inorganic nitrogen amendments to support growth. The landscape consists of rolling hills and elevated plateaus, creating an undulating and elevated terrain, with minimum elevation at 919 m asl and maximum elevation at 964 m asl (Eurodem).

The Pine forest (Figure 1C) is a planted silviculture composed of pine (*Pinus pinaster*), being a coniferous forest, primarily consisting of a pure stand (monoculture) or in some areas a mixed stand. Managed as an even-aged high forest, trees are planted in rows and harvested through clear-cutting and timber extraction, with biomass residues removed as part of site management. Wildlife control measures include the use of physical barriers and deterrents to minimize animal disturbances. This site is characterized by a more homogeneous terrain than the oak forest, with minimum elevation at 1015 m asl and maximum elevation at 1078 m asl.

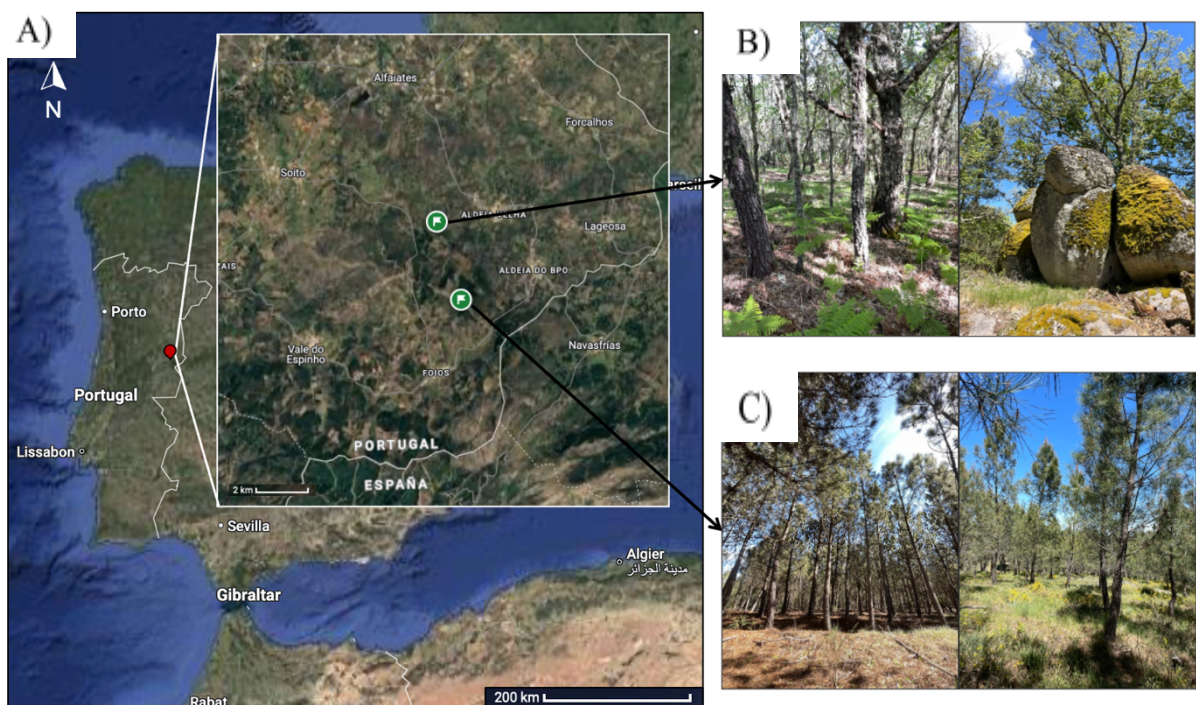


Figure 1: A) Map showing the two forest sampling locations in central Portugal. B) Photographic overview of the studied *Quercus* (oak) forest, representative of a low-impact management regime with high structural complexity and natural understory. C) Photographic overview of the *Pinus* (pine)

plantation forest under active management, characterized by more uniform structure and reduced understory vegetation.

## 2.2 Sampling Design

Sampling for this study was conducted in alignment with the BENCHMARKS project protocol for variance sites (Symanczik et al., 2025). To capture spatial heterogeneity across the forest sites, the sampling design employed a k-means clustering approach developed by the project consortium. This method generated 25 stratified sampling points in a 25-hectare site, resulting in a sampling density of approximately one point per hectare (Brus, 2019). In total, each site included 13 random points, 25 k-means points, and 1 LUCAS reference point (Figure 2A, B), with point selection guided by environmental covariates. Topographic variation was incorporated using data from the EuroDEM Digital Elevation Model, while soil and vegetation characteristics were derived from a Principal Component Analysis (PCA) of a cloud-free Sentinel-2 satellite image. The PCA layers were resampled to 10-meter resolution to retain fine-scale spectral information. In addition, Normalized Difference Vegetation Index (NDVI) was calculated as a proxy for vegetation vigor, allowing classification of sampling cells based on green biomass. To improve the robustness of the stratified design and enable the assessment of small-scale variability, an additional 12 randomly located samples were collected per site. This enhanced spatial replication supports more accurate estimates of intra-site heterogeneity and strengthens the statistical power of ecological comparisons.

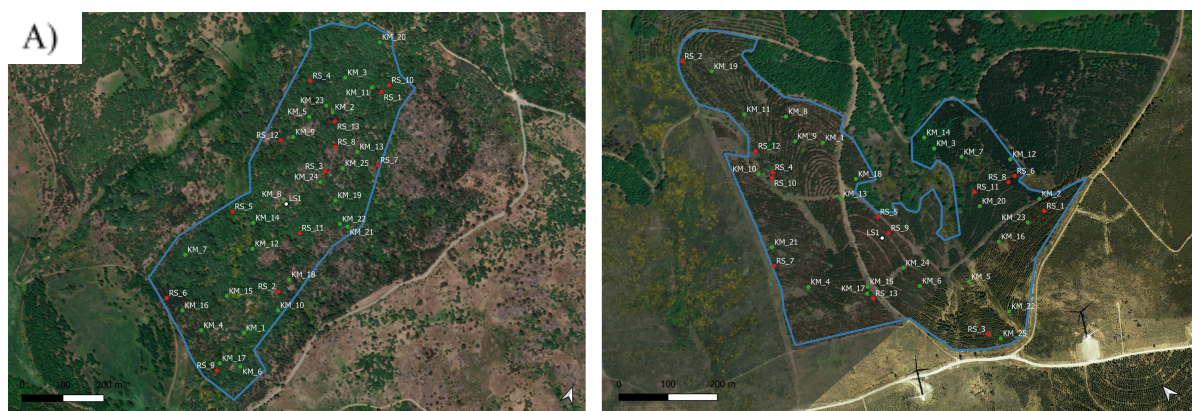


Figure 2: A) OAK 25 sampling points per 25-hectare site, corresponding to a density of one point per hectare, resulting in each system 13 random points (RS (red)) 25 k-means points (KM (green)) and 1 LUCAS point (LS (white)). B) Pine 25 sampling points per 25-hectare site, corresponding to a density of one point per hectare, resulting in each system 13 random points (RS (red)) 25 k-means points (KM (green)) and 1 LUCAS point (LS (white)).

### *Sample Collection*

For the case study sites, soil was sampled following the BENCHMARKS standardized protocol (Symanczik et al., 2025). Sample collection took place at the beginning of May 2024, with pitfall traps installed and retrieved after approximately 8-10 days. In the Sabugal case study, macrofauna sampling was carried out in addition to the standard suite of BENCHMARKS soil health indicator measurements. In total, 39 pitfall traps were installed per system, one at each sample point just to the north, outside the composite soil sampling area (Figure 3b). Each trap was filled with ethylene glycol, and lids were used to reduce rainwater accumulation and prevent dilution, helping to minimise organism degradation. After collection, the samples were preserved in 96% ethanol at room temperature until further analysis.

At each sampling point, soil was collected as a composite sample, consisting of 15 randomly selected subsamples (0–20 cm deep) within a 1-meter radius circle, around the designated sample point coordinates (Figure 3a). The sampling process followed the official protocol for "variance sites" as outlined by the project consortium (Symanczik et al., 2025). Wet subsamples were sieved and weighed in the field, while air dry samples were dried and weighed the following day. Processing, storage and shipment to contributors for analysis was conducted according to the BENCHMARKS processing protocol. Soil sampling at the designated LUCAS point was conducted in accordance with the standardized European protocol established by Fernandez Ugalde et al. (2022) (Figure 4a). A single composite sample was created for each point by pooling five individual subsamples. Using a spade, the first subsample was obtained from the geographical centre of the field. Four additional subsamples were then collected from points located 2 meters away from the centre, one in each of the four cardinal directions (north, east, south, and west). The collection of each subsample involved digging a V-shaped hole to a depth of 20 cm and then extracting a 3 cm-thick vertical slice from one of the hole's faces, as illustrated in Figure 4b.

The mesofauna sample was obtained from within the northern subsample area, while bulk density samples were taken from within the western, eastern, and southern subsample zones.

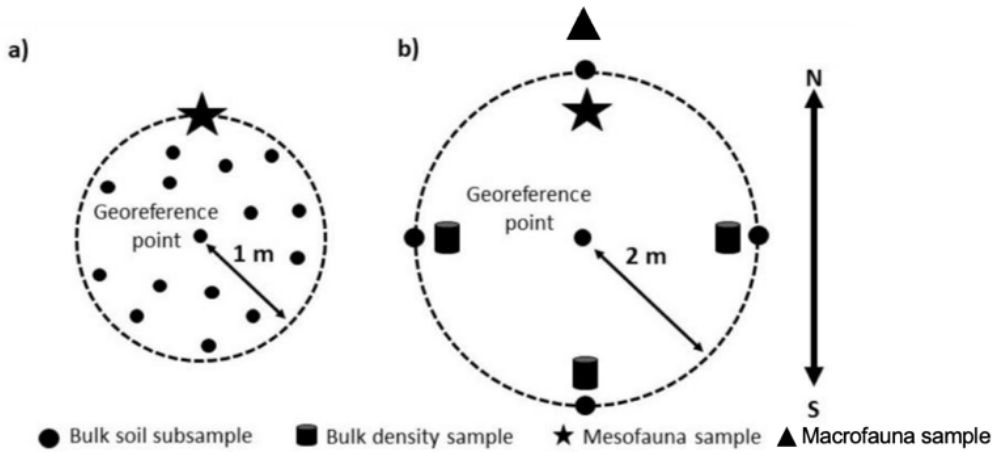


Figure 3: BENCHMARKS sampling approach: a) The composite bulk soil sample consists of 15 subsamples randomly collected within a 1-meter radius circle around the georeferenced point. b) The mesofauna sample is taken from the north side within the 2 m radius of the georeference point. The macrofauna is taken from the north side outside the 2 m radius, the bulk density sample from the south east and west, and the bulk density and earthworm samples from the east. A separate plastic composite sample (0–10 cm) is taken from 15 random locations within a 2-meter circle, avoiding plastic contamination.

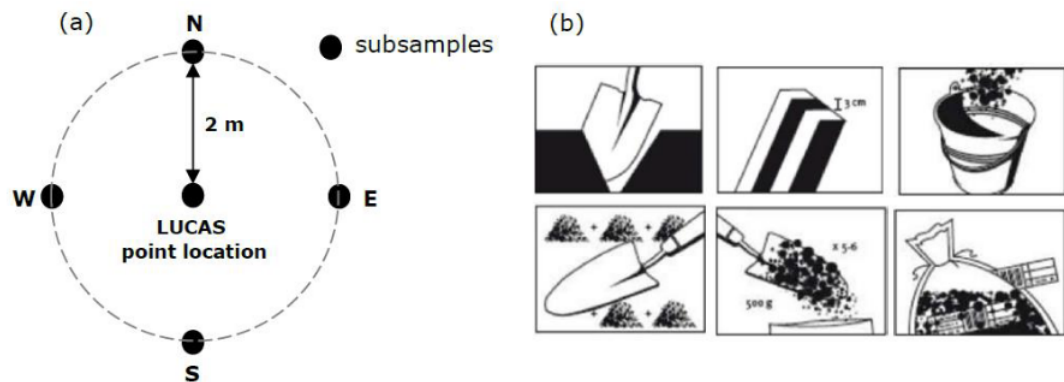


Figure 4: The LUCAS protocol sampling design, as outlined by Fernández Ugalde et al. (2022), includes one central and four peripheral subsamples collected 2 meters from the center in the four cardinal directions (north, east, south, and west). Each subsample is taken by digging a V-shaped hole to 20 cm depth, from which a 3 cm-thick vertical soil slice is extracted.

#### *Environmental characterisation of Soil Samples*

In total, a total of sixteen soil parameters were analyzed to describe the abiotic environment at each study site and for each sample (Figure 2). These included key indicators of soil fertility and nutrient availability, such as pH, available phosphorus ( $P$  and  $PO_4$ ), exchangeable potassium ( $K$  and  $K_2O$ ), total organic carbon (TOC), and total nitrogen (TN). In addition, exchangeable cations including

calcium (Ca), magnesium (Mg), sodium (Na), aluminium (Al), iron (Fe), and manganese (Mn) were measured, along with phosphorus expressed in cmolc/kg. The H-value (reflecting hydrogen ion concentration) and cation exchange capacity (CEC) were also assessed to evaluate the soil's buffering capacity and nutrient retention potential. All chemical and physical analyses were conducted using harmonized protocols developed by the BENCHMARKS consortium to ensure methodological consistency across case studies (Symanczik et al., 2025). These parameters were used in subsequent analyses to investigate potential environmental drivers of soil macrofauna community composition and diversity.

## 2.3 Taxonomic Identification

### 2.3.1 Morphological Identification

Macroinvertebrates were identified using traditional taxonomic methods, employing dichotomous keys that focused on the organisms' morphological traits. Samples were examined under a low-power microscope, and the organisms were classified to taxonomic groups based on physical characteristics, guided by relevant taxonomic references (Quigley & Madge, 1988) and expert knowledge. To prevent cross-contamination between samples, cleaning protocols were strictly followed. After each sample, tweezers were sanitized with 3% sodium hypochlorite, followed by two rinses with distilled water or by flaming them for 5-10 seconds to ensure the denaturation and destruction of any DNA. Other materials, such as trays, were cleaned with 70% alcohol. The sorted specimens were then preserved in 96% alcohol at room temperature until the completion of all sample processing. Additionally, 15 random samples were selected, consisting of 8 samples from the oak forest and 7 samples from the pine forest. They were separated according to their taxonomic group. The specimens were dabbed to remove any excess ethanol. Each group was weighed three times using a scale with a precision of 0.0005 g decimals to account for scale variability. The mean biomass for each group was then assessed based on the three recorded weights.

### 2.3.2 Molecular Identification and Metabarcoding Pipeline

#### *Bulk Sample Preprocessing*

To proceed with molecular species identification using COI gene metabarcoding , bulk samples were dried overnight in an incubator at 56°C. In cases where the ethanol did not fully evaporate, excess was removed manually with pipettes from each sample individually. A second drying step was done overnight. The lids were unscrewed and placed on top of each container. After the specimens were fully dried, they were transferred into Falcon Tubes

50mL. Based on the amount of biological material, one to four 8mm glass beads were added to the bulk sample. The samples were turned into fine powder using the Bullet Blender® 50 Gold+ (Next Advance, NY, USA), for 15 minutes at maximum velocity or until fully homogenized.

#### *DNA Extraction Protocol*

For DNA extraction 10mg homogenized powder was used per sample. If less than 10 mg of sample powder was available, the entire sample was processed. DNA was extracted using the Mag-Bind® Blood & Tissue DNA HDQ 96 Kit (Omega Bio-Tek, GE, USA). For high-throughput processing, the extractions were automated on the Opentrons OT-2 pipetting robot (Opentrons, NY, USA) using an adapted version of the manufacturer's protocol. Samples with limited tissue quantity were extracted manually in parallel using single-tube workflows.. First, to each well, 250 µL of TL Buffer was added. Proteinase K (20 µL) was added to initiate digestion, and samples were vortexed to ensure proper mixing. Lysis was carried out at 55°C for 2 hours in a water bath. Manual vortexing was performed every 20–30 minutes. Manually extracted samples underwent a digestion step in a Thermomixer-Mixer HC (Starlab, Hamburg, Germany). The incubation was performed for 2 hours at 55 °C with interval mixing. Following lysis, samples were centrifuged at 20,000 × g for 5 minutes to pellet insoluble debris. 200 µL of the clear supernatant was transferred to a fresh 96-deepwell plate. Subsequently, 230 µL of AL Buffer was added, and samples were mixed by vortexing (10 minutes with 500 rpm) using the Multi Plate Shaker MPS-1 (Biosan, Riga, Latvia) to ensure complete homogenization.

To bind genomic DNA, 320 µL of HDQ Binding Buffer (pre-diluted with 100% isopropanol as per manufacturer's instructions) and 20 µL of Mag-Bind® Particles HDQ were added. The mixture was vortexed under the same conditions as in the previous step. Next, 600 µL (for manual) and 540 µL (for automatic) of VHB Buffer (prepared with ethanol) was added, and samples were vortexed for 15 seconds before being placed on a magnetic separation device. Once particles had cleared from the solution, the supernatant was discarded. This wash step was repeated to improve purity. An additional wash was performed using 600 µL (for manual) and 540 µL (for automatic) of SPM Buffer (prepared with ethanol). The supernatant was removed after magnetic separation, and the particles were then air-dried for 10 minutes to remove residual ethanol, (as extended drying improves downstream elution efficiency.) DNA was eluted by adding 50 µL (for manual) and 55 µL (for automatic) of pre-warmed Elution Buffer (70°C). Samples were vortexed for 5 minutes to facilitate release of DNA

from the magnetic particles. After magnetic separation, the cleared eluate containing purified DNA was transferred to a new 96-well microplate and stored at 4°C. To evaluate the quality and quantity of extracted DNA a Nanodrop spectrophotometer was used, the analysis allows also to understand possible sources of contamination. DNA integrity was confirmed by running an agarose gel electrophoresis (1%) alongside a 1 kb DNA ladder (150V for 45 minutes). All extracted samples showed clear, visible DNA bands, while negative controls (blanks) showed no bands, indicating no contamination.

*Amplicon PCR and Library Preparation:*

For Illumina library preparation a two-step PCR protocol was followed (Figure 5). The PCR was performed using the BF3 (CCHGAYATRGCHTTYCCHCG) and BR2 (TCDGGRTGNCCRAARAAYCA) primer pair, which includes Illumina adapters and targets a 418 bp fragment of the mitochondrial cytochrome oxidase I (COI) gene (Elbrecht et al., 2019).

To accommodate diverse downstream amplification needs and improve sequencing performance, I prepared four separate primer mixes containing different combinations of 1 to 4 unique primer variants. For the first PCR (PCR1), fusion primers were designed based on the broad-spectrum COI primers BF3 and BR2 (Elbrecht et al., 2019). Each primer was modified to include a variable-length nucleotide insert (0–3 bp) between the Illumina adapter tail and the target-specific sequence. These inserts serve to increase sequence complexity at the start of sequencing reads, enhancing base-calling accuracy on Illumina platforms. In total, four forward and four reverse variants were used, enabling combinatorial diversity across samples. The final primer structure consisted of an Illumina adapter tail (partial), followed by the variable-length insert, and ending with the target-specific COI primer sequence. A separate master mix was prepared for each primer insert set. The reaction mixes for a single sample ( $n=1$ ) consisted of 5 µL of Qiagen Multiplex Master Mix (QIAGEN, Hilden, Germany), 0.3 µL of the forward primer (10 nM), 0.3 µL of the reverse primer (10 µM), and 3.4 µL of H<sub>2</sub>O, for a total master mix volume of 9 µL per reaction. PCR reactions were prepared by combining 9 µL of master mix with 1–3 µL of DNA template, previously diluted to 1:5, 1:10 or 1:20. The amount and dilution of each DNA templated was based on the previously determined optimal conditions for each sample. Derived from the intensity and clarity of the DNA bands retrieved from electrophoresis gel and the given Nanodrop values 1–3 µL of DNA template was selected (Table 1). PCR conditions were tested and optimized, bands with smearing or no amplification were diluted accordingly. This approach aimed to

normalize the amount of viable, high-molecular-weight DNA template while minimizing the impact of potential PCR inhibitors. Reactions were assembled in a 96-well plate and subjected to thermocycling using the following conditions: an initial denaturation at 95 °C for 15 minutes; followed by 30 cycles of denaturation at 94 °C for 30 seconds, annealing at 50 °C for 60 seconds, and extension at 72 °C for 60 seconds; with a final extension step at 72 °C for 5 minutes. Amplification success was verified using 2% agarose gel electrophoresis, which showed clear bands for all samples, while the extraction blanks and PCR negative controls showed no evidence of contamination.

Table 1: Guidelines for adjusting DNA input volume for PCR based on DNA quality (assessed via agarose gel) and concentration (measured by Nanodrop). Recommended dilution and input volumes were adapted to optimize amplification efficiency across a range of sample conditions. Samples with high concentrations and strong bands were diluted to reduce PCR inhibition, while lower-quality or lower-concentration samples were used undiluted with adjusted input volumes.

<b>DNA Quality (Agarose Gel)</b>	<b>DNA Concentration (Nanodrop)</b>	<b>Action Taken</b>	<b>µL Added</b>
Strong/Good Band	> 100 ng/µL	Dilute sample 1:10	1 µL of diluted sample
Strong/Good Band	< 100 ng/µL	Use neat (undiluted)	1 µL
Medium Band	> 100 ng/µL	Use neat	1 µL
Medium Band	< 100 ng/µL	Use neat	2 µL
Weak Band	> 100 ng/µL	Use neat	2 µL
Weak Band	< 100 ng/µL	Use neat	3 µL

Smearing/Dragging	Any	Dilute sample 1:10 or 1:20	1 µL of diluted sample
-------------------	-----	-------------------------------	---------------------------

The PCR products were diluted at a 1:4 ratio, followed by a second PCR to add the 7-base pair identification indexes along with the Illumina P5 and P7 sequencing adapters. Indexing PCR was done using 7.0 µL of Kapa HiFi Hot Start mix (Roche, Penzberg, Germany) 2.8 µL of H<sub>2</sub>O, 0.7 µL of each indexing primer (10 nM) and 2.8 µL of the previous diluted PCR product. Resulting in a final reaction volume of 14 µL per well. The amplification program was set with an initial denaturation step at 95°C for 3 minutes. Followed by 8 cycles, each consisting of denaturation at 95°C for 30 seconds, primer annealing at 55°C for 30 seconds, and extension at 72°C for 30 seconds. A final extension was performed at 72°C for 5 minutes. The program concluded with a hold step at 4°C. After completion of the PCR program, the samples were stored at 4 °C until further processing. A 2% agarose gel electrophoresis was performed for all PCR products to assess amplification success. Samples displaying faint bands were re-amplified using a 1:1 dilution of the original template. All samples ultimately produced visible bands upon gel electrophoresis.

Fragmented DNA samples (4–9 µL) were purified using KAPA HyperPure Beads at a 0.7X bead-to-sample volume ratio. The beads were first equilibrated to room temperature and thoroughly resuspended by vortexing. For each sample, 0.7 volumes of beads were added (e.g., 6.3 µL beads for 9 µL DNA sample), and the mixture was mixed thoroughly by pipetting up and down. The samples were then incubated at room temperature for 5 minutes to allow DNA binding to the beads. Following incubation, the tubes were placed on a magnetic rack until the solution cleared, allowing the beads to separate. The supernatant was carefully removed and discarded without disturbing the beads. While remaining on the magnet, the beads were washed twice with 100 µL of freshly prepared 80% ethanol. Each wash involved adding ethanol, incubating for 30 seconds, then carefully removing the ethanol. After the second wash, the beads were air-dried at room temperature for 3 to 5 minutes, avoiding over-drying to prevent reduced DNA yield. The tubes were then removed from the magnet, and the beads were resuspended in 20 µL of elution buffer (nuclease free water). Samples were incubated for 2 minutes at room temperature to elute the DNA from the beads. Finally, the tubes were placed back on the magnetic rack until the solution cleared, and the clear supernatant containing purified DNA was transferred to a new plate. Purified DNA was stored at 4°C until further processing.

### *Quality Check, Normalization and Sample Pooling*

A subset of five samples was evaluated using the 4150 Agilent TapeStation System (Agilent Technologies, Santa Clara, CA, USA) with the D1000 ScreenTape for fragment size distribution and further quantified using a NanoDrop Spectrophotometer (Thermo Fisher Scientific, Wilmington, DE, USA). Based on quantification results, all samples were normalized to a final concentration of 12 nM using 5 µL of cleaned PCR product.

Following normalization, 4 µL of each sample was pooled into two separate libraries. Samples that could not be normalized due to low DNA concentration, were added directly to the sequencing pool without dilution. Then 150 µL of each pool was used for a second bead cleanup with a 0.65× bead-to-sample ratio to perform size selection, targeting fragments greater than 400 bp. Final library quality and fragment distribution were verified using the TapeStation, and concentrations > 5 ng/ µL were confirmed. Finally the prepared libraries were sequenced at Novogene (Cambridge, UK) using the Illumina Novaseq Platform.

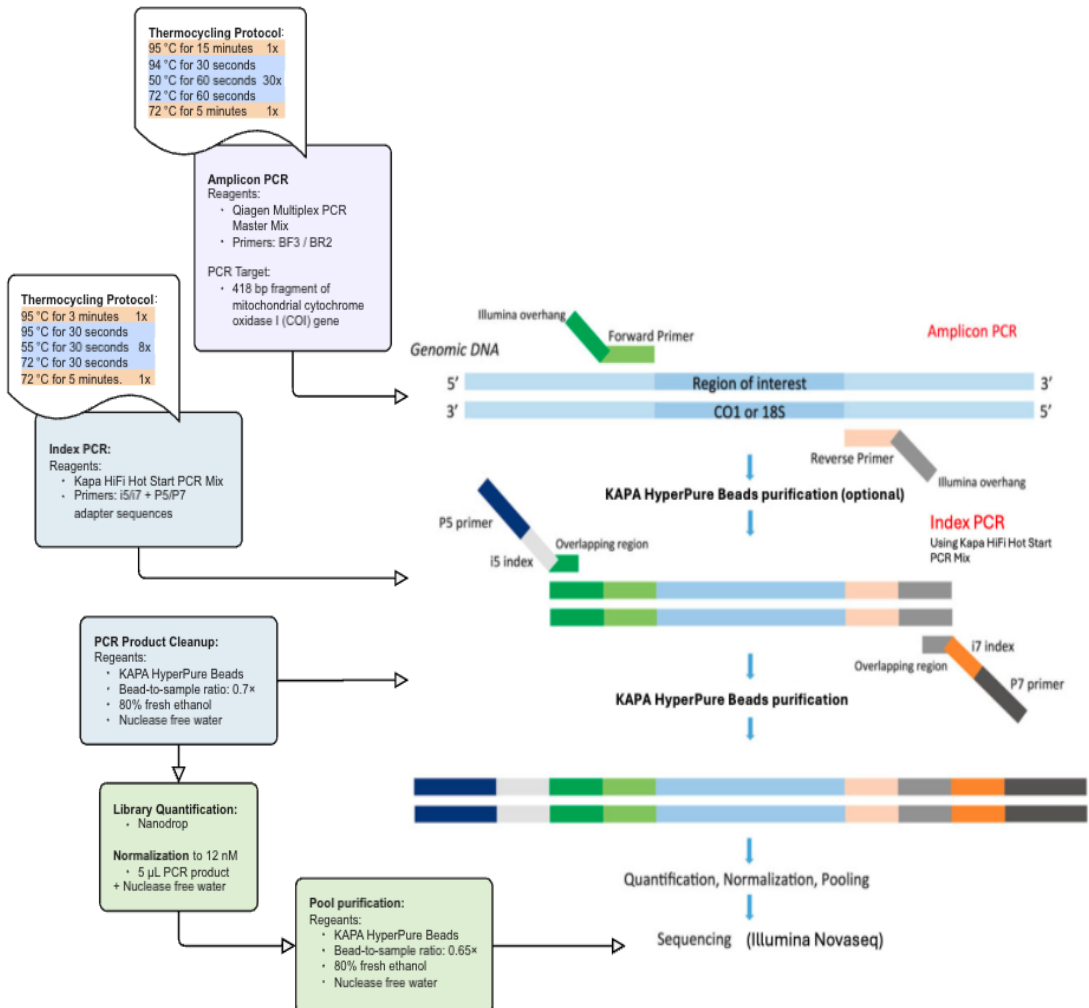


Figure 5: Overview of the two-step library preparation workflow for COI gene metabarcoding. The process begins with amplicon PCR using Qiagen Multiplex PCR reagents and fusion primers BF3 and BR2 targeting a ~418 bp fragment of the mitochondrial cytochrome c oxidase subunit I (COI) gene. Thermocycling parameters for amplicon and indexing PCR are shown. Following initial amplification, products undergo cleanup using KAPA HyperPure beads before index PCR with i5/i7 adapters using KAPA HiFi HotStart polymerase. A second bead cleanup step follows before samples are quantified via Nanodrop, normalized to 12 nM, pooled, and purified. Final library validation was performed using TapeStation. Adapted from Bourlat et al., (2016) and Illumina, 2013.

### Bioinformatic Pipeline

Sequence processing and denoising were conducted using OBITools4, in combination with VSEARCH and LULU. Initially, paired-end reads were merged via “obipairing,” with any unaligned sequences being discarded. From the original reads, sample assignment and primer sequence trimming were performed using the “obimultiplex” command, allowing up to four mismatches per primer sequence. The remaining reads were then dereplicated into unique sequences using “obiuniq,” and singletons were removed with “obigrep.”

Subsequently, the remaining exact sequence variants were aggregated into a single file and processed using VSEARCH. Reads were dereplicated again with the “--derep\_fulllength” command and then denoised using “--cluster\_unequal”, resulting in the removal reads due to presumed PCR and sequencing errors. Chimeric sequences were identified and removed using “--uchime3\_denovo,” eliminating additional reads. The remaining sequences were then grouped based on a 99% similarity threshold using “--cluster\_size,” defining 4,934 operational taxonomic units. LULU was used to identify and curate putative NUMTs and other artifacts, which is essential for preventing the artificial inflation of diversity estimates caused by pseudogenes or PCR artifacts. This process reduced the Operational Taxonomic Unit (OTU) count thus removing spurious variants. Taxonomic assignment was performed using Boldigger, which queried representative OTU sequences against the BOLD database. For the metabarcoding data further filtering of sequences was needed after taxonomic assignment. OTUs assigned to taxa outside the scope of soil macrofauna or assigned only at a rank higher than Class were excluded. Additionally, I have retained only those OTUs that showed a percent sequence identity of >85% to their best match in the BOLD reference database.

## 2.4 Statistical Analysis

All statistical analyses and data visualization were performed in R Version Version 2025.05.1+513. All statistical analyses were performed in the R programming environment (R Core Team, 2023). Alpha diversity was analyzed using the iNEXT package (v3.0.0; Hsieh et al., 2016), which uses rarefaction and extrapolation to standardized sample coverage for robust diversity estimation. Community-level analyses were primarily performed using the vegan package (v2.6-10; Oksanen et al., 2022), which was used for data transformation (decostand), calculating beta diversity dissimilarity matrices (vegdist), performing ordinations (NMDS with metaMDS; dbRDA with dbRDA), generating rarefaction curves (rarecurve), and conducting Mantel tests. The homogeneity of multivariate dispersion among groups was tested with the betadisper function. Beta diversity was further partitioned into its turnover and nestedness components using the betapart package (Baselga & Orme, 2012). Indicator species analysis to identify taxa associated with specific forest types was carried out with the indicspecies package (multipatt function; De Cáceres & Legendre, 2009).

Spatial analyses, including the generation of distance-based Moran's Eigenvector Maps (dbMEMs) and forward selection of predictors, were conducted using the adeSpatial (Dray et al., 2023) and ape (Paradis & Schliep, 2019) packages. Model validation was performed using standard diagnostic checks, including the calculation of the Variance Inflation Factor (VIF) with the car package (Fox & Weisberg, 2019).

All publication-quality figures were created using the ggplot2 package (v3.4.2; Wickham, 2016), with figures arranged and enhanced using ggpubr (v0.6.0; Kassambara, 2023). Venn diagrams showing shared and unique taxa between groups were generated with ggVennDiagram (v1.2.3; Gao et al., 2021), and clustered heatmaps were created with pheatmap (Kolde, 2019). Data, code, and bioinformatic pipelines used in this study are available on GitHub (<https://github.com/luiscunhamx/ENGELUC/>)

### 2.4.1 Comparative Performance of Sampling Strategies

In this section, the methods used to evaluate and compare the performance of the k-means and random sampling strategy are described. The primary goal was to determine which design was more effective in capturing the underlying spatial variability of species richness within the study area.

### *Exploratory Analyses and Visualization:*

The performance of the k-means and random sampling strategies was evaluated. First, the distributions of site-level species richness were visualized and compared using box plots for the k-means, random, and reference LUCAS datasets. This provided a direct comparison of the richness values captured by each design. Second, to assess the uniqueness and overlap of the captured species pools, Venn diagrams were constructed to illustrate the number of distinct and shared species among the three sampling strategies. Finally, to provide a standardized comparison of sampling efficacy that accounts for differences in sampling effort, sample-based rarefaction and extrapolation (R/E) curves were generated for species richness using the iNEXT R package (Hsieh et al., 2016). This allowed for the comparison of diversity at standardized sample sizes, offering robust insights into sampling completeness and efficiency for each design. In all analyses, the LUCAS data served as an external reference point.

### *Statistical Assessment of Captured Variability:*

To evaluate the variability captured by different sample designs, the coefficient of variation (CV) was calculated for species richness and for each chemical parameter. This was performed at each site, both for the entire dataset and for subsets partitioned by oak and pine forest types. To statistically compare the variation around the means within and across sites, Levene's test for homogeneity of variance was applied as a measure of relative variation (Schultz, 1985). This procedure was repeated for both chemical variables and richness. To validate LUCAS as a reliable and effective reference point to represent the broader distribution of taxonomic richness, it was checked whether the point falls outside the distribution of each sample strategy for each system individually. Bootstrapping was employed to account for non-normal distribution, and a 95% CI was created and tested if LUCAS falls within or outside this predicted range.

Moreover, to determine if there were significant differences in community heterogeneity captured by each sampling design a comparative analysis of multivariate homogeneity of group dispersion was done using the “betadisper” function from the “vegan” package and tested for significance with “permutest” (999 permutations) for statistical difference. However as LUCAS is only a single observation per forest site there is no distribution to be assessed and therefore was excluded from this analysis, further investigating k-means against random sampling per system (Oak and Pine). This comparison was systematically applied across both data collection methodologies (morphological identification and molecular

taxonomic assignment) and two aspects of diversity (taxonomic richness and abundance structure), resulting in four distinct analyses per forest system:

- For taxonomic richness based on morphological identification, community data was converted to presence/absence, and heterogeneity was assessed using a Jaccard dissimilarity matrix.
- For abundance structure based on morphological identification, raw abundance counts were first Hellinger-transformed to down-weight the influence of hyper-abundant taxa. The analysis was then performed on a resulting Bray-Curtis dissimilarity matrix.
- For taxonomic richness based on molecular assignment, the OTU table was converted to presence/absence, and dispersion was again assessed using a Jaccard dissimilarity matrix.
- For abundance structure based on molecular assignment, raw read counts were first normalized to relative abundance (decostand, method = "total") to account for uneven sequencing depth. Heterogeneity was then tested using a Bray-Curtis dissimilarity matrix derived from this normalized data.

Furthermore, this method calculates the multivariate dispersion (i.e., distance to group centroid) for each sample in ordination space, (based on Bray–Curtis dissimilarity for abundance data and Jaccard dissimilarity for occurrence data). Boxplots of centroid distances were used to visualize differences in dispersion between the k-means and random sampling designs. A lower average distance to centroid indicates greater compositional homogeneity within a group.

## 2.4.2 Biodiversity Assessment

### *Exploration and Visualization*

Boxplots were generated to compare the median, interquartile range, and overall distribution of both taxonomic richness and total abundance between the two forest types. For the specific purpose of improving the visual clarity of the abundance boxplots, extreme outliers (defined as samples with a count >100 individuals) were excluded from the plot generation; however, these data points were retained for all subsequent statistical analyses. To visualize and compare the taxonomic composition of each forest type, bar plots were created to depict the mean abundance and standard deviation for each identified taxonomic group, allowing for a direct comparison of the dominant taxa in each system.

### *Analysis of Alpha Diversity*

Alpha diversity of each forest type was analysed using Hill numbers using the iNEXT R package (Hsieh et al., 2016). The first three Hill numbers were calculated, corresponding to species richness, the exponential of Shannon's entropy, and the inverse of Simpson's concentration index. Rarefaction/extrapolation curves for species richness were generated to visualize sampling sufficiency. A curve that approaches an asymptote, coupled with a high sample coverage value, indicates that the sampling effort was sufficient to capture most of the "true" diversity within each forest type. Alpha diversity estimates were compared among forest systems based on the 95% confidence intervals generated by the (iNEXT) bootstrapping procedure. If CIs between the two systems were non-overlapping, they were interpreted as a significant difference. For complementation alpha diversity indices, the Shannon index, Simpson index and Pielou's evenness index for each individual sample and for each forest type were calculated using the vegan R package. Data were checked for normality and homogeneity of variances. Difference in taxonomic richness between the forest systems was tested employing the Wilcoxon rank-sum test.

### *Analysis of Beta Diversity*

To investigate beta diversity and compare community composition between pine and oak forests, a multi-step approach was used. A Jaccard dissimilarity matrix was first calculated from species presence-absence data to quantify compositional differences among samples. These patterns were visualized using Non-Metric Multidimensional Scaling (NMDS) based on the Jaccard matrix, with stress values below 0.2 indicating a reliable ordination. To verify the reliability of the ordination community distance was tested for unequal dispersion. To statistically test for differences in community structure between oak and pine forest, a Permutational Multivariate Analysis of Variance (perMANOVA) was conducted using the "adonis2" function from the "vegan" package in R, with significance assessed via 999 permutations. To determine the relative contributions of species turnover and nestedness to overall beta diversity, a partitioning analysis was conducted using the "betapart" R package. Total beta diversity, as measured by the Jaccard dissimilarity index ( $\beta_{jac}$ ), was decomposed into its two additive components: spatial turnover ( $\beta_{jtu}$ ) and nestedness-resultant dissimilarity ( $\beta_{jne}$ ) using the "beta.multi" function. This analysis was performed on presence-absence matrices derived from both the morphological and the OTU-based metabarcoding datasets. The partitioning was conducted independently for the Oak and Pine forest systems to assess the dominant community assembly process within each habitat.

To quantify the level of congruence between morphological and metabarcoding identification methods, a Mantel test was performed using the "mantel" function from the "vegan" R package. The test calculated the Pearson correlation coefficient between two community dissimilarity matrices: one generated from the morphological presence-absence data and the other from the metabarcoding presence-absence data. Both dissimilarity matrices were calculated using the Jaccard index. The statistical significance of the correlation was evaluated using 999 permutations. This analysis was conducted independently for the Oak and Pine forest datasets to determine if the congruence between methods varied by habitat.

#### **2.4.3 Analysis of Environmental and Spatial Drivers**

All soil chemical data used in this study were provided by the Austrian Agency for Health and Food Safety (Ages) as part of the Benchmarks Consortium.

##### *Exploration of Chemical Measurements*

An initial exploratory analysis was performed by generating boxplots for each chemical variable to visualize its median, interquartile range, and distribution across the two forest types. Prior to analysis, all chemical variables (e.g., pH, phosphate, TOC, TN) were scaled to a mean of zero and unit variance. For subsequent modeling, multicollinearity was rigorously assessed. First, a pairwise Spearman correlation matrix was calculated using the "rcorr" function from the "Hmisc" package. Variable pairs exhibiting a Spearman correlation coefficient ( $\rho$ ) with an absolute value greater than 0.7 were flagged as highly correlated. Second, to further diagnose collinearity within the full suite of predictors, Variance Inflation Factors (VIFs) were calculated. Based on the results of the correlation matrix and VIF analysis, a final, reduced set of non-collinear variables was selected for use in all subsequent constrained analyses. To identify the principal axes of variation within the multidimensional environmental dataset, a Principal Component Analysis (PCA) was performed using the "prcomp" function from the base R stats package.

##### *Assessment of Community to Chemical Relationship*

Distance-based redundancy analysis (db-RDA) was used to examine the relationships between community composition and soil chemical variables, assessing how much variation in community structure could be explained by environmental factors. Analyses were performed using the "dbrda" function from the "vegan" package in R, based on Jaccard dissimilarities. Permutation-based ANOVA tests (999 permutations) using "anova.cca"

function were used to evaluate the significance of the overall model and individual predictors. Separate analyses were conducted for oak and pine forest types to identify forest-specific patterns. Model selection was carried out using the “ordistep” function to identify the most parsimonious set of explanatory variables. If no suitable model could be fitted, non-metric multidimensional scaling (NMDS) was used as an alternative, allowing for the exploration of community–environment relationships in a less constrained ordination space.

#### *Linking Community to Chemical and Spatial Dependency*

To explore the relative contributions of environmental filtering and spatial processes on macrofauna community composition, a multi-step analytical approach was applied separately for oak and pine forest, using the “vegan” and “sf” packages. First, community dissimilarity was calculated using the Jaccard distance (`vegan::vegdist`) and environmental distances were computed using the Euclidean distance, applied to filtered and scaled chemical variables. The site coordinates (in WGS84, CRS:4326) were converted into a simple feature (`sf`) object using the `st_as_sf` function. This object was then projected into the Universal Transverse Mercator (UTM) coordinate system (CRS: 25830) (`sf::st_transform`) to convert geographic degrees into accurate distance measurement. For subsequent analysis into a standard distance. Mantel tests (`vegan::mantel`) were then performed to assess the direct correlation between community dissimilarity and the environmental and geographic distance matrices. Following correlations were evaluated:

- Community dissimilarity and geographic distance, to evaluate spatial structuring suggestive of dispersal limitation.
- Environmental distance and geographic distance, to assess whether environmental variables were spatially autocorrelated.
- Community dissimilarity and environmental distance, testing whether variation in soil chemistry structures community composition (environmental filtering).

These tests were conducted using Pearson's correlation coefficient, with statistical significance evaluated through 999 permutations. To visualize how the spatial autocorrelation in the community data changed across different spatial scales, Mantel correlograms were generated using the “mantel.correlog” function. Mantel correlations for n = 8 distance classes were calculated, based on the maximum distance observed between two samples, providing insight into the spatial scale at which community shows autocorrelation or similarity decays.

Variation partitioning was conducted using the “varpart” function from the vegan package, partitioning the explained variation in community composition into:

[E|S]: the pure environmental fraction (independent of spatial structure),

[S|E]: the pure spatial fraction (e.g., dispersal limitation), and

[E ∩ s]: the shared fraction (spatially structured environmental effects).

Finally, distance-based redundancy analysis (db-RDA) and partial db-RDA using the “dbrda” and “Condition” function from vegan package and partial db-RDA were used to further explore and quantify these relationships, explicitly controlling for spatial and environmental variables.

#### **2.4.4 Taxonomic Response to Environmental and Spatial Variability**

To further evaluate how spatial and environmental variability drives community composition and how this separation is reflected by individual taxonomic, following analyses were performed.

To compare community structure between methodologies and within forest systems, both the morphological and specimen-based metabarcoding datasets were analyzed. For abundance-based analyses, the raw molecular read counts were normalized into Relative Read Abundance (RRA) by dividing the counts for each taxon by the total library size of each sample (vegan::decostand, method="total"). For presence-absence analyses, a taxon was considered present if its RRA exceeded a threshold of 0.0001%.

Indicator species analysis was conducted to identify taxa significantly associated with either the Oak or Pine forest types. This was performed using the multi-level pattern analysis function “multipatt” from the “indicspecies” package, with 999 permutations to assess statistical significance. The analysis was run on both the morphological count data and the molecular RRA data.

To identify taxa with non-random spatial distributions, Global Moran's I tests were performed for each key taxonomic group using the Moran.I function from the ape package. This analysis was conducted at two different resolutions to align with the nature of each dataset:

- Count abundance (Morphological Dataset)
- Relative read abundance grouped into taxonomic groups

Species with insufficient variation were excluded from this analysis, as they cannot exhibit spatial patterns due to low general variance. For taxa exhibiting significant global spatial autocorrelation, a Local Indicators of Spatial Association (LISA) analysis was conducted to identify the location of spatial clusters. This was performed using Local Moran's I to classify sample locations into significant high-high ("hotspot"), low-low ("coldspot"), or high-low/low-high (spatial outlier) clusters, based on a neighborhood defined by the k=5 nearest neighbors.

#### **2.4.5 Comparative Analysis of Morphological and Molecular Data**

##### *Sample completeness*

The efficacy of the sampling effort was assessed using the vegan package in R. First, sample-based rarefaction curves were generated via the "rarecurve" function to visualize the relationship between sampling intensity (reads) and observed taxonomic richness. All curves were standardized to the smallest sample size in the dataset for valid comparison. Second, the total expected taxonomic richness for each forest type was estimated using the "specpool" function, which calculates non-parametric estimators like Chao2 for pooled samples. The overall sampling completeness for each system was then quantified by expressing the total number of observed taxa as a percentage of the estimated total richness derived from the Chao2 estimator.

### 3 Results

#### 3.1 Comparative Performance of Sampling Strategies

In the oak forest, the k-means sampling approach detected a higher median richness (6 taxonomic groups) compared to the random sampling strategy (5 groups), with mean richness values of 5.88 (SD = 1.45) and 5.39 (SD = 0.87), respectively (Figure 6A). A similar pattern was observed in the pine forest, where the k-means strategy also resulted in a higher median of 6 taxonomic groups than random sampling with 5 groups, although the mean richness values were nearly identical 5.80 (SD = 1.47) 5.77 (SD = 1.01) (Figure 6B). The LUCAS point (7 taxonomic groups) fell outside the 95% confidence interval of both sampling distributions in the oak forest. In the pine forest, the LUCAS point fell within the confidence 95% intervals for k-means and random sampling.

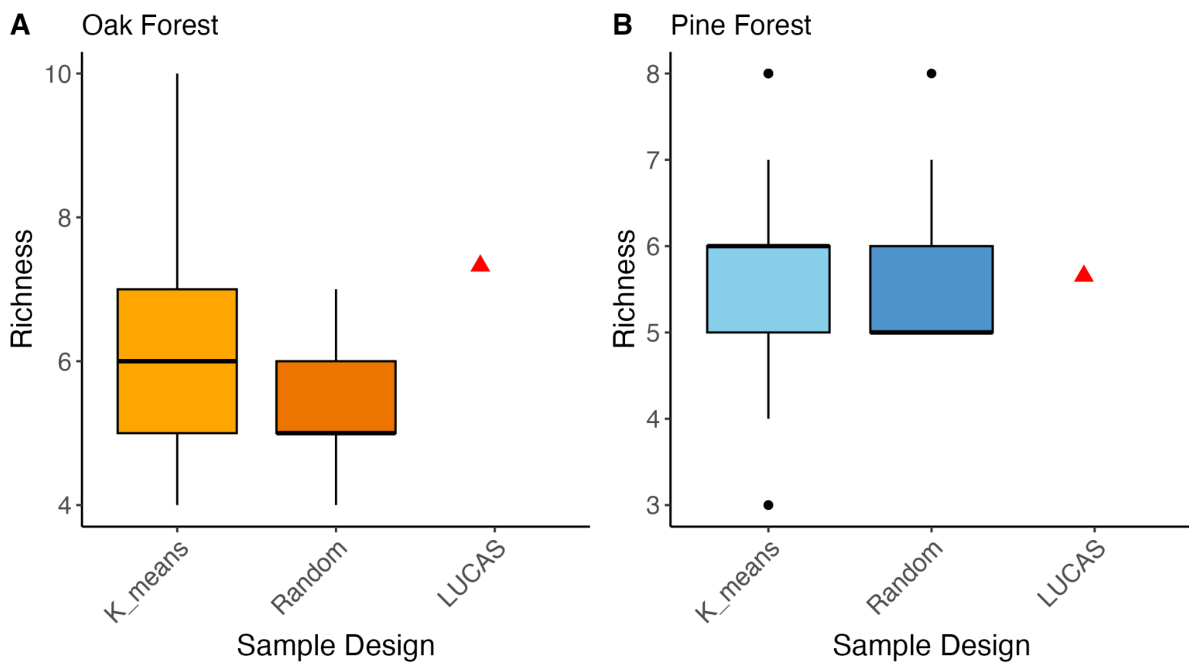


Figure 6: Box and whisker plots morphological taxonomic richness distribution captured by k-means and random sampling strategies in two forest ecosystems. (A) Display of the distribution of richness values selected via the k-means (orange) and random (dark orange) in the oak forest. (B) Display of the distribution of richness values selected via the k-means (lightblue) and random (steelblue) in the pine forest. The richness value of the single LUCAS point in each ecosystem is shown as a red triangle.

To assess the variability of taxonomic richness captured by each strategy comparing effectiveness across the two first types, standard deviation (sd), the coefficient of variation (CV) and Levene's test for homogeneity of variance were used to evaluate the variability discrimination. Descriptively, the k-means sampling approach consistently captured greater richness variability in both ecosystems. In the oak forest, the CV for k-means was 24.7% compared to 25.4% in the pine forest. A similar pattern was observed for the random sampling, with CVs of 16.2% and 17.6% in the oak and pine forest, respectively. Formal statistical testing with Levene's test indicated that these differences in variance were not statistically significant, with variance homogeneity observed across the forest systems ( $p > 0.05$ , Table 2).

Table 2: Mean (M), standard deviation (sd) and coefficient of variation (CV) for taxonomic richness, in the oak and pine forests, for coupled k-means - random observations (all), k-means, and random observations. M and sd are expressed in the parameter unit, and CV is expressed in % variation around the mean.

Parameter:	Oak			Pine			p-value
	Mean	SD	CV	Mean	SD	CV	
Richness							(oak-pine)
all	5.744	1.292	0.225	5.795	1.301	0.225	0.796
k_means	5.88	1.453	0.247	5.8	1.472	0.254	1
random	5.385	0.87	0.162	5.769	1.013	0.176	0.818
p-value	0.196			0.37			
(k-means - random)							

In the oak forest a total of 14 distinct taxonomic groups were identified (Figure7). 7 (50%) groups were captured by all three designs. Beyond this shared central group, the k-means and random sampling methods both detected an additional 3 taxonomic groups (21.4%). The k-means design was the only strategy to capture unique taxa, identifying 4 groups (28.6%) that were not found by either the random or LUCAS methods. Overall, k-means captured all 14 taxonomic groups (100%) observed in the study. The Random sampling captured a total of

10 groups (71.4%), while at the LUCAS point the 7 groups (50%) found were common to all approaches.

In the pine forest, a comparison of the taxonomic groups captured by the k-means, random, and LUCAS sampling designs revealed a total of 13 distinct macroinvertebrate groups (Figure 7). A core set of 6 taxonomic groups, representing 46.2% of the total taxonomic richness, was detected by all three methodologies. The k-means and random designs captured an additional 4 groups (30.8%). The random sampling was the only strategy to recover unique taxonomic groups, identifying 3 groups (23.1%) that were not found by the other methods. Overall, the random sampling captured all 13 taxonomic groups (100%). The k-means design recovered 10 groups (76.9%), while the LUCAS design captured the smallest core set of 6 groups (46.2%). It is important to note, however, that these raw totals do not account for differences in sampling effort between the designs.

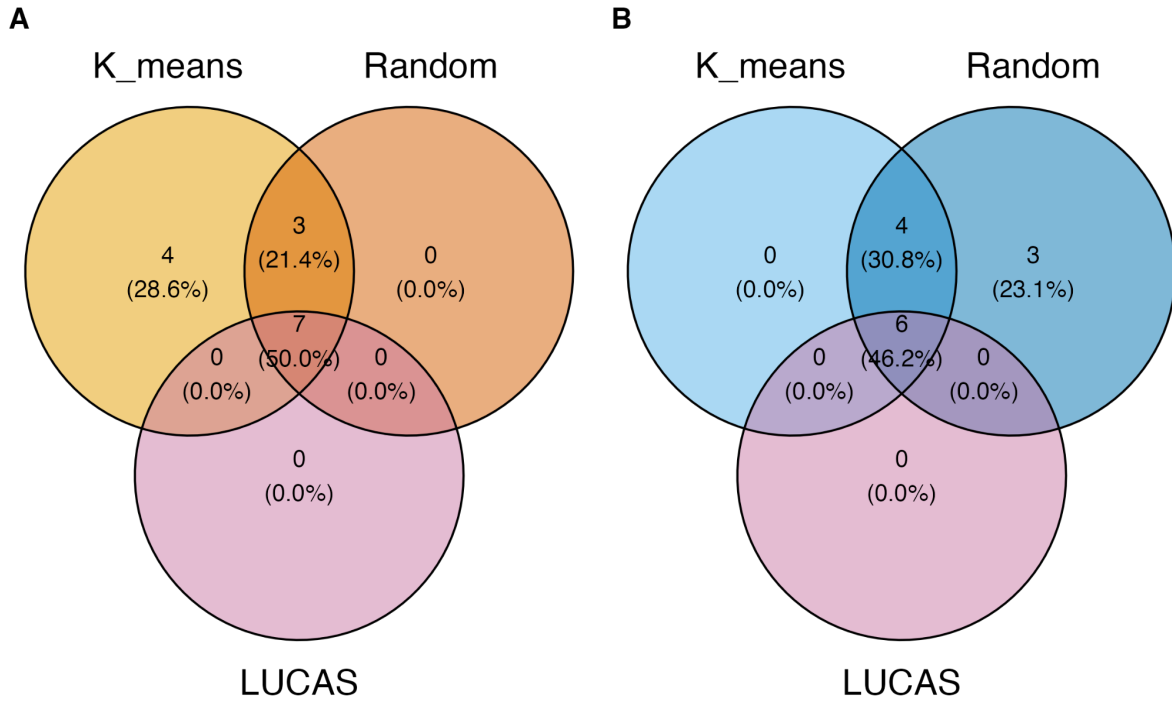


Figure 7: Venn Diagram of morphological identified taxonomic groups captured by each sampling strategy. The circle presents the fraction of captured taxonomic richness in total unique taxa found and in proportion (%), overlap demonstrates overlapping proportion shared by either one other fraction, or in the center by all three indicating similar taxa found. The size of the circles is not representative of the richness. (A) Taxonomic groups found in the oak forest by k-means sampling (light orange), random (orange), LUCAS (purple). (B) Taxonomic groups found in the pine forest by k-means sampling (light blue), random (blue), LUCAS (purple).

Rarefied coverage-based comparison (Figure 8A) shows k-means potentially capturing higher levels of diversity than random, with reaching sample coverage close to 1 showing higher species diversity measures. Extrapolated coverage-based comparison (Figure 8B) revealed that the k-means design as well as random sampling achieved sampling completeness reaching a clear asymptote, with sample coverage values approaching 1.0 at approximately 10 sampling units. However, visually overlapping confidence intervals in both analyses suggest no significant difference in sample performance comparing k-means to random sampling.

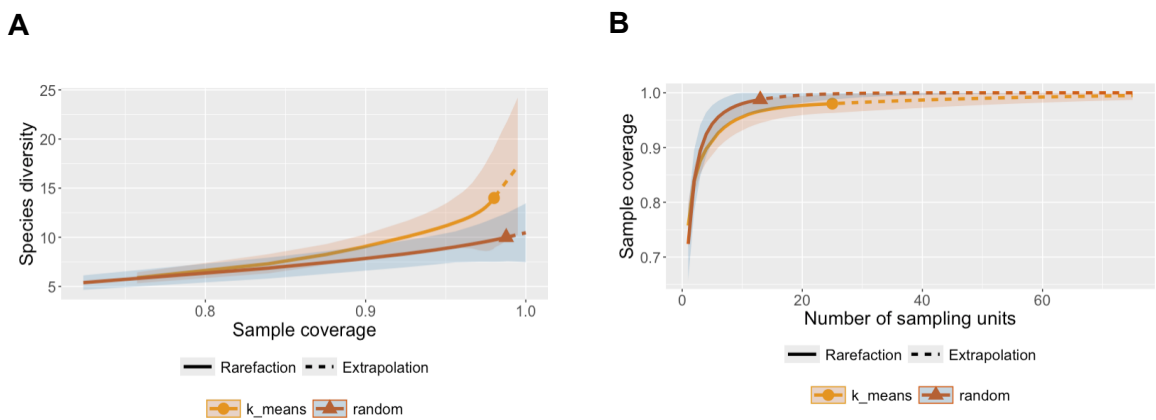


Figure 8: Comparison of sampling design performance (k-means vs. random) in the oak forest system using rarefaction and extrapolation analysis. (A) Sample-size-based rarefaction and extrapolation curves showing observed and estimated species diversity as a function of sample coverage. Shaded areas indicate 95% confidence intervals. (B) Sample coverage as a function of the number of sampling units. The k-means design consistently achieved higher coverage and captured more diversity with fewer samples, suggesting improved efficiency in detecting macrofaunal richness. Curves were generated using the iNEXT package in R (Hsieh et al., 2016).

In the pine forest, the results of the rarefaction (Figure 9A) revealed that the random sampling design shows potentially higher efficiency than the k-means strategy. At any given level of sample coverage, the rarefaction curve for the random design indicates a consistently higher taxonomic diversity, however it also exhibits a large confidence interval. The extrapolated sample-size-based analysis (Figure 9B) shows that k-means design reaches an asymptote close to 1 at approximately 10 sampling units, confirming the sampling effort was sufficient. While random sampling reaches the asymptote at approximately 0.93 accounting for 10 sampling units, and only reaches full sample coverage with extrapolation to 30 - 40 sampling units with a broad confidence interval, giving uncertainty to the estimation.

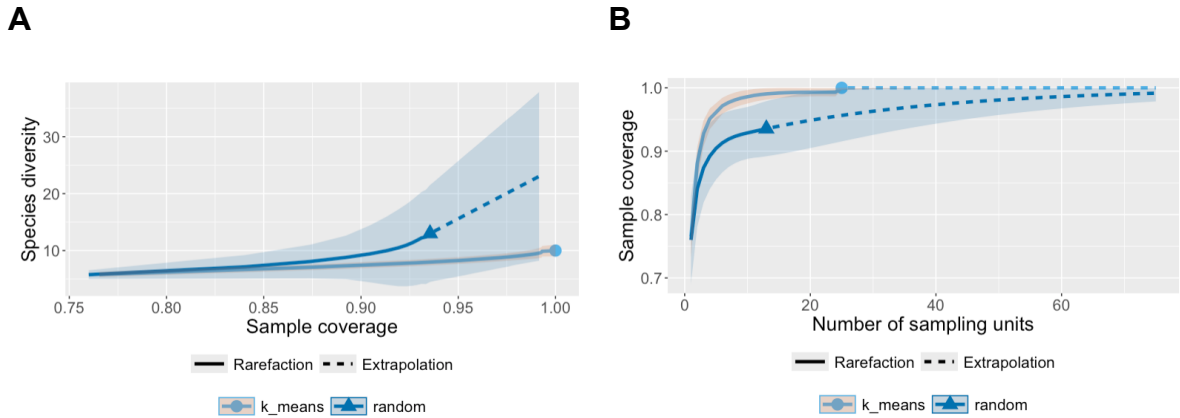


Figure 9: Comparison of sampling design performance (k-means vs. random) in the pine forest system using rarefaction and extrapolation analysis. (A) Sample-size-based rarefaction and extrapolation curves illustrate species diversity as a function of sample coverage. The random sampling design yielded higher extrapolated diversity and broader confidence intervals, indicating greater richness captured or projected. (B) Sample coverage relative to the number of sampling units, showing slightly more efficient accumulation under the random design. Curves were generated using the iNEXT package in R (Hsieh et al., 2016).

#### *Effectiveness of Capturing Variability in Community Composition:*

The non-metric Multidimensional Scaling (NMDS) ordination for each forest system revealed no clear visual separation or clustering of samples based on the sampling approach (K-means, Random, and LUCAS). The stress value for both the oak and pine ordinations was 0.201(Supplementary Figure 1, 2). To formally validate this lack of visual separation, a permutational multivariate analysis of variance (perMANOVA) was performed. This test confirmed that there were no significant differences in the community composition captured by the different sampling designs in either the oak forest ( $p > 0.05$ ) or the pine forest ( $p > 0.05$ ). Beta dispersion analyses revealed contrasting outcomes between forest systems. In the oak forest, the k-means sampling design resulted in lower dispersion compared to random sampling, across both count-based and RRA-derived data (Figure 10a, 10c respectively). This suggests that k-means sampling captured more compositionally homogeneous macrofauna communities in this system. Conversely, in the pine forest, the random sampling design consistently yielded lower dispersion values, indicating greater internal similarity among samples (Figure 10b, 10e). This effect was especially pronounced in the RRA data, where random sampling produced a much tighter distribution of distances to centroid. These results indicate that sampling design influences within-group variability, but the direction and magnitude of this effect depend on both the ecosystem and the type of data used.

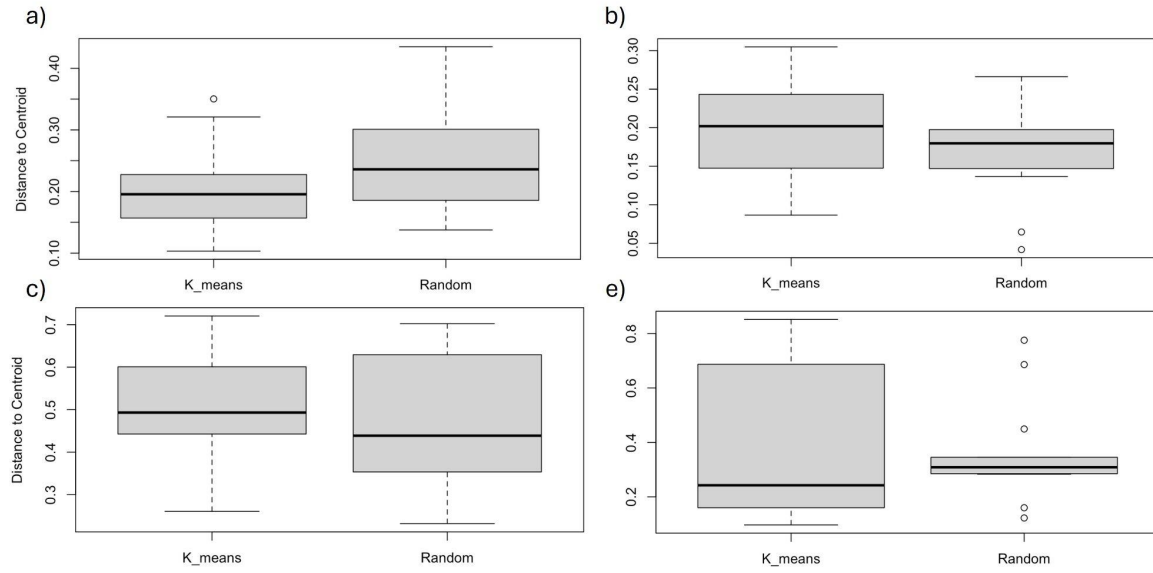


Figure 10: Beta dispersion of soil macrofauna communities across oak and pine forest systems under k-means and random sampling designs. Panels show distances to group centroids (based on Bray–Curtis dissimilarity) calculated for different community data types: a) Oak with count abundance data; b) Pine for count abundance data; c) Oak with relative read abundance (RRA); e) Pine with relative read abundance (RRA). Lower values indicate greater within-group homogeneity in community composition.

#### *Capturing variance in chemical parameters*

To evaluate how effectively different sampling strategies captured environmental variability, Levene's test for homogeneity of variance was applied. The test was used to compare variation in soil chemical properties between forest types (oak vs. pine) within each sampling design, and between sampling designs (k-means vs. random) within each forest type.

For pH, Levene's test indicated significantly different variances between forest types: variance was greater in oak under random sampling ( $p = 0.017$ ) and in pine under k-means sampling ( $p = 0.010$ ). However, within-system comparisons (i.e., between sampling designs) showed no significant differences in pH variance. For phosphate, variance was significantly different between oak and pine under k-means sampling ( $p = 0.005$ ), with no significant variance differences between sampling methods within oak or pine. The same pattern was observed for phosphorus under k-means sampling ( $p = 0.005$ ), but not significantly different within systems between methods. For potassium oxide ( $K_2O$ ), both k-means ( $p < 0.0001$ ) and random sampling ( $p = 0.012$ ) showed significant differences in variance between oak and pine, with no significant differences between sampling designs within a forest type. For calcium, a significant variance difference between forest types was observed under k-means

sampling ( $p = 0.016$ ). Similarly, magnesium showed significantly different variance between oak and pine under both k-means ( $p = 0.008$ ) and random sampling ( $p = 0.017$ ). In the case of potassium (cmolc/kg) and manganese, significant differences in variance between forest types were found under both designs (k-means  $p < 0.001$  and  $p < 0.002$ ; random  $p = 0.017$  and  $p = 0.012$ , respectively), but no significant differences were detected between designs within either forest. Notably,  $H^+$  values in pine, where variance differed significantly between sampling designs, with greater heterogeneity under k-means ( $p = 0.007$ ). In contrast, no significant differences in variance were detected for total organic carbon (TOC), total nitrogen (TN), cation exchange capacity (CEC), iron, aluminium, or sodium—neither between forest types nor between sampling strategies which suggests consistency in these variables across both design and system (Supplementary Table 1).

Table 3: Mean (M), standard deviation (sd) and coefficient of variation (CV) for pH, Phosphate (mg/k100g), Phosphorus (mg/kg), Potassiumoxide (mg/100g), Potassium (mg/kg), Calcium (cmolc/kg), Magnesium (cmolc/kg), Potassium (cmolc/kg), Manganese (cmolc/kg), H value (cmolc/kg) in the oak and pine forest. For coupled kmeans-random observations (all), k-menas, and random observations. M and sd are expressed in the parameter unit, and CV is expressed in % variation around the mean. Significant p values ( $p < 0.05$ , Levene's test) are highlighted. \*CV of pH is not calculated because mathematically not correct, as pH does not have a true 0 value.

Parameter	Oak			Pine			p-value (oak-pine)	
	Mean	SD	CV	Mean	SD	CV		
pH	all	4.31	0.14	*	4.25	0.1	*	0.12
	k_means	4.31	0.15	*	4.25	0.12	*	0.65
	random	4.32	0.13	*	4.24	0.06	*	<b>0.02</b>
p-value (k_means - random)	0.79			<b>0.01</b>				
Phosphate	all	1.97	1.88	0.95	0.86	0.34	0.39	<b>0.00</b>
	k_means	1.75	1.3	0.74	0.76	0.32	0.42	<b>0.00</b>
	random	1.87	1.97	1.05	1.03	0.3	0.29	0.15
p-value (k_means - random)	0.79			0.84				
Phosphorus	all	17.64	8.02	0.45	12.92	1.4	0.11	<b>0.00</b>
	k_means	16.72	5.59	0.33	12.48	1.36	0.11	<b>0.00</b>
	random	17.23	8.52	0.49	13.69	1.18	0.09	0.14
p-value (k_means - random)	0.77			0.82				
Potassiumoxide	all	6.29	2.75	0.44	2.36	0.71	0.3	<b>0.00</b>
	k_means	6.42	2.94	0.46	2.3	0.78	0.34	<b>0.00</b>
	random	6.24	2.49	0.4	2.52	0.58	0.23	<b>0.01</b>
p-value (k_means - random)	0.56			0.62				
Potassium	all	52.23	22.78	0.44	19.62	6.02	0.31	<b>0.00</b>
	k_means	53.32	24.35	0.46	19.04	6.62	0.35	<b>0.00</b>
	random	51.69	20.49	0.4	21	4.81	0.23	<b>0.01</b>
p-value (k_means - random)	0.52			0.58				
Calcium	all	0.84	0.71	0.85	0.59	0.27	0.47	<b>0.02</b>
	k_means	0.91	0.87	0.95	0.54	0.27	0.5	<b>0.02</b>
	random	0.71	0.3	0.42	0.69	0.27	0.39	0.53
p-value (k_means - random)	0.1			0.88				
Magnesium	all	0.35	0.24	0.68	0.16	0.06	0.35	<b>0.00</b>
	k_means	0.37	0.28	0.76	0.16	0.06	0.39	<b>0.01</b>
	random	0.33	0.13	0.41	0.17	0.05	0.26	<b>0.03</b>
p-value (k_means - random)	0.23			0.2				
Potassium_cmolc	all	0.17	0.07	0.41	0.06	0.02	0.36	<b>0.00</b>
	k_means	0.18	0.07	0.41	0.05	0.02	0.4	<b>0.00</b>
	random	0.16	0.06	0.39	0.06	0.02	0.28	<b>0.02</b>
p-value (k_means - random)	0.64			0.84				
Manganese	all	0.14	0.1	0.67	0.02	0.01	0.54	<b>0.00</b>
	k_means	0.14	0.1	0.69	0.02	0.01	0.55	<b>0.00</b>
	random	0.14	0.1	0.68	0.02	0.01	0.54	<b>0.01</b>
p-value (k_means - random)	0.98			0.72				
H_value	all	0.09	0.02	0.23	0.11	0.02	0.19	0.58
	k_means	0.09	0.02	0.24	0.11	0.03	0.23	0.17
	random	0.09	0.02	0.23	0.12	0.01	0.11	0.22
p-value (k_means - random)	0.99			<b>0.01</b>				

### **3.2 Biodiversity Assessment**

#### *Exploration of Abundance and Richness on the Morphology-based approach*

An analysis of the macrofauna community in the Oak and Pine forests reveals notable differences in abundance but similar levels of taxonomic richness across the sampled locations. In the Oak forest, the abundance of macrofauna across the 39 samples ranged from a minimum of 5 to a maximum of 428 individuals (Figure 11A). The median abundance was 46, with 50% of the samples containing between 29 and 64.5 individuals (the interquartile range). The mean abundance for the Oak forest was calculated to be 62.77. The specific LUCAS sample for the Oak forest recorded an abundance of 41 individuals, which falls near the median of the broader sample set. In terms of taxonomic richness (Figure 11B), the number of different taxonomic groups per sample varied from 4 to 10, with a median of 6 and a mean of 5.74. The LUCAS sample had a richness of 7, which is slightly above the mean and median for the Oak forest. In the Pine forest, the macrofauna abundance in the 39 samples ranged from 12 to 73 individuals (Figure 11A). The median abundance was 38, and the interquartile range was between 30 and 50.5. The mean abundance in the Pine forest was 39.41, substantially lower than that observed in the Oak forest. The LUCAS sample for the Pine forest showed an abundance of 39, a value that aligns closely with both the mean and median of the other samples. Despite the lower abundance, the taxonomic richness in the Pine forest was very similar to the Oak forest (Figure 11B). The number of taxonomic groups ranged from 3 to 8, with a median of 6 and a mean of 5.80. The LUCAS sample's richness was 6, matching the median and closely reflecting the mean richness for the Pine forest

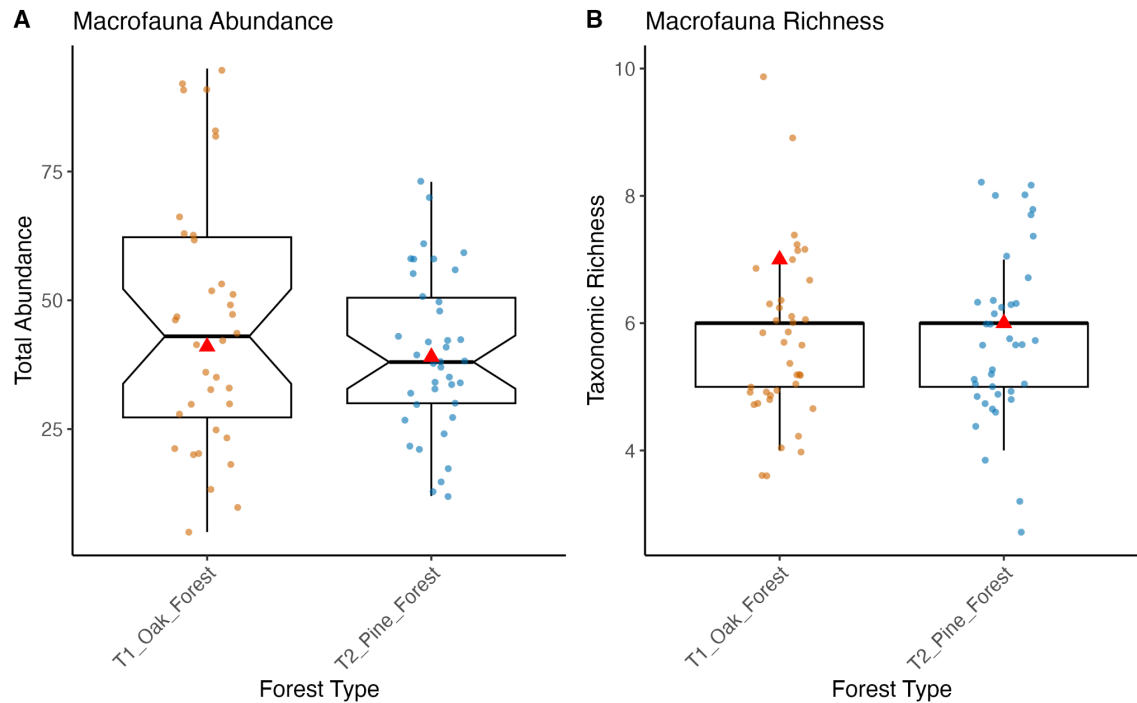


Figure 11: Box and whiskers plot (A) shows the abundance distribution and (B) shows the total taxonomic richness distribution collected from the Oak forest with observation points of each sample (orange) and Pine forest with observation points of each sample (blue). Red triangles represent LUCAS observation at each system.

An analysis of the taxonomic composition of macrofauna in the oak forest and the pine forest revealed distinct differences in the abundance of various groups (Figure 12). The total average abundance of macrofauna was higher in the Oak forest ( $49.22 \pm 63.85$ ) compared to the Pine forest ( $39.41 \pm 30.98$ ). The most dominant taxonomic group in the Oak forest was Hymenoptera, with a mean abundance of  $31.72 \pm 64.59$ . This was followed by Araneae with an abundance of  $17.21 \pm 20.10$  and Coleoptera with  $7.33 \pm 6.17$ . Several taxonomic groups, including Dermaptera, Embioptera, Opiliones, and Scorpiones, were not observed in the Oak forest samples. In the T2 Pine forest, the most abundant group was Coleoptera, with a mean abundance of  $15.26 \pm 10.17$ , which was notably higher than in the Oak forest. The next most abundant group was Hymenoptera with a mean of  $13.28 \pm 9.99$ , followed by Araneae with a much lower abundance of  $4.77 \pm 2.31$  compared to the Oak forest. Diplopoda, Pseudoscorpiones, and Scorpiones were absent from the Pine forest samples. Some taxonomic groups showed comparable abundance in both forest types, including Larvae ( $2.05 \pm 1.97$  in Oak forest;  $2.10 \pm 2.16$  in Pine forest) and Hemiptera ( $1.62 \pm 1.84$  in Oak forest;  $1.82 \pm 1.70$  in Pine forest). In contrast, groups like Isopoda were more prevalent in the Oak forest ( $0.23 \pm 0.43$ ) than in the Pine forest ( $0.03 \pm 0.16$ ), while Archaeognatha was more common in the Pine forest ( $0.92 \pm 1.91$ ) than in the Oak forest ( $0.03 \pm 0.16$ ).

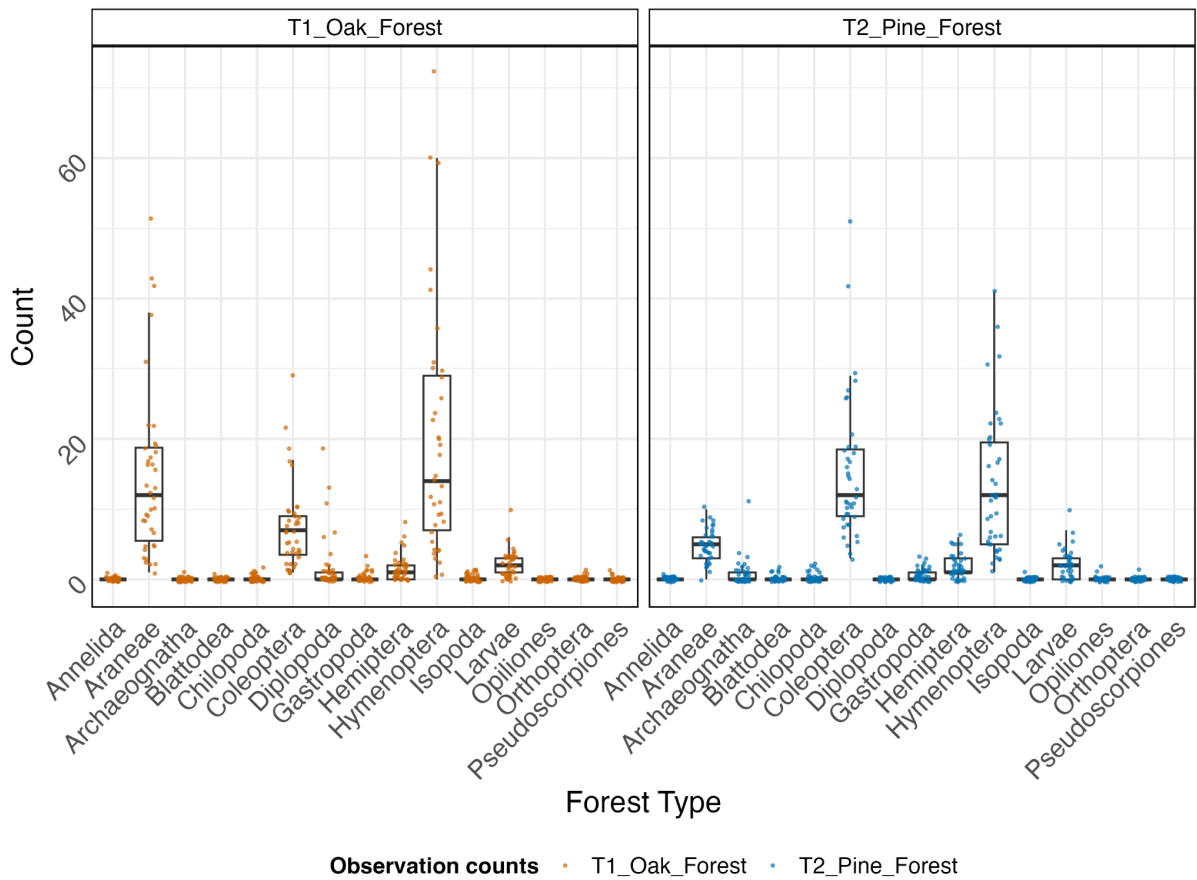


Figure 12: Boxplots showing the absolute counts of macrofauna taxonomic groups collected from the T1 Oak forest (orange) and T2 Pine forest (blue). The line within each box represents the median, the box boundaries represent the 25th and 75th percentiles, and the whiskers extend to 1.5 times the interquartile range. Individual points represent the counts from each individual sample. Outliers from the oak forest datasets, including Araneae count of 115 individuals and two Hymenoptera counts of 111 and 400 individuals ,were removed to improve visual clarity.

The abundances of individual taxonomic groups were compared between the oak and pine forest (Figure 13). The analysis showed significant differences for five of the fifteen taxonomic groups. Specifically, the abundance of Araneae, Diplopoda, and Isopoda was significantly higher in the Oak forest ( $p.\text{adj} < 0.05$ ). Conversely, the Pine forest supported a significantly higher abundance of Coleoptera and Archaeognatha ( $p.\text{adj} < 0.0001$ ) (Supplementary Table 2).

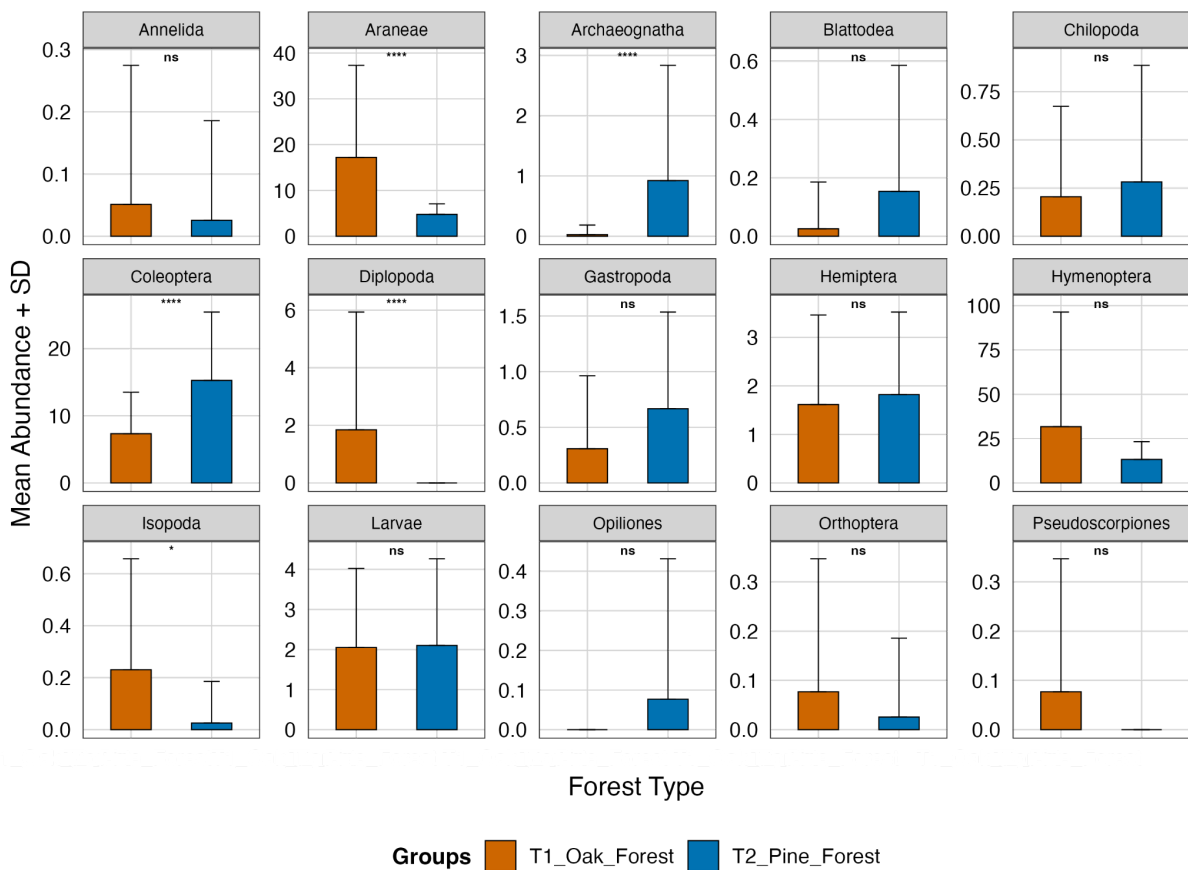


Figure 13: Comparison of mean macrofauna abundance between T1 Oak forest and T2 Pine forest. Each panel shows the mean abundance (+SD) for a specific taxonomic group. Statistical significance between the two forest types was determined by a Welch's t-test or Mann-Whitney U test with significance levels denoted as: ns = not significant; \* =  $p < 0.05$ ; \*\*\*\* =  $p < 0.0001$ .

#### *Exploration of OTU Richness and Morphological Abundance*

From the 78 samples sequenced, a total of 10,829,219 reads were generated, corresponding to 1,989 molecular operational taxonomic units (OTUs). After filtering for the target group, 604 OTUs, representing 8,037,146 reads, were identified as soil macrofauna. These target OTUs were classified into seven classes and 21 orders. The average number of reads per sample library for the target macrofauna was 103,040.3 ( $\pm 109,572.2$  SD) (Figure 14A).

The traditional morphological identification of specimens from the 78 samples resulted in the enumeration of 3,985 individuals. These were assigned to 14 distinct taxonomic groups, plus a separate "larvae" category. The average abundance per sample, based on morphological counts, was 51.05 individuals ( $\pm 53.17$  SD) (Figure 14B).

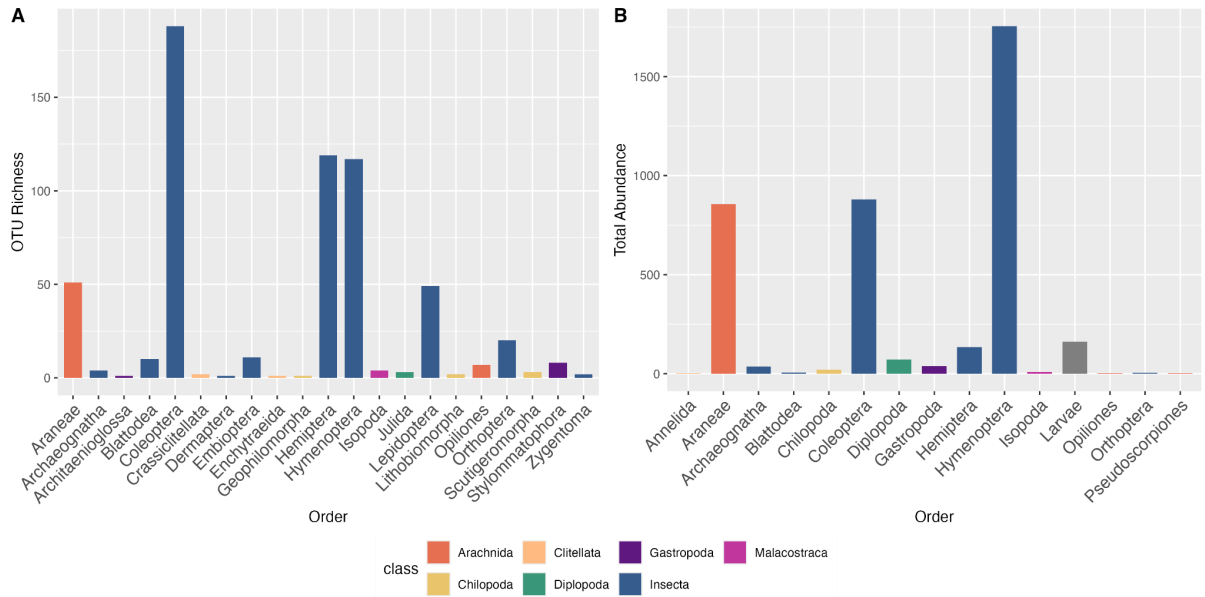


Figure 14: Comparison of taxonomic composition based on (A) molecular OTU richness and highlights that the insect orders (blue bars) are the most diverse in terms of unique OTUs (B) morphological total abundance. It shows that while Hymenoptera is the most numerically abundant order, Araneae also represent a major component of the community in terms of individual counts. Bars show the distribution of diversity and abundance across taxonomic orders, which are colored by class. Colors represent macrofauna taxonomic classes: Arachnida are shown in terracotta red, Insecta in deep slate blue, Malacostraca in magenta pink, Gastropoda in dark plum purple, Chilopoda in muted golden yellow, and Diplopoda in forest green. These color assignments facilitate visual differentiation of macrofauna groups across sampling plots.

The Oak forest accounted for 406 of the macrofauna OTUs from a total of 2,987,926 reads. The average number of reads per PCR in the Oak forest samples was  $76,613.49 \pm 72,274.63$  SD). Accounting for 7 classes and 20 orders (Figure 15A).

The highest mean read count was attributed to Coleoptera ( $31,176.26 \pm 54,104.26$  SD), followed by Araneae ( $12,901.49 \pm 25,337.96$  SD) and Myriapoda ( $11,602.23 \pm 33,827.26$  SD). Other taxa with high mean read counts included Julida ( $9,349.74 \pm 31,484.24$  SD) and Hymenoptera ( $8,375.41 \pm 25,304.78$  SD). Taxa with the lowest read abundance included Dermaptera ( $0.13 \pm 0.57$  SD) and Zygentoma ( $0.18 \pm 0.85$  SD). The total number of reads across all samples was highest for Coleoptera (1,215,874), followed by Araneae (503,158) and Myriapoda (452,487) (Figure 15A).

The morphological analysis of the same 39 samples resulted in the identification of 2,448 individuals from the target macrofauna groups. These individuals were classified into 13 distinct taxonomic groups, in addition to a "larvae" category. The mean abundance per

sample in the Oak forest, based on these direct counts, was 62.77 individuals ( $\pm$  72.29 SD)(Figure 15B).

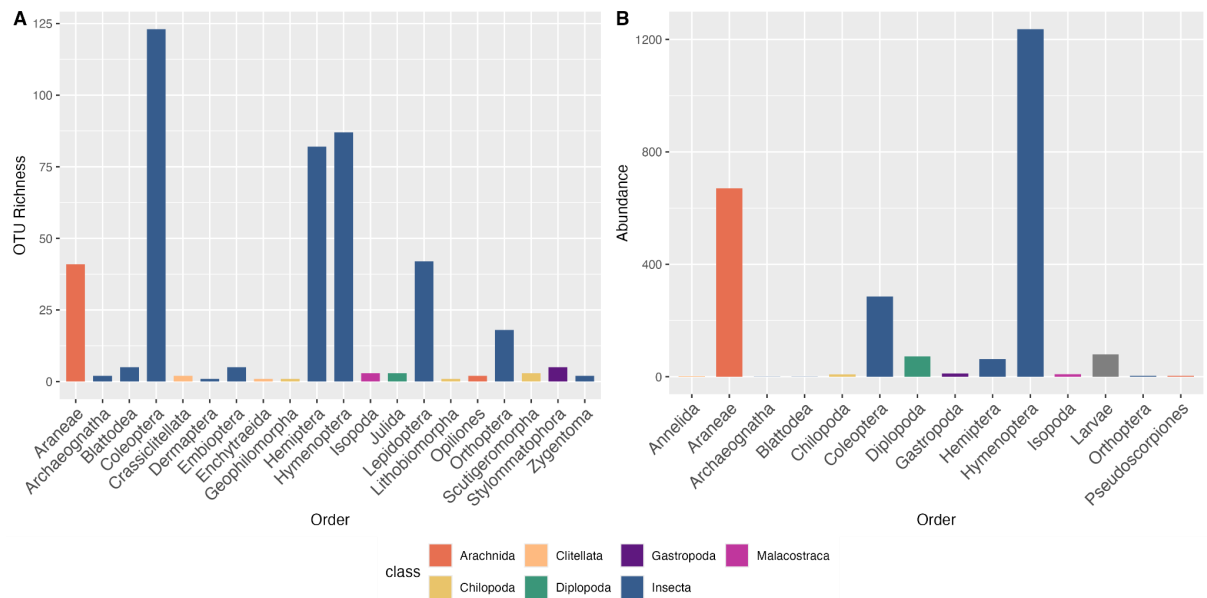


Figure 15: Comparison of taxonomic composition in the Oak forest based on (A) molecular OTU richness indicates that Coleoptera represent the most diverse order in terms of unique OTUs. (B) morphological total abundance. Demonstrates that Hymenoptera are the most numerically abundant group, with Araneae also being a major component of the community based on individual counts. Bars show the distribution of diversity and abundance across taxonomic orders. Colors represent macrofaunal taxonomic classes: Arachnida are shown in terracotta red, Insecta in deep slate blue, Malacostraca in magenta pink, Gastropoda in dark plum purple, Chilopoda in muted golden yellow, and Diplopoda in forest green. These color assignments facilitate visual differentiation of macrofaunal groups across sampling plots.

The Pine forest yielded 372 macrofauna OTUs from a significantly higher number of reads (5,049,220). The average reads per PCR in the Pine forest was identical to the Oak forest at 76,613.49 ( $\pm$  72,274.63 SD). Figure 16A provides a detailed summary of the OTU richness for each identified taxonomic order. Accounting for 6 classes and 17 orders.

The highest mean read count was attributed to Coleoptera ( $86,153.67 \pm 96,427.74$  SD), which also accounted for the highest total reads (3,359,993). This was followed by Hymenoptera ( $17,789.23 \pm 43,118.27$  SD), Hemiptera ( $9,345.87 \pm 19,144.73$  SD), and Araneae ( $7,214.74 \pm 16,467.85$  SD). In contrast to the Oak forest, Archaeognatha also showed a high mean read count ( $4,760.44 \pm 16,525.05$  SD). Several taxa had very low read counts, including Julida ( $0.26 \pm 1.60$  SD), Isopoda ( $0.31 \pm 1.42$  SD), Embioptera ( $0.51 \pm 1.52$  SD), and Architaenioglossa ( $0.74 \pm 4.64$  SD).

Morphological identification yielded a total of 1,494 individuals. These specimens were assigned to 12 distinct taxonomic groups and a "larvae" category, indicating a slightly lower taxonomic richness at this level compared to the Oak forest. The mean abundance per sample was 39.32 individuals ( $\pm 15.54$  SD)(Figure 16B).

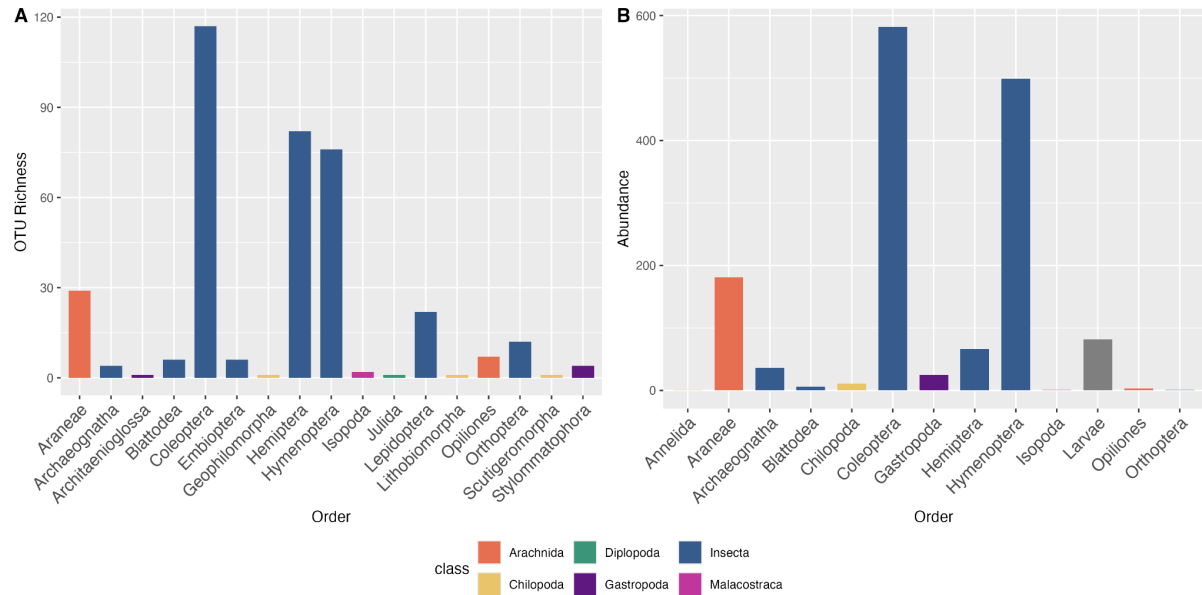


Figure 16: Comparison of taxonomic composition in the Pine forest based on (A) molecular OTU richness. The plot indicates that Coleoptera represents the most diverse order in terms of unique OTUs. (B) morphological total abundance which demonstrates that Coleoptera are also the most numerically abundant group, followed closely by Hymenoptera. Bars show the distribution of diversity and abundance across taxonomic orders. Colors represent macrofaunal taxonomic classes: Arachnida are shown in terracotta red, Insecta in deep slate blue, Malacostraca in magenta pink, Gastropoda in dark plum purple, Chilopoda in muted golden yellow, and Diplopoda in forest green. These color assignments facilitate visual differentiation of macrofaunal groups across sampling plots.

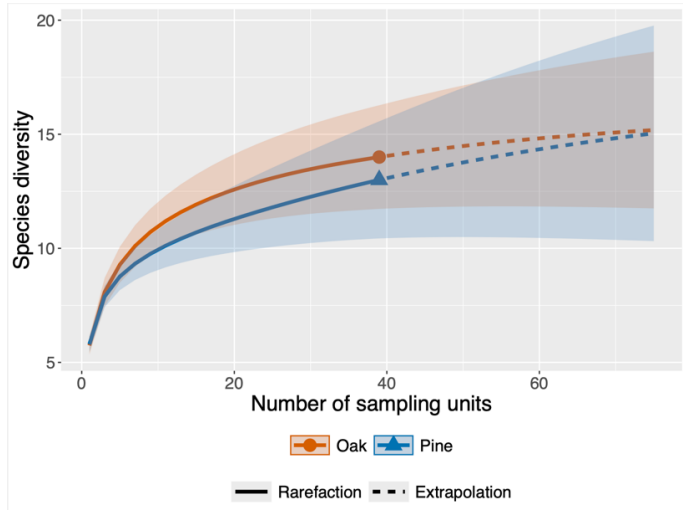
#### *Assessment of Alpha Diversity*

Analysis of sample-based rarefaction and extrapolation curves indicated that, despite slight visual differences in mean diversity estimates, the 95% confidence intervals largely overlapped across forest types (Figure 17A,B,C). This overlap suggests that there are no statistically significant differences in alpha diversity between oak and pine forests. This analysis is further supported by Wilcoxon rank sum tests, which revealed no significant differences in species richness ( $p = 0.67$ ), Shannon diversity ( $p = 0.53$ ), Simpson diversity ( $p = 0.59$ ), or Pielou's evenness ( $p = 0.30$ ).

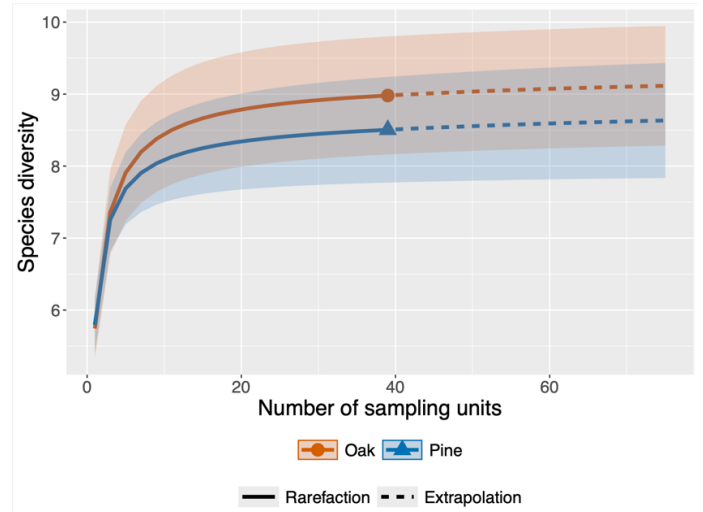
Extrapolation curves (Figure 17D) confirmed that the sampling effort was highly sufficient in both systems. The curves for both forest types rose steeply before reaching a clear asymptote

at a sample coverage value approaching 1.0. This indicates that the vast majority of the local taxonomic diversity was captured. Although the pine forest assemblage appeared to reach a high level of coverage with slightly fewer sampling units, the overlapping 95% confidence intervals at their respective asymptotes show no significant difference in the overall sampling completeness achieved between the two forest ecosystems.

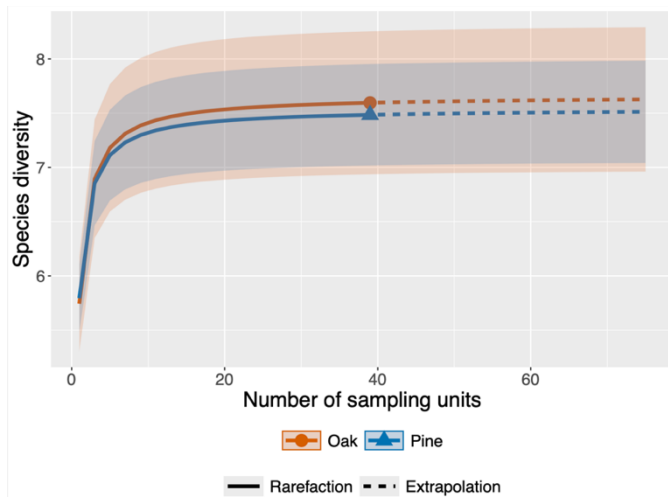
**A**



**B**



**C**



**D**

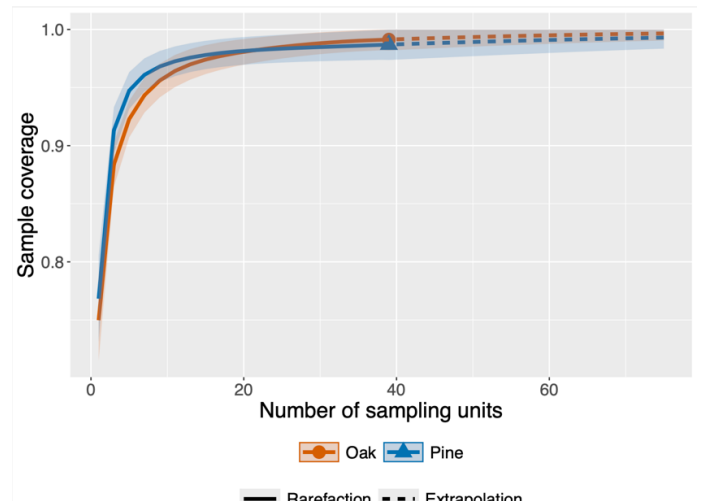


Figure 17: Sample-size-based rarefaction and extrapolation curves for macrofauna diversity in the Oak (orange) and Pine (blue) forests. Panels show the diversity estimates for Hill numbers of order: (A)  $q=0$  (species richness), (B)  $q=1$  (exponential of Shannon's entropy), and (C)  $q=2$  (inverse Simpson index). Panel (D) shows the corresponding sample coverage for each forest type. Solid lines

represent rarefaction (interpolation), while dashed lines represent extrapolation up to double the sample size. Shaded areas denote the 95% confidence intervals. The solid points mark the observed diversity and sample size for each forest.

### *Community Structure based on Morphological Diversity*

The analysis of the macrofauna community structure showed a clear separation between the two forest systems as visible in the NMDS plot (stress value = 0.201) (Figure 18). This is statistically confirmed by a perMANOVA (999 permutations). The results underline that the type of forest has a significant effect on community composition ( $F = 7.9764, p = 0.001$ ). This factor explained 9.5% of the variation in the community structure ( $R^2 = 0.09498$ ).

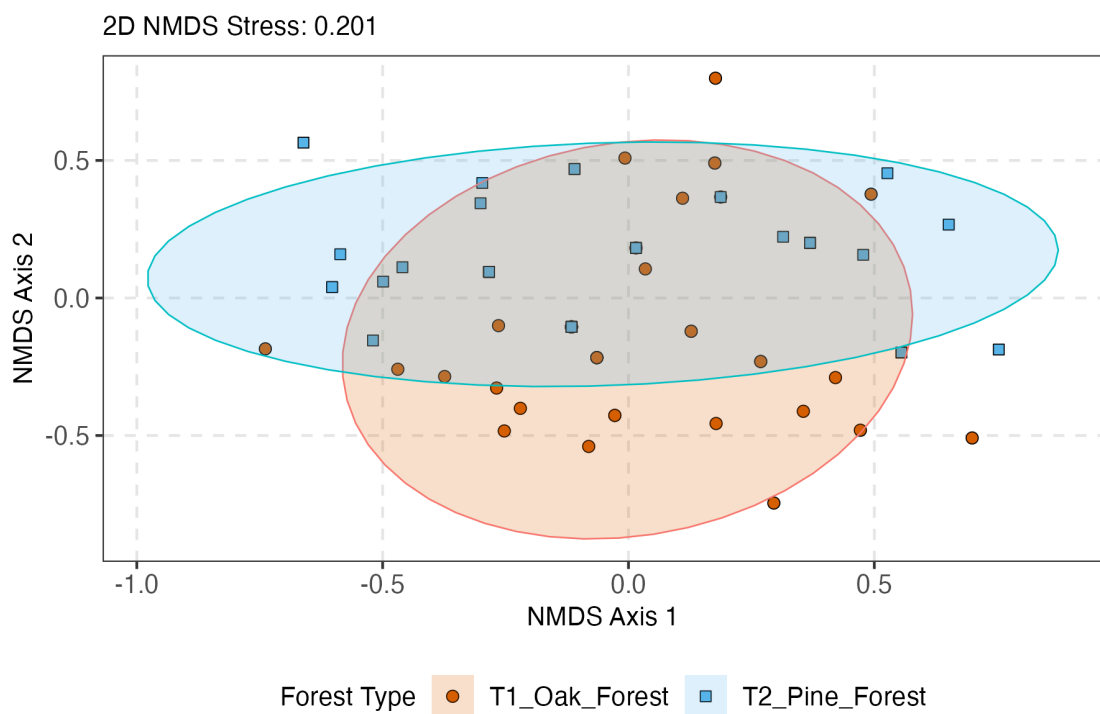


Figure 18: NMDS ordination illustrating the differences in macrofauna community composition between the Oak and Pine forests. The analysis was performed using a Jaccard dissimilarity matrix on morphological occurrence data. Each point corresponds to a single sample and is colored according to its forest type (orange for oak, blue for pine). The shaded ellipses represent the 95% confidence intervals around the group centroids. Ordination stress = 0.201.

### *Community Structure based on Molecular Diversity*

The overall macrofauna community structure, as determined by the sequencing data, was significantly different between the Oak and Pine forests. PerMANOVA confirmed that forest

type had a significant effect on community composition (perMANOVA:  $R^2 = 0.082$ ,  $p = 0.001$ ). The 'Forest Type' factor explained 8.2% of the variation in the macrofauna community, while the remaining 91.8% was attributed to residual, unexplained variance.

This significant separation between the two habitats is visualized in the Non-Metric Multidimensional Scaling (NMDS) ordination plot (Figure 19). The plot shows a distinct clustering of samples according to their forest of origin..

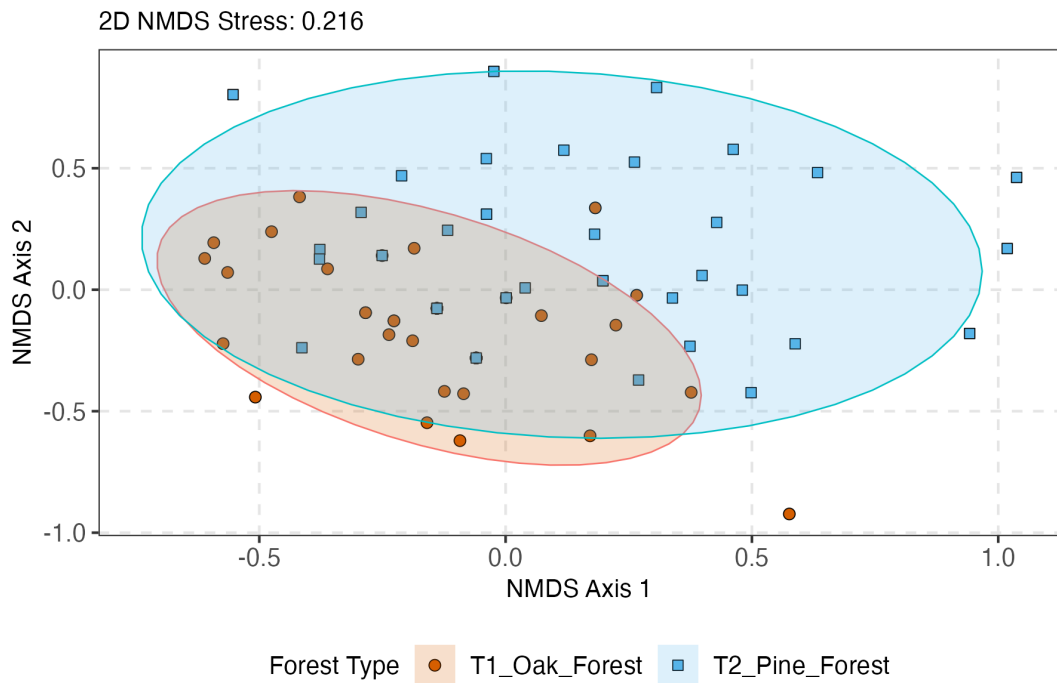


Figure 19: NMDS ordination illustrating the differences in macrofauna community composition between the Oak and Pine forests. The analysis was performed using a Jaccard dissimilarity matrix on molecular presence/absence data. Each point corresponds to a single sample and is colored according to its forest type (orange for Oak, blue for Pine). The shaded ellipses represent the 95% confidence intervals around the group centroids. Ordination stress = 0.216.

#### Beta diversity partitioning

The beta diversity partitioning revealed a consistent pattern across both forest types and both analytical methodologies (Table 4). The overall multiple-site beta diversity ( $\beta_{jac}$ ) was exceptionally high in all four scenarios, indicating substantial community variation within each system.

This level of community differentiation was driven by the species turnover component ( $\beta_{jtu}$ ). In contrast, the contribution from the nestedness component ( $\beta_{jne}$ ) was negligible in all cases.

Table 4: Results of the beta diversity partitioning for the Morphological and Metabarcoding datasets within the Oak and Pine forest systems. Values represent the total multiple-site dissimilarity ( $\beta_{jac}$ ) and its turnover ( $\beta_{jtu}$ ) and nestedness-resultant ( $\beta_{jne}$ ) components.

<b>Dataset</b>	<b>System</b>	<b>Total Beta (<math>\beta_{jac}</math>)</b>	<b>Turnover (<math>\beta_{jtu}</math>)</b>	<b>Nestedness (<math>\beta_{jtu}</math>)</b>
Morphology	Oak	0.91	0.843	0.068
Metabarcoding	Oak	0.903	0.821	0.082
Morphology	Pine	0.901	0.81	0.092
Metabarcoding	Pine	0.922	0.852	0.07

Furthermore, the assessment of spatial correlation of community composition patterns between morphological and molecular identification methods, revealed a difference between the two methodologies depending on the forest system. In the Pine system, the Mantel test showed a significant positive correlation between morphological and molecular community dissimilarities (Mantel's  $r = 0.161, p = 0.033$ ). In the Oak system, no significant correlation was found (Mantel's  $r = -0.061, p = 0.736$ ). The correlation coefficient was close to zero, indicating a statistical independence between the community structures captured by the two methods.

### 3.3 Analysis of Chemical Soil Parameters

#### *Exploratory Analyses of Chemical Variables*

Boxplot analyses revealed distinct patterns in soil chemical profiles between forest types. Oak forest soils exhibited greater chemical heterogeneity, characterized by broader distributions and a higher frequency of outliers across multiple chemical variables (Figure 20), while Pine forest soils displayed a more constrained and homogeneous profile. These visual trends were supported by statistical analyses, which identified significant differences between forest types for nearly all measured parameters, with the exception of calcium ( $p =$

0.19) (Supplementary Table 3). Pine forest soils showed significantly higher concentrations of total organic carbon (TOC) and total nitrogen (TN), corresponding with elevated cation exchange capacity (CEC) and hydrogen ion ( $H^+$ ) concentrations. In contrast, Oak forest soils exhibited significantly higher pH and greater median concentrations of magnesium, manganese, and all three measured forms of potassium. Aluminium concentrations were significantly higher in the more acidic Pine forest soils. LUCA's observations generally aligned with the observed distributions: in Oak forest soils, values for aluminium, calcium, CEC, manganese, sodium, iron, and TOC fell within the interquartile range, while values for  $H^+$ , magnesium, pH, phosphate, phosphorus, TN, and all potassium forms fell outside. In Pine forest soils, LUCA's values for aluminium, calcium, CEC,  $H^+$ , iron, magnesium, manganese, phosphorus, sodium, TN, and all potassium forms were within the interquartile range, whereas phosphate, TOC, and pH were outside.

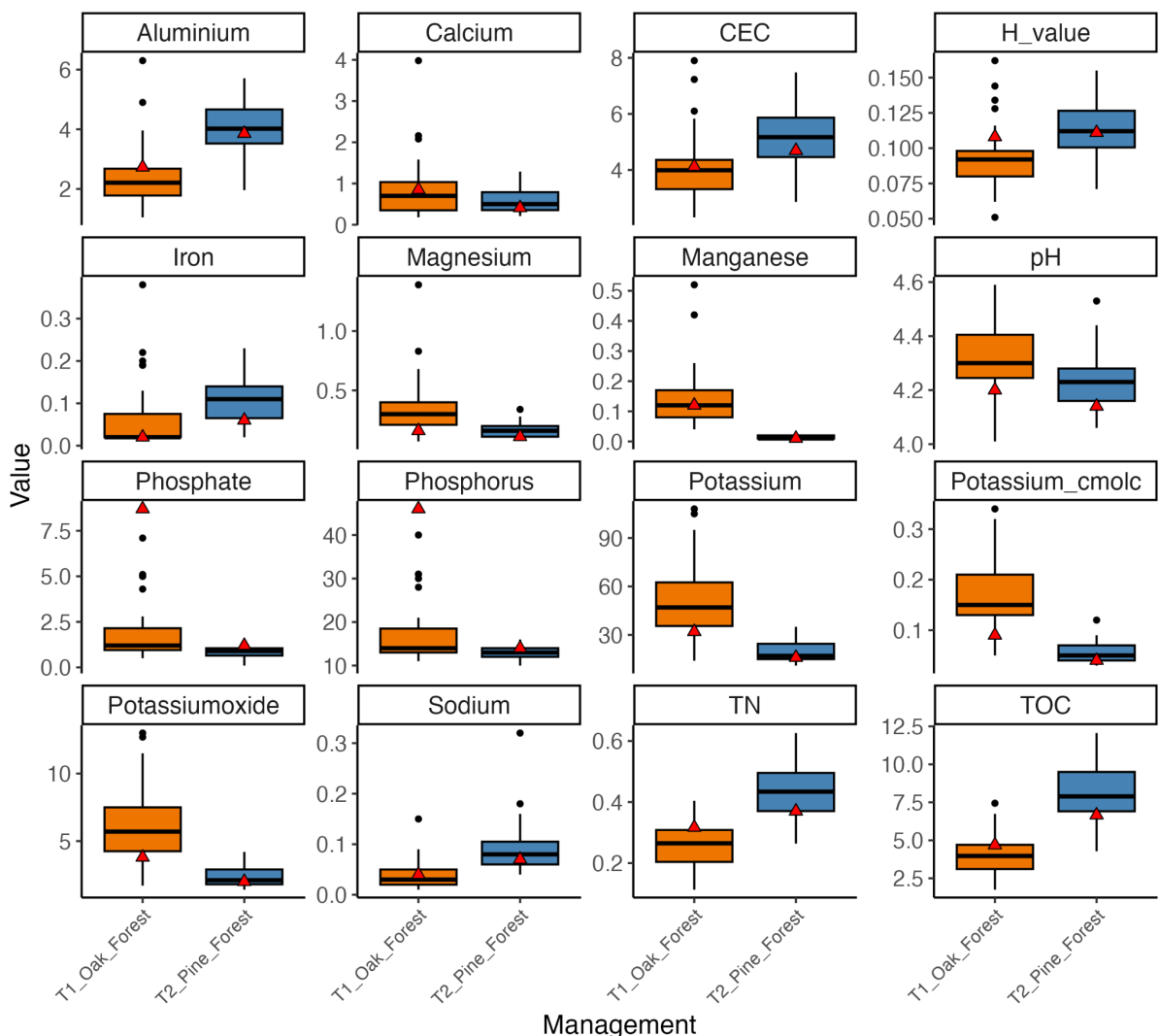


Figure 20: Boxplots illustrating the variation in soil chemical properties between Oak (orange) and Pine (blue) forest soils. Displayed variables include total organic carbon (TOC), total nitrogen (TN), cation exchange capacity (CEC), hydrogen ion concentration ( $H^+$ ), pH, calcium (Ca), magnesium (Mg), manganese (Mn), aluminium (Al), iron (Fe), sodium (Na), phosphorus (P), phosphate ( $PO_4^{3-}$ ), and three potassium-related measures: total potassium (K), potassium oxide ( $K_2O$ ), and exchangeable potassium (Potassium, cmol/kg). Red triangles indicate values recorded at the LUCAS sampling point for each respective variable.

An initial correlation analysis revealed strong relationships between several variables. In the Oak forest, a strong inter-correlation was identified among a group of variables that included pH, Aluminium, Magnesium, Potassium oxide, Potassium, Total Organic Carbon (TOC), and Phosphorus (Figure 21A). Consequently, Aluminium, Potassium oxide, Potassium (cmolc), and the H-value were excluded from the final Oak forest variable set. Similarly, in the Pine forest, high correlations were observed among Cation Exchange Capacity (CEC), TOC, Aluminium, H-value, multiple forms of Potassium, and Phosphate (Figure 21B). Based on these relationships, several variables were removed to ensure independence: Aluminium was excluded due to its strong correlation with multiple other key parameters (e.g., CEC, TOC, and pH); Potassium oxide and Potassium (cmolc) were removed for redundancy with the primary Potassium measurement; and Phosphate and the H-value were also excluded from the final Pine forest variable set. This process resulted in two distinct sets of largely independent environmental variables for subsequent analysis of each habitat.

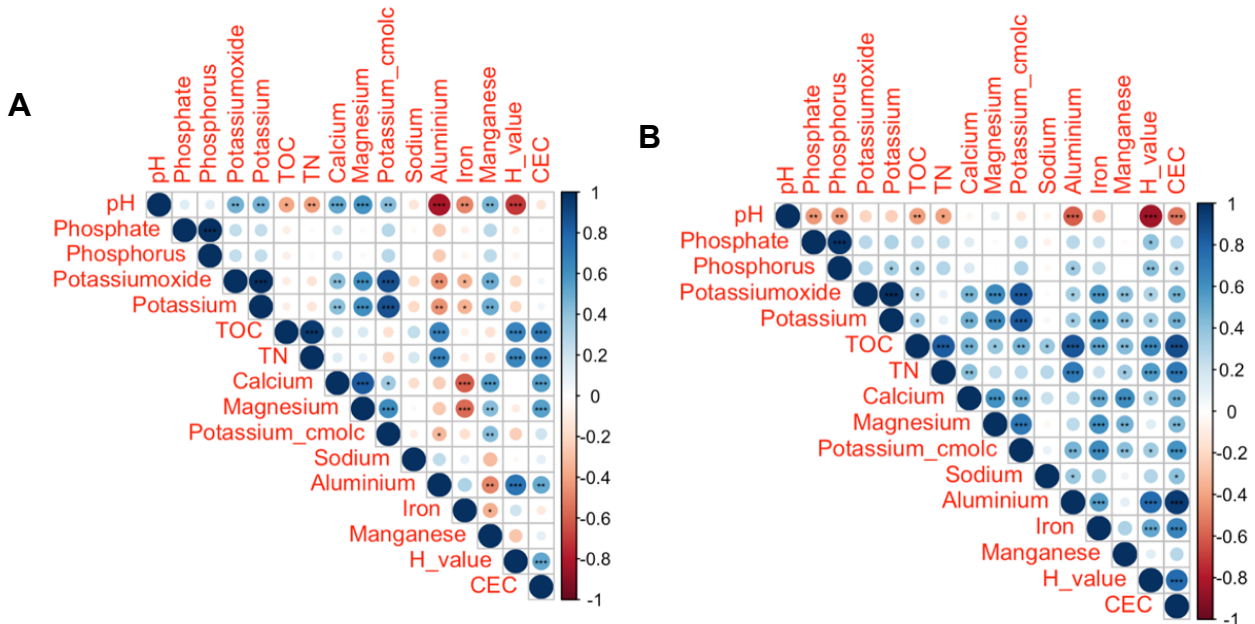


Figure 21: Spearman correlation matrices of soil chemical properties in (A) Oak forest and (B) Pine forest habitats. Each plot displays pairwise correlation coefficients among all measured soil parameters. The color and size of the circles represent the strength and direction of the correlations,

with dark blue indicating strong positive correlations and dark red indicating strong negative correlations. Correlations that are not statistically significant ( $p > 0.05$ ) are omitted from the plots. These matrices were used to inform variable selection by identifying and excluding highly collinear parameters ( $|r| > 0.7$ ) to retain a final set of independent soil variables for subsequent analyses.

To visualize the nature of measured chemical variables, a Principal Component Analysis (PCA) was performed. The first two principal components collectively explained 67.4% of the variance in the dataset (PC1 = 43.1%, PC2 = 24.3%) and clearly separated the two groups (Figure 22). The primary axis of variation, PC1, was driven by a contrast between soil nutrients and organic content. It was strongly positively correlated with pH (0.42), Potassium (0.44), and Phosphorus (0.26), and strongly negatively correlated with Total Organic Carbon (TOC) (-0.47) and Iron (-0.41). This axis effectively separated the Oak forest samples, which aligned with higher pH and nutrient values, from the Pine forest samples, which were associated with higher organic carbon. The second principal component (PC2) represented a secondary axis of variation, defined largely by strong negative loadings from Calcium (-0.62) and Cation Exchange Capacity (CEC) (-0.59). Furthermore, the PCA biplot highlighted a marked difference in chemical heterogeneity; the widely dispersed Oak forest samples indicated greater overall variability in soil chemistry compared to the tightly clustered and more homogeneous Pine forest samples. A perMANOVA confirmed the significant difference in the overall soil chemical environment between the two forest types, with the management type explaining 24.2% of the total variance ( $R^2 = 0.24$ ,  $F = 24.31$ ,  $p = 0.001$ ).

PCA - Biplot

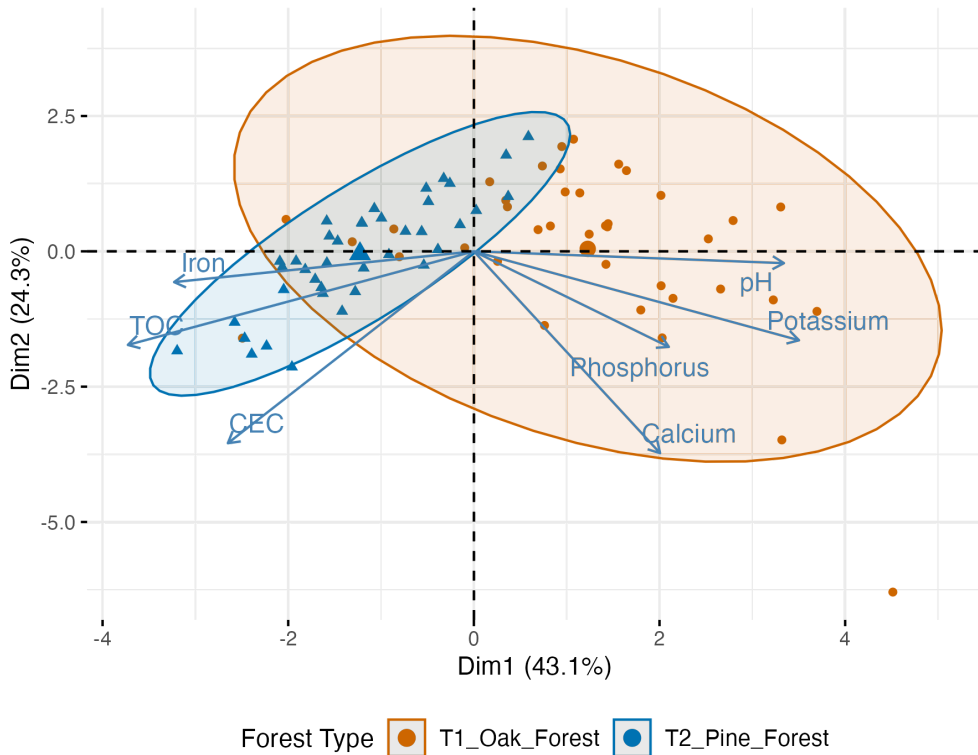


Figure 22: Principal Component Analysis (PCA) of soil chemical variables from Oak (orange) and Pine (blue) forest samples. Environmental variables are shown as blue vectors. The first two components are displayed and explain 67.4% of the total variance (PC1 = 43.1%, PC2 = 24.3%).

The PCA of the Oak forest's environmental data revealed two primary axes of variation, which together explained (55 %) of the total variance (Figure 23A). The first principal component (PC1), accounting for (37.3%) of the variance, described a strong gradient separating samples with high pH on the right side of the axis from those with higher concentrations of Total Organic Carbon (TOC), Sodium, and Iron on the left. The second principal component (PC2), which explained (17.7%) of the variance, was primarily defined by a contrast between high pH and Manganese concentrations in the positive direction and high Phosphate, Calcium, and TOC in the negative direction.

In the Pine forest, the first two principal components together accounted for ( 59.1%) of the total variance in the soil chemical data (Figure 23B). A very strong environmental gradient was evident along the first principal component (PC1, (41.9%) of variance). This axis clearly separated samples with high pH on the right from those on the left characterized by high concentrations of nutrients, including Total Nitrogen (TN), Phosphorus, TOC, Calcium, Potassium, Magnesium, and Iron. The second principal component (PC2, (17.2%) of

variance) described a secondary gradient, separating samples with higher concentrations of Magnesium and Manganese from those with higher Sodium and Phosphorus.

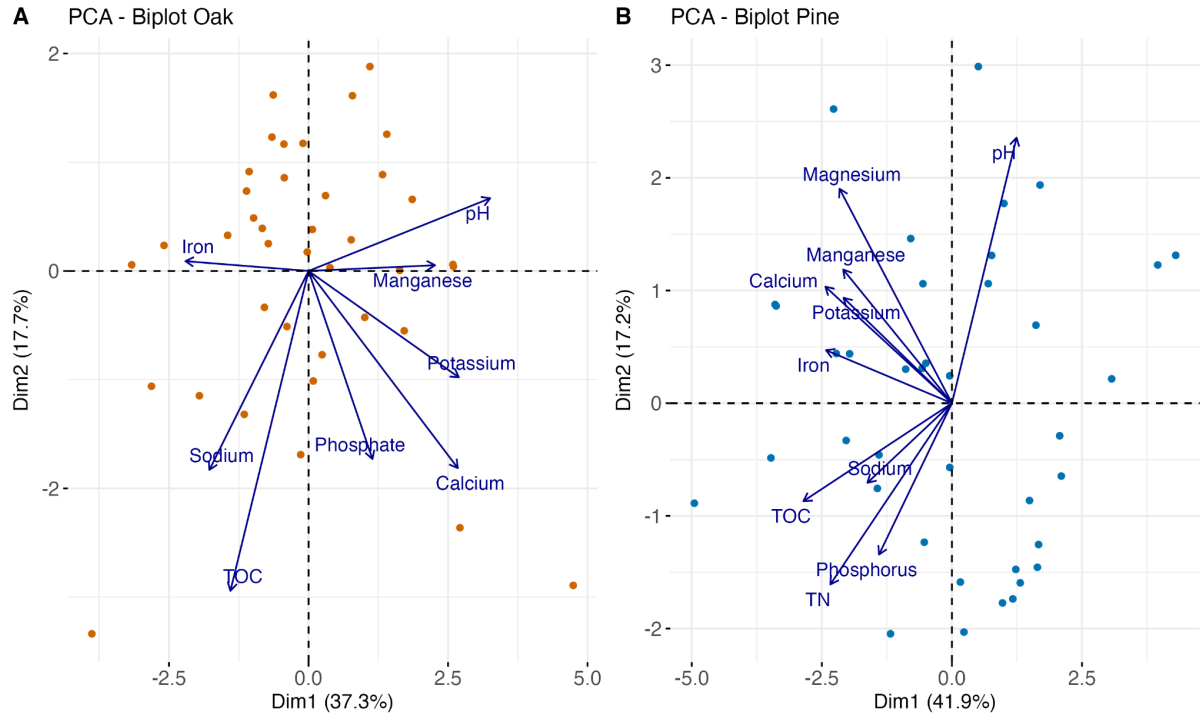


Figure 23: Principal Component Analysis (PCA) of soil chemical variables for the (A) Oak forest and (B) Pine forest. The plots illustrate the major axes of variation within the environmental data for each habitat. Individual soil samples are shown as points (orange for Oak, blue for Pine). The blue vectors represent the soil chemical variables; the direction and length of each vector indicate the variable's contribution to the first two principal components. The first two components (PC1 and PC2) are displayed, which together explain (55 %) of the total variance in the Oak forest data and (59.1%) of the variance in the Pine forest data.

### 3.4 Linking Community Structure to Chemical Soil Parameters

#### *Assessment based Morphological Taxonomic Occurrence*

The full model of distance-based Redundancy Analysis (db-RDA), that incorporated all selected chemical predictors, was found to be non-significant and explained only a negligible amount of the community variation (Adjusted  $R^2 = 0.03$ ). This conclusion was reinforced by a stepwise model selection procedure, which resulted in a final model containing only the intercept ( $\sim 1$ ). This indicates that no combination of the tested variables provided a better explanation of the community structure than a null model.

However, despite the overall model's lack of significance, an analysis of the marginal effects of each predictor when considered independently suggests that pH ( $p = 0.009$ ) and TOC ( $p = 0.03$ ) may have a weak but potential association with the macrofauna community.

A Non-metric Multidimensional Scaling (NMDS) ordination of the oak forest macrofauna presence absence revealed distinct community groupings in a reliable two-dimensional plot (stress = 0.13)(Figure 24) An “envfit” analysis was used this analysis revealed that none of the measured chemical variables had a statistically significant correlation with the community structure.

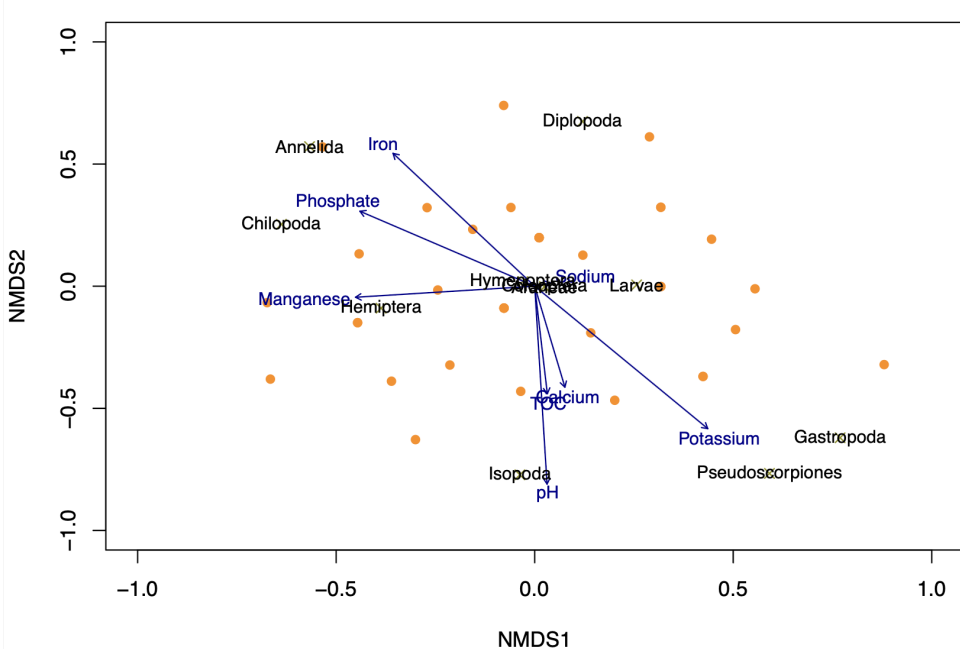


Figure 23: NMDS ordination biplot of the Oak forest morphological community (Stress = 0.16). The plot shows the distribution of sample sites (orange points), the relative positions of the dominant taxonomic groups (black text), and the correlation of environmental variables (blue vectors) with the ordination axes. The stress value of 0.16 indicates a good fit.

A distance-based Redundancy Analysis (db-RDA) with forward model selection (ordistep) was performed. The procedure was successful, identifying a significant model that explained 25% of the community variation ( $p = 0.001$ , Adjusted  $R^2 = 0.25$ ).

The final model included the predictor variables pH, TOC, and TN (Figure 25). When assessing the effect of each variable within the context of this model, both pH ( $p = 0.002$ ) and Total Nitrogen (TN,  $p = 0.015$ ) were found to have a significant independent influence on the community structure. The significance of the first constrained axis (RDA1,  $p = 0.002$ ) further

confirms that the model has successfully captured a meaningful gradient in the data that is directly related to these key chemical predictors.

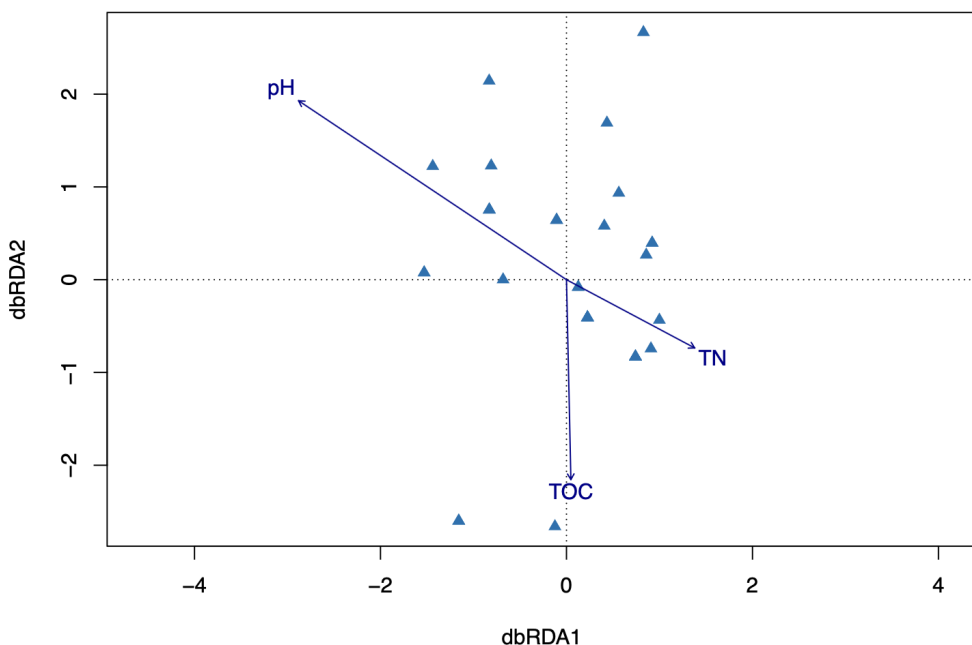


Figure 25: db-RDA ordination showing the influence of soil chemistry on the Pine forest morphological community composition. The plot displays the distribution of sample sites (blue triangles) along the primary axes of environmental variation defined by pH, Total Nitrogen (TN), and Total Organic Carbon (TOC). This constrained ordination visualizes the significant relationship between the soil environment and community structure (Overall model:  $p = 0.001$ , Adjusted  $R^2 = 0.25$ ).

#### *Assessment Through Molecular Taxonomic Occurrence*

In the Oak forest the forward selection procedure (“ordistep”) identified Total Organic Carbon (TOC) and Iron as the most influential environmental drivers of macrofauna community composition in the Oak forest (Figure 26). The resulting model was statistically significant ( $p = 0.024$ ) and explained 6.0% of the community variation (adjusted  $R^2 = 0.06$ ). Within this model, Iron was identified as the primary significant driver of community structure ( $p = 0.031$ ).

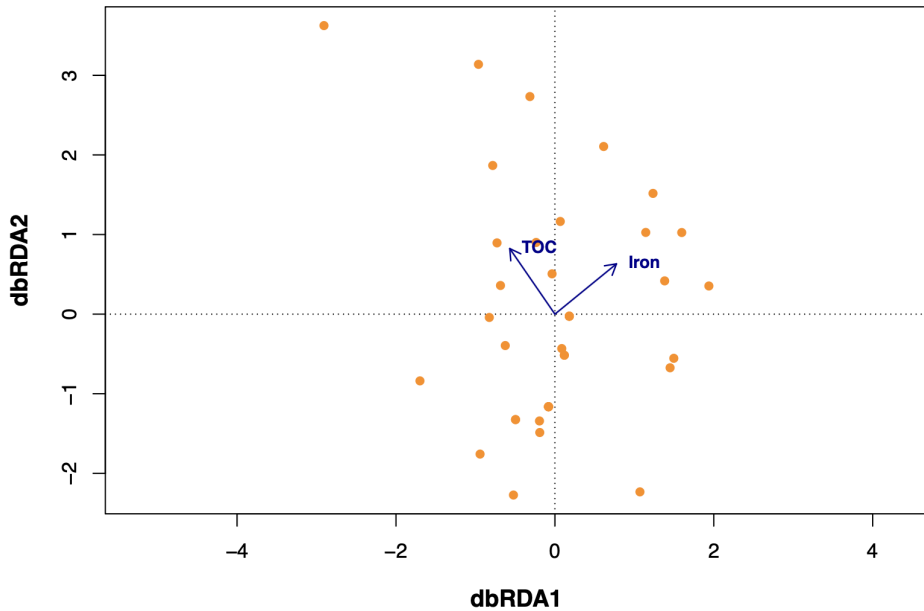


Figure 26: db-RDA ordination showing the influence of the most significant soil variables on the Oak forest molecular community composition. The plot displays the distribution of sample sites (orange points) along the two primary axes of environmental variation defined by Total Organic Carbon (TOC) and Iron. This constrained ordination visualizes the significant, but modest, relationship between the soil environment and community structure (Overall model:  $p = 0.024$ , Adjusted  $R^2 = 0.06$ ).

In the Pine forest, a distance-based redundancy analysis (db-RDA) was performed. The model tested the influence of five selected variables (“ordistep”) (Phosphorus, Total Nitrogen, Magnesium, Sodium, and Iron) on the Jaccard dissimilarity molecular presence-absence data (Figure 27). The overall model was highly significant ( $p = 0.001$ ) and explained approximately 15.6% of the total variation in community structure (adjusted  $R^2 = 0.156$ ). An ANOVA-like permutation test of the individual terms within the model revealed that Magnesium ( $p = 0.004$ ) and Iron ( $p = 0.009$ ) were the two highly significant predictors of OTU community composition. In contrast, Phosphorus, Total Nitrogen (TN), and Sodium did not have a statistically significant unique effect in the context of the full model.

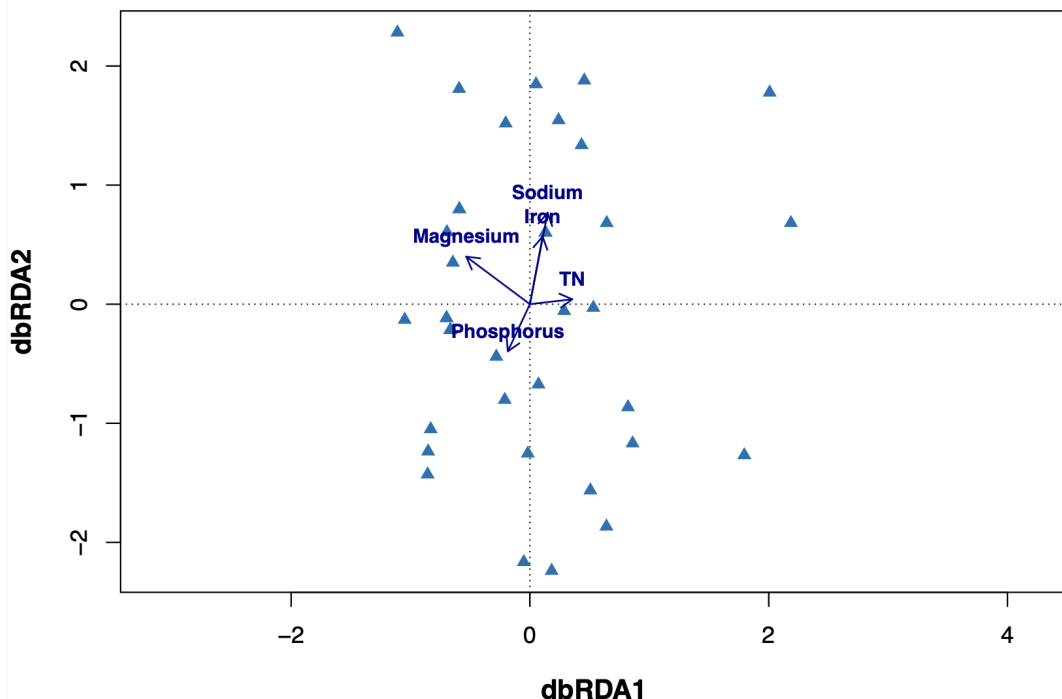


Figure 27: db-RDA ordination showing the influence of soil chemistry on the Pine forest molecular community composition. The plot displays the distribution of sample sites (blue triangles) along the primary axes of environmental variation defined by the predictor variables (blue vectors). This constrained ordination visualizes the significant relationship between the soil environment and community structure (Overall model:  $p = 0.001$ , Adjusted  $R^2 = 0.156$ ).

#### *Spatial Dependency of Community and Environmental Variables*

##### Morphological Assessment

In oak forest sites, a global Mantel test detected a significant positive correlation between spatial distance and community composition ( $\text{Mantel } r = 0.162, p = 0.009$ ), indicating that spatial distance is associated with community turnover. However, no significant global relationships were found between spatial distance and environmental variables ( $r = 0.070, p = 0.205$ ) (Supplementary Figure 3A), or between environment and community composition ( $r = 0.024, p = 0.390$ ) (Supplementary Figure 3B), suggesting that environmental factors do not broadly structure community patterns across space.

Mantel correlograms further revealed fine-scale spatial structuring of communities. Specifically, community composition showed significant positive spatial autocorrelation at the smallest distance class (~69 m), with a Mantel  $r$  of 0.167 ( $p = 0.002$ ) (Figure 28), indicating that communities closer together are more similar in composition. Weak or non-significant correlations at broader distances suggest that this spatial structure is not

consistent beyond local scales. In contrast, environmental variables showed only a marginally significant positive autocorrelation at approximately 69 m ( $p = 0.064$ ), and no spatial structure beyond that.

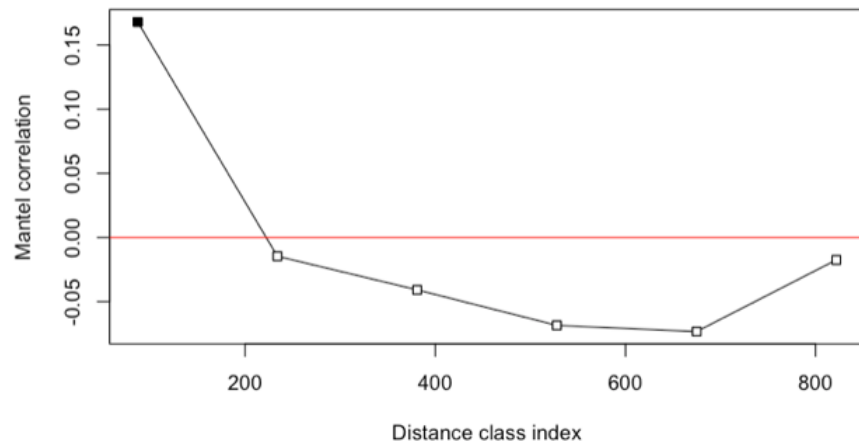


Figure 28: Mantel correlogram illustrating the spatial structure of the macrofauna community on morphology-based data from oak forest. The plot shows the correlation (Mantel  $r = 0.162$ ,  $p = 0.009$ ) between community similarity and geographic distance at increasing distance classes. The red line represents a correlation of zero. A significant positive autocorrelation (filled point) is evident only at the shortest distance class, demonstrating that the community is spatially structured at a local scale, with similarity decaying rapidly with distance.

In pine forest sites, Mantel tests revealed no significant global correlations between spatial distance and community composition (Mantel  $r = 0.077$ ,  $p = 0.108$ ) (Supplementary Figure 4), environmental variables (Mantel  $r = 0.059$ ,  $p = 0.191$ ), or between environment and community composition (Mantel  $r = 0.053$ ,  $p = 0.232$ ). However, Mantel correlograms revealed that environmental variables showed significant positive spatial autocorrelation at short distances (64 m) ( $p = 0.019$ ) (Figure 29A), but this structure dissipates beyond 170 m. Similarly, the relationship between community composition and environmental variables exhibited a significant positive autocorrelation at very fine scales (1.3 m) ( $p = 0.04$ ), and a significant negative autocorrelation at around 4.8m ( $p = 0.027$ ) (Figure 29B).

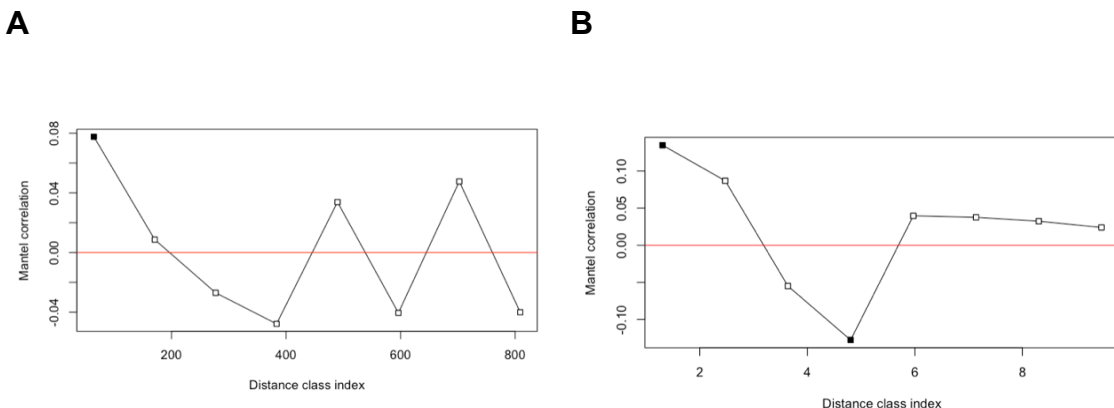


Figure 29: Mantel correlogram illustrating the spatial similarity of the macrofauna community and environmental variables morphology-based data from pine forest. The red line represents a correlation of zero. (A) shows the correlation (Mantel  $r = 0.059$ ,  $p = 0.191$ ) between environmental similarity and geographic distance at increasing distance classes. A significant positive autocorrelation (filled point) is evident only at the shortest distance class (64 m)( $p = 0.019$ ), demonstrating that the environment is spatially structured at a local scale, with similarity decaying rapidly with distance. (B) shows the correlation (Mantel  $r = 0.053$ ,  $p = 0.232$ ) between community similarity and environmental similarity at increasing distance classes. A significant positive autocorrelation (filled point) is evident at the shortest distance class (1.3 m)( $p = 0.04$ ), a significant negative correlation is observed at the fourth distance class 4.8m ( $p = 0.027$ ).

### Molecular assessment

In the oak forest the primary test for spatial autocorrelation, comparing community dissimilarity to geographic distance (Geo vs Comm), found no significant relationship (Mantel  $r = 0.007$ ,  $p = 0.459$ ). Similarly, there was no evidence that the environmental conditions were spatially structured, with the test comparing environmental dissimilarity to geographic distance (Geo vs Env) also yielding a non-significant result (Mantel  $r = 0.070$ ,  $p = 0.188$ ). Finally, the test for a direct relationship between the environment and the community (Env vs Comm) was also not significant (Mantel  $r = 0.036$ ,  $p = 0.360$ ).

In the pine forest the test for spatial autocorrelation in the community (Geo vs Comm) was not significant (Mantel  $r = 0.037$ ,  $p = 0.307$ ), indicating that there is no overarching spatial structure to the macroinvertebrate community across the entire pine system. Similarly, the environmental variables themselves were not significantly spatially structured, with the Geo vs Env test also returning a non-significant result (Mantel  $r = 0.067$ ,  $p = 0.173$ ). But revealed significant positive spatial autocorrelation only at the shortest spatial scale (Figure 30A). In the first distance class, representing sites separated by an average of 64.5 meters, a significant positive Mantel correlation was observed ( $r = 0.078$ ,  $p = 0.018$ ). This indicates that sites that

are close to each other are also more similar in their overall soil chemistry. This relationship disappeared at all larger distance classes, with no significant correlation found from the second distance class onwards (average distance = 170.8 meters). Finally, the test for a direct relationship between the environment and the community (Env vs Comm) was also not significant (Mantel  $r = 0.058$ ,  $p = 0.256$ ). However, a significant relationship was found only at the smallest scale of environmental difference (Figure 30B). In the first distance class, representing the most environmentally similar sites, a significant positive correlation was found ( $r = 0.097$ ,  $p = 0.039$ ).

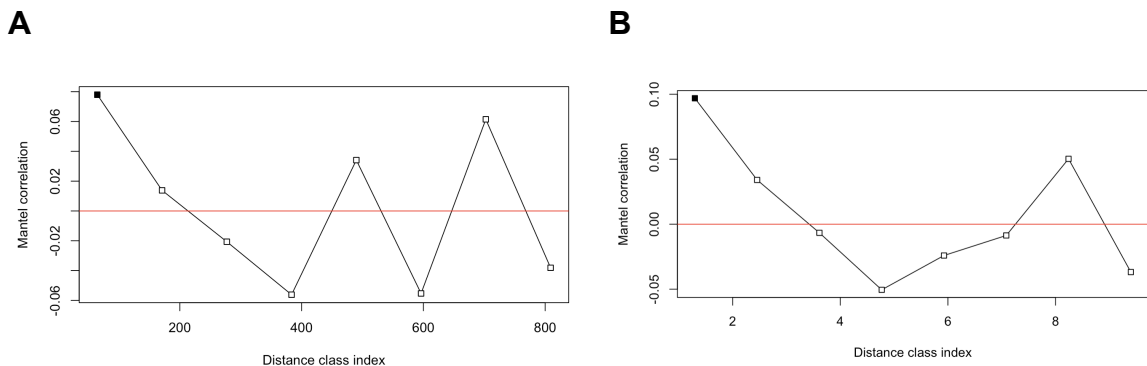


Figure 30: Mantel correlograms for the Pine forest molecular data, showing Spearman's correlation coefficient (Mantel  $r$ ) is plotted against distance classes. (A) environmental spatial autocorrelation (Mantel  $r = 0.067$ ,  $p = 0.173$ ). A significant positive autocorrelation (filled point) is evident at the shortest distance class (64.5 m)( $p = 0.018$ ); (B) The community-environment relationship across spatial scales (Mantel  $r = 0.058$ ,  $p = 0.256$ ). A significant positive autocorrelation (filled point) is evident at the shortest distance class ( $p = 0.039$ )

### Variance Partitioning

In the oak forest, variation partitioning revealed that spatial and environmental variables together explained approximately 19.6 % of the variation in community composition (adjusted  $R^2 = 0.196$ )(Figure 31). Of this, pure spatial structure accounted for a substantial proportion ( $[b] = 16\%$ ,  $p = 0.002$ ), while the pure environmental fraction was very small ( $[a] = 1\%$ ) and could not be tested for significance due to model fitting limitations. The shared fraction between environment and space ( $[c]$ ) explained an additional 3% of the variation. Spatial variables alone ( $b + c$ ) explained 19% of the variation ( $p = 0.001$ ), whereas environmental variables alone ( $a + c$ ) explained only 3.8% ( $p = 0.117$ ), suggesting a relatively weak environmental signal. The unexplained residual variation ( $[d]$ ) remained high at 80.4%, highlighting the presence of other unmeasured or stochastic factors influencing community composition.

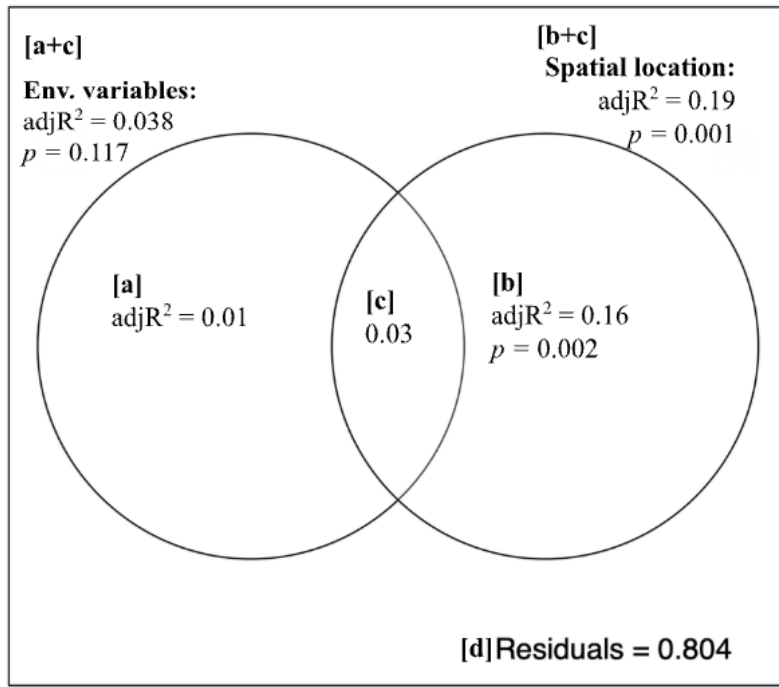


Figure 31: Venn diagram illustrating the results of the Variance Partitioning Analysis for the Oak forest macrofauna community. The analysis partitions the total variation in community composition (based on [e.g., Jaccard] dissimilarities) between two groups of explanatory variables: environmental variables (left circle) and spatial location (right circle). The values shown are the adjusted R<sup>2</sup> values, representing the proportion of variance explained by each component. [a] represents the pure effect of the environmental variables (1.0%). This component was not statistically significant (p = 0.117); [b] represents the pure effect of spatial location (16.0%); [c] represents the shared variance that is explained by both the environment and space (3.0%); [d] represents the unexplained or residual variance (80.4%).

In the pine forest, variation partitioning showed that spatial and environmental variables together explained 21.6% of the variation in community composition (adjusted R<sup>2</sup> = 0.216) (Figure 32). The pure environmental component ([a]) explained a small but statistically significant portion (0.6%, p = 0.001), while the pure spatial fraction ([b]) accounted for 4% (p = 0.003). The shared fraction between space and environment ([c]) contributed the largest explainable component, at 12%, indicating substantial spatial structuring of environmental variables. Spatial variables alone (b + c) explained 15% (p = 0.001), and environmental variables alone (a + c) explained 18% (p = 0.001). The residual unexplained variation remained high at 78.4%, suggesting that other unmeasured environmental or biotic factors may influence community patterns in these pine forests.

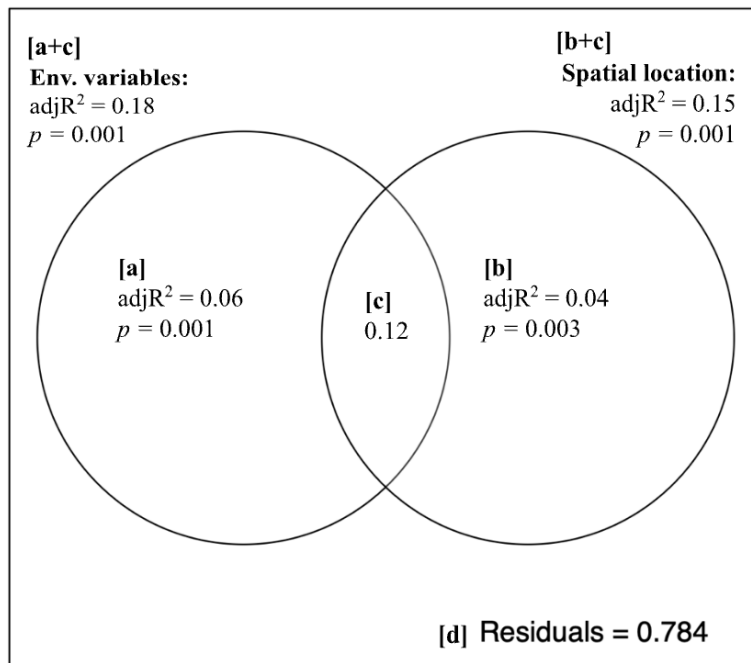


Figure 32: Venn diagram illustrating the results of the Variance Partitioning Analysis for the Pine forest macrofauna community. The analysis partitions the total variation in community composition (based on Jaccard dissimilarities) between two groups of explanatory variables: environmental variables (left circle) and spatial location (right circle). The values shown are the adjusted R<sup>2</sup> values, representing the proportion of variance explained by each component. [a] represents the pure effect of the environmental variables (6.0%); [b] represents the pure effect of spatial location (4.0%); [c] represents the shared variance that is explained by both the environment and space (i.e., spatially structured environmental variation) (12.0%); [d] represents the unexplained or residual variance (78.4%). All components shown were statistically significant ( $p < 0.005$ ).

#### *Global Moran's I Analysis of Taxonomic Abundance Patterns*

The analysis of global morans i for abundance data revealed that several key taxa exhibited significant positive spatial autocorrelation, revealing a clustering of their distribution in space. In the oak forest the strongest spatial clustering was observed for the orders Isopoda (Moran's I = 0.28,  $p = 0.003$ ) and Coleoptera (Moran's I = 0.26,  $p = 0.003$ ). Significant, though slightly weaker, spatial clustering was also detected for the class Annelida (Moran's I = 0.17,  $p = 0.013$ ) and the order Hemiptera (Moran's I = 0.14,  $p = 0.033$ ). The remaining taxonomic groups tested did not show significant spatial patterns (Table X)

In the pine forest the strongest spatial pattern was exhibited by the order Coleoptera, which showed significant positive spatial autocorrelation (Moran's I = 0.30,  $p = 0.001$ ), indicating a highly clustered or patchy distribution. Significant, positive clustering was also observed for Hymenoptera (Moran's I = 0.20,  $p = 0.014$ ), unidentified Larvae (Moran's I = 0.20,  $p =$

0.008), and Hemiptera (Moran's I = 0.17, p = 0.026). The class Annelida was the only taxon to exhibit significant negative spatial autocorrelation (Moran's I = -0.005, p = 0.013).

To explore the nature of these non-random patterns, I have further investigated the species with the strongest spatial autocorrelation using Local Moran's I (LISA). (Supplementary material Figure 5)

Table 5: Moran's I test for spatial autocorrelation of individual taxon abundances in the Oak and Pine forests. The observed Moran's I statistic and associated p-value are shown for each taxonomic group. Significant p-values ( $p < 0.05$ ), indicating a non-random spatial distribution, are highlighted in bold.

Species	Oak		Pine	
	Observed Moran I	<i>p</i> value	Observed Moran I	<i>p</i> value
Coleoptera	0.25689894	<b>0.003</b>	0.302599708	<b>0.001</b>
Isopoda	0.28222222	<b>0.003</b>	-0.031578947	0.7105
Annelida	0.17297297	<b>0.0125</b>	-0.005263158	<b>0.0125</b>
Hemiptera	0.14130952	<b>0.0325</b>	0.17453271	<b>0.026</b>
Pseudoscorpiones	0.10555556	0.033	-	-
Gastropoda	0.12264151	0.056	-0.204651163	0.9955
Araneae	0.01828826	0.229	-0.008415466	0.377

<b>Larvae</b>	0.01914008	0.271	0.195408605	<b>0.008</b>
Diplopoda	-0.01850775	0.405	-	-
Archaeognatha	-0.02631579	0.541	-0.082815965	0.837
Blattodea	-0.02631579	0.569	0.056521739	0.1375
<b>Hymenoptera</b>	-0.03182103	0.512	0.198469877	<b>0.014</b>
Orthoptera	-0.07222222	0.625	-0.047368421	0.954
Chilopoda	-0.07116564	0.69	-0.007380074	0.361
Opiliones	-	-	-0.048387097	0.6415

A Global Moran's I analysis through the OTU-based community data employing relative read abundance of key taxonomic groups revealed distinct results comparative to the morphological assessment.

In the oak forest the analysis found a significant spatial pattern for the subphylum Myriapoda (Moran's I = 0.13, p = 0.042). In the pine forest a significant positive spatial autocorrelation was detected for the order Archaeognatha (Moran's I = 0.11, p = 0.037), indicating that their relative abundance was spatially clustered. Furthermore, a significant positive spatial clustering was observed for the order Embioptera (Moran's I = 0.003, p = 0.001). Although the Moran's I statistic itself is low, the highly significant p-value confirms a non-random, aggregated distribution.

To gain deeper insight into the observed non-random spatial patterns, I have conducted a Local Moran's I (LISA) analysis on the taxa exhibiting the strongest global spatial autocorrelation (Supplementary Figure 6)

Table 6: Moran's I test for spatial autocorrelation of individual OTU abundances in the Oak and Pine forests. The observed Moran's I statistic and associated p-value are shown for each taxonomic group. Significant p-values ( $p < 0.05$ ), indicating a non-random spatial distribution, are highlighted in bold.

Species	Oak		Pine	
	Observed Moran I	P Value	Observed Moran I	P Value
<b>Myriapoda</b>	0.13385776	<b>0.042</b>	0.012090752	0.208
Coleoptera	0.06635173	0.147	-0.053819803	0.577
Isopoda	0.033226116	0.101	-0.071915814	0.9175
Opiliones	-0.006038628	0.197	-0.048371374	0.548
Clitellata	-0.020707071	0.313	-	-
Clitellata	-0.020707071	0.291	-	-
Orthoptera	-0.020814236	0.367	-0.009643993	0.395
Hymenoptera	-0.040428184	0.479	0.020108894	0.286
Lepidoptera	-0.026789296	0.442	-0.011115228	0.348
Araneae	-0.147573769	0.934	-0.067633784	0.662

<b>Archaeognatha</b>	-0.055323735	0.834	0.106722038	<b>0.037</b>
Gastropoda	-0.046745762	0.917	-0.024785322	0.424
Blattodea	-0.02884405	0.602	-0.027306328	0.506
Dermoptera	-0.042179534	0.9175	-	-
<b>Embioptera</b>	-0.039764836	0.665	0.003390444	<b>0.001</b>
Hemiptera	-0.111891745	0.856	-0.040151596	0.531

### 3.5 Community Response to Environmental and Spatial Variability

To identify the most significant environmental and spatial predictors of macroinvertebrate community composition in oak and pine forests, a distance-based redundancy analysis (db-RDA) was performed using presence-absence data of morphologically identified taxa. The analysis was based on morphological richness and aimed to assess how community patterns are shaped by environmental conditions and spatial variables across the two forest types.

The analysis used a forward-selection process to identify the most significant predictors, resulting in a final model that included one environmental variable (Total Organic Carbon - TOC) and four spatial variables (MEM2, MEM4, MEM6, and MEM10). The overall db-RDA model was highly significant and explained a substantial portion of the variation in the community data (PERMANOVA:  $F = 3.03$ ,  $p = 0.001$ ). The model accounted for 21.1% of the total constrained variance in community composition (Adjusted  $R^2 = 0.211$ ). An analysis of the individual terms within the model revealed that the community structure was primarily driven by spatial factors. Four separate spatial eigenvectors, representing different scales of spatial patterning, were found to be significant predictors: MEM2 ( $F = 4.69$ ,  $p = 0.003$ ), MEM4 ( $F = 3.99$ ,  $p = 0.002$ ), MEM6 ( $F = 2.72$ ,  $p = 0.026$ ) and MEM10 ( $F = 2.65$ ,  $p = 0.035$ ).

In the Pine forest, a distance-based Redundancy Analysis (db-RDA) was conducted. Following a forward-selection process, the final, most parsimonious model included one environmental variable (pH) and two spatial variables (MEM1 and MEM7). The overall model was highly significant and explained a large and significant portion of the community variation (PERMANOVA:  $F = 5.38$ ,  $p = 0.001$ ). In total, the model accounted for 25.7% of the total constrained variance in community composition (Adjusted  $R^2 = 0.257$ ). An analysis of the significance of the individual terms revealed that, in stark contrast to the oak forest, the community in the pine system was most strongly driven by an environmental variable. Soil pH was the single most important and highly significant predictor of community composition ( $F = 8.67$ ,  $p = 0.001$ ). In addition to this strong environmental filtering effect, two spatial eigenvectors were also retained in the final model as significant predictors, indicating that pure spatial processes also play a role MEM1 ( $F = 4.30$ ,  $p = 0.014$ ), MEM7 ( $F = 3.17$ ,  $p = 0.022$ )

#### *Linking Molecular Community Response to Environmental and Spatial Variability*

To identify the most significant environmental and spatial predictors of macroinvertebrate community composition in the Oak forest and pine forest, a distance-based Redundancy Analysis (db-RDA) was conducted based on taxonomic OTU presence absence.

The final model for the oak forest, determined via a forward-selection process, retained two environmental variables (pH and Iron) and one spatial variable (MEM7). The overall model was statistically significant and explained a significant portion of the community variation (PERMANOVA:  $F = 2.28$ ,  $p = 0.007$ ). An analysis of the marginal effects of each term in the model revealed that the community structure was significantly influenced by both an environmental and a spatial factor. Iron was found to be a significant environmental predictor of community composition ( $F = 2.80$ ,  $p = 0.025$ ). The spatial eigenvector MEM7, representing a specific scale of spatial patterning, was also a significant predictor ( $F = 2.45$ ,  $p = 0.031$ ). In contrast, after accounting for the effects of Iron and the spatial term, pH was not a significant individual predictor ( $F = 1.60$ ,  $p = 0.170$ )

The final distance based redundancy analysis model for the pine forest, determined through a forward-selection process, included Phosphorus, Total Nitrogen (TN), Magnesium, Sodium, and Iron. The overall model containing these five environmental predictors was statistically significant and explained a significant portion of the community variation (PERMANOVA:  $F = 2.36$ ,  $p = 0.002$ ). An analysis of the marginal effects of each variable within the model (a

ANOVA) revealed that Magnesium and Iron were the most influential individual predictors. Both were found to have a highly significant relationship with community composition Magnesium ( $F = 3.39$ ,  $p = 0.005$ ) and Iron ( $F = 3.22$ ,  $p = 0.008$ ). The other variables included in the model Phosphorus, TN, and Sodium were not found to be individually significant predictors after accounting for the effects of Magnesium and Iron.

### **3.6 Investigating Taxonomic Indicator Response to Soil Variability**

To identify taxa that were strongly associated with each habitat, an indicator species analysis was performed on both the morphological and molecular datasets. The results revealed both areas of congruence and key differences in the insights provided by each method.

Based on the morphological data, the Oak forest was significantly indicated by two detritivore groups: Diplopoda (Indicator Value [IndVal] = 0.641,  $p = 0.001$ ) and Isopoda (IndVal = 0.456,  $p = 0.019$ ). In striking contrast, the analysis of the molecular data did not identify any significant OTU indicators for the Oak forest habitat.

For the Pine forest, the results showed a clear point of agreement between the two methods. Archaeognatha was identified as a highly significant indicator of the Pine forest in both the morphological analysis (IndVal = 0.642,  $p = 0.001$ ) and the molecular analysis (IndVal = 0.528,  $p = 0.007$ ), underscoring its strong and consistent fidelity to this ecosystem. The molecular data further identified an additional significant indicator for the Pine forest, Blattodea (IndVal = 0.411,  $p = 0.031$ ), a distinction not captured by the morphological counts. Overall, while both methods highlighted the unique affinity of Archaeognatha for the pine habitat, the morphological data exclusively identified indicators for the oak system, and the molecular data exclusively identified an additional indicator for the pine system.

### **3.7 Comparative Analysis of Morphological and Molecular Data**

While the individual sample rarefaction curves indicated sufficient sequencing depth for each sample analyzed, a pooled analysis of the overall sampling completeness for the Oak forest was conducted using non-parametric richness estimators. The analysis revealed that the total observed OTU to quantify the overall sampling completeness for the entire Oak forest ecosystem. By comparing the total number of observed OTUs across all samples to the richness accounted for 62.25% of the estimated total richness for the habitat, indicating that while a majority of total expected OTU richness estimated by the Chao2 non-parametric

estimator, the analysis revealed that the sampling campaign successfully recovered the diversity was captured, additional sampling would likely reveal rarer OTUs.

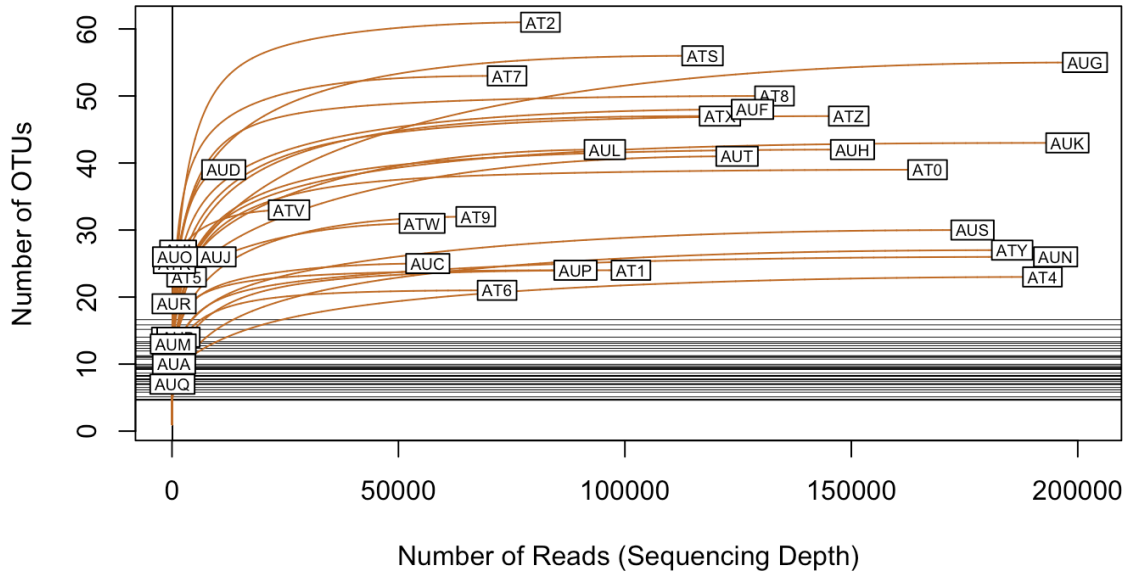


Figure 33: Sample-based rarefaction curves for the molecular (OTU) dataset. Each curve represents an individual sample, plotting the cumulative number of unique Operational Taxonomic Units (OTUs) observed as a function of increasing sequencing depth (number of reads). The curves were generated to assess the completeness of the sequencing effort for each sample. The shape of the curves, particularly the leveling off or plateauing for most samples, indicates that the sequencing depth was sufficient to capture the vast majority of the OTU diversity present in those samples.

The adequacy of the molecular sequencing effort was evaluated at two scales: the individual sample level and the entire ecosystem level. At the individual sample level, rarefaction curves were generated to assess sequencing depth (Figure 34). The resulting curves consistently approached an asymptote, demonstrating that the sequencing for each sample was sufficient to capture the vast majority of the OTU diversity contained within it.

To assess the overall sampling completeness for the entire Pine forest habitat, the total observed OTU richness was compared to the total estimated richness using a non-parametric estimator (Chao2). This analysis revealed that the sampling campaign successfully recovered 70.73% of the estimated total OTU diversity present within the Pine forest

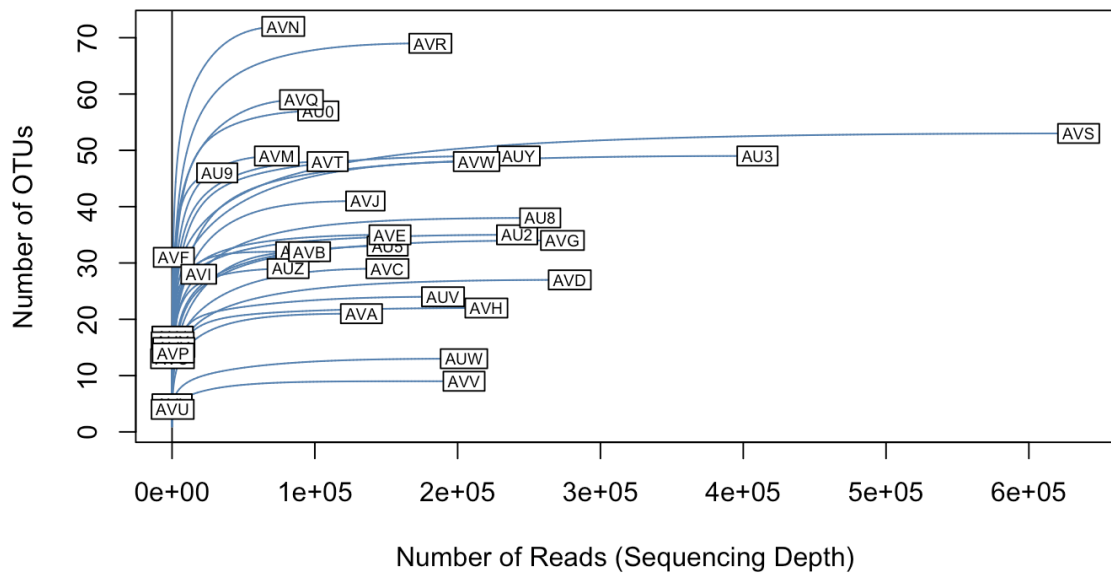


Figure 34: Sample-based rarefaction curves for the Pine forest molecular (OTU) dataset. Each blue curve represents an individual sample, plotting the cumulative number of unique Operational Taxonomic Units (OTUs) observed as a function of increasing sequencing depth. The curves were generated to assess the completeness of the sequencing effort for each sample. The pronounced leveling off (plateauing) of nearly all curves indicates that the sequencing depth was sufficient to capture the vast majority of the OTU diversity present within each individual sample.

## 4 Discussion

This study demonstrates that the performance of biodiversity sampling strategies is highly context-dependent and strongly influenced by forest type and community structure (Catford et al., 2022). Oak forests supported higher macrofauna richness and abundance overall; however, the efficiency of sampling designs varied. In the structurally complex oak forest, k-means sampling more effectively captured species richness and yielded more consistent community profiles. Conversely, in the more homogeneous pine forest, random sampling outperformed k-means in terms of stability and representativeness. These findings emphasize the importance of adapting biodiversity monitoring frameworks to local ecological and spatial conditions, rather than applying a one-size-fits-all approach (Hoffman et al., 2013; Catford et al., 2022).

### 4.1 Evaluating the Performance of Spatial Sampling Strategies

To evaluate sampling design performance, this study focused on the spatial structure of macroinvertebrate communities and the ability of sampling schemes to capture biodiversity and environmental variability. Macrofaunal communities often respond to fine-scale heterogeneity rather than broad gradients (Decaëns, 2010), and uniform sampling strategies frequently overlook this complexity. The k-means clustering approach, developed to target environmental variability, was compared with random sampling and the LUCAS single-point protocol.

Overall, comparative analysis of k-means and random sampling strategies in oak and pine forests yielded critical insights into their respective efficacies. While the k-means approach consistently demonstrated descriptive advantages in its capacity to capture both taxonomic and environmental variability, these distinctions frequently lacked statistical significance.

Rather, the most pronounced distinctions emerged from ecological contrasts between the forest systems themselves. In the oak forest, characterized by structurally complex vegetation and topography, k-means sampling yielded more consistent beta diversity patterns, suggesting that it better captured underlying environmental gradients. In contrast, the pine forest, more homogeneous in vegetation and management, was better represented by random sampling, which avoided overemphasis on environmental edges or outliers. Interestingly, relative read abundance (RRA)-based molecular data revealed more pronounced differences between sampling designs than traditional morphological count data, indicating that molecular beta diversity may be more sensitive to spatial structure.

Environmental variables further substantiated these patterns. Across most soil parameters, both sampling methods identified significantly greater variance in the oak forest than in the pine forest, particularly for potassium oxide, magnesium, potassium, and manganese. The k-means approach also captured higher variability in phosphate, phosphorus, and calcium within the oak forest. These results confirm that both designs were sensitive to large-scale ecological differences between systems, while within-system distinctions remained subtle. One exception occurred in the pine forest, where k-means detected significantly greater variance in H<sup>+</sup> values, suggesting a potential advantage in capturing structured chemical gradients.

Altogether, these results indicate that while stratified sampling designs like k-means can enhance biodiversity and environmental signal detection in complex systems, their benefits may diminish in more uniform settings. The comparison also underscores the limitations of the LUCAS approach for local-scale assessments and highlights the need for flexible, landscape-adapted strategies in soil biodiversity monitoring.

## 4.2 Community Composition Shaped by Forest Type and Turnover Patterns

It was hypothesized that oak and pine forests would support significantly different macrofaunal communities due to differences in soil chemistry, vegetation structure, and management. This hypothesis is strongly supported by the data. While both investigated forest systems shared a similar number of taxonomic groups and revealed no significant differences in alpha diversity metrics, this apparent similarity in species richness masked profound differences in community composition. Indeed, the perMANOVA results provide strong evidence that the community composition is significantly different between the forest types. This statistical separation is visually represented in the NMDS ordination plot, which shows two distinct, non-overlapping clusters of samples corresponding to their forest of origin. This indicates that while both forests may support a similar number of taxa, the identities of those taxa are fundamentally different.

Beta diversity partitioning further clarified this pattern. Indeed, in both systems, high beta diversity was almost entirely attributable to species turnover, with negligible nestedness. This indicates that the pine forest is not a species-poorer subset of the oak forest, but rather supports a fundamentally different set of species, suggesting strong environmental filtering between systems, where abiotic factors select for distinct species traits (Baselga, 2010; Kraft et al., 2015).

Compositional differences in macroinvertebrate communities were reflected in distinct taxonomic signatures detected by both morphological and molecular data. In oak forests, morphological data showed that groups like Isopoda and Diplopoda are significant indicators. These are key detritivores that thrive in environments typical of healthy broadleaf systems. Deciduous trees provide high-quality litter, leading to a higher proportion of earthworms and more diverse detritivore assemblages (Ganault et al., 2021). This suggests a complex, resource-rich temperate deciduous ecosystem with active detritivore guilds. The sensitivity of the broader Myriapoda group, as identified by molecular data, further supports the role of these organisms in indicating specific soil conditions within these systems. The collective presence and activity of these groups strongly support a litter-rich environment that fosters robust decomposer activity.

Interestingly, the lack of correlation between the molecular and morphological community data itself reflects the oak system's complexity. This discrepancy is likely a product of the forest's inherent heterogeneity. While morphology tallies individual organisms, metabarcoding sensitive to biomass, cryptic species, and gut contents captures a broader ecological signal, including trophic links. This statistical independence underscores the multidimensional nature of biodiversity in heterogeneous systems. In contrast, the pine forest community appeared shaped by harsher environmental filters. Molecular data revealed dominance by Coleoptera, while decomposer taxa like millipedes were absent, likely due to recalcitrant litter limiting detritivore guilds (Berg & McClaugherty, 2003; Kaneko & Salamanca, 1999). Morphological results confirmed lower mean abundance (approximately 39 individuals/sample), indicating a resource-limited system. Interestingly, in pine forests, molecular and morphological data were significantly correlated, suggesting that in less complex or more environmentally constrained ecosystems, different biodiversity assessment methods are more likely to converge on similar patterns (Rooney et al., 2006). The dominance of beetles was consistently reflected in both data types, pointing to a community strongly shaped by abiotic constraints. Many beetle families are known to be well-adapted to the harsh conditions, such as low pH and physically complex litter layers, allowing them to thrive where other detritivore guilds are excluded (Persson et al., 1980; Van Breemen & Buurman, 2002). Together, these results confirm that environmental filtering, via soil chemistry and vegetation type, plays a dominant role in structuring macrofaunal communities (Wardle et al., 2004), and that community complexity mediates the degree of alignment between morphological and molecular assessments (Cavander-Bares et al. 2009). In complex systems like oak forests, both methods provide complementary insights, while in simpler systems like pine forests, their signals converge.

### **4.3 Soil Chemistry as a Filter of Community Structure**

It was hypothesized that macrofaunal community structure is significantly influenced by key environmental variables, particularly pH and organic matter content (e.g., TOC and TN), and that the identity and strength of these predictors would differ between forest types. The results strongly support this hypothesis, revealing how vegetation, soil chemistry, and faunal composition are intricately linked. The observed biological patterns are not random; they are tightly coupled to the contrasting environmental conditions characterizing the two forest systems (Wardle et al., 2004).

While the hypothesis highlighted soil chemistry, vegetation, and management as potential drivers, the findings suggest a cascade of effects: vegetation type fundamentally shapes soil chemistry (Augusto et al., 2002), which in turn serves as the primary environmental filter for the faunal community. The Principal Component Analysis (PCA) of soil chemical properties confirmed that forest type explains a significant portion of variation in soil chemistry, specifically, 24.2% of the total variance. The first principal axis clearly separated oak and pine forest samples, underscoring the ecological divergence between systems. This finding aligns with ecological theory emphasizing the role of environmental heterogeneity in maintaining distinct community structures through processes like species sorting (Leibold et al., 2004; Kraft et al., 2015).

The oak forest was characterized by higher pH and elevated concentrations of key nutrients such as potassium and phosphorus conditions typical of a “mull” humus profile found in broadleaf forests (Augusto et al., 2002). These environments support rapid organic matter turnover and nutrient cycling (Scheu & Setälä, 2002), creating favorable conditions for diverse and abundant soil faunal communities. (Gonzalez & Seastedt, 2001).

Conversely, the pine forest exhibited lower pH and higher concentrations of Total Organic Carbon and iron, hallmarks of a “mor” humus system associated with acidic, recalcitrant needle litter (Van Breemen & Buurman, 2002). Such conditions are known to impose physiological stress on many invertebrates and reduce nutrient availability (Augusto et al., 2002), thereby favoring a narrower set of tolerant taxa (Hättenschwiler et al., 2005), which in this study included a dominance of Coleoptera. The tight clustering of pine samples in the PCA further suggests a chemically homogenous environment, consistent with the reproducible community composition observed across both morphological and molecular datasets.

When modeling community composition, a striking contrast emerged between forest types. In the pine forest, morphological abundance data revealed a strong, predictable structure: broad taxonomic groups varied systematically in response to dominant chemical gradients. This pattern was echoed by molecular data, where OTU-level composition was significantly shaped by magnesium and iron availability, suggesting a hierarchy of environmental filters (Cavander-Bares et al. 2009), broad chemical constraints followed by finer-scale nutrient limitations.

In contrast, no significant explanatory model (e.g., db-RDA) could be identified for the oak forest using abundance-based morphological data. This suggests that in more complex, heterogeneous systems like oak forests, macrofaunal abundance patterns are shaped not solely by chemical variables, but also by unmeasured factors such as microhabitat variation, biotic interactions, or legacy effects. However, when community structure was analyzed at higher taxonomic resolution using OTU data, a modest but significant relationship emerged, with Total Organic Carbon (TOC) and iron identified as key predictors. TOC likely represents the quantity and quality of decomposable substrate, while iron, an essential micronutrient, may act as a selective constraint in certain microhabitats.

Together, these findings reveal a dual pattern: environmental filtering exerts a dominant structuring force in more homogeneous systems like pine forests, while in heterogeneous environments like oak forests, community assembly is driven by a combination of chemical, spatial, and biotic processes, highlighting the need for multi-scalar, high-resolution approaches in biodiversity monitoring.

#### **4.4 Spatial Structure vs. Environmental Filtering in Community Assembly**

In this study it was aimed to determine the relative importance of spatial structure and environmental filtering in shaping macrofauna community composition within oak and pine forest systems. I have hypothesized that spatial distance would be a stronger predictor of community composition in oak forests, due to greater microenvironmental heterogeneity, whereas in pine forests, abiotic filtering would play a more dominant role (Cavander-Bares et al. 2009). The results largely support this hypothesis and reveal two distinct modes of community assembly.

In the oak forest, spatial location exerted a stronger influence than measured soil chemistry. Variance partitioning analysis showed that the pure spatial fraction ([b]) explained 16% of community variation, while the pure environmental component ([a]) was negligible and

non-significant. This suggests that key structuring factors are spatially autocorrelated but not captured by the measured chemical variables. This finding is corroborated by Mantel tests, which revealed a significant global correlation between spatial distance and community dissimilarity. Spatial correlograms further confirmed that nearby sites harbored more similar communities, regardless of soil chemistry. These spatial patterns likely reflect unmeasured spatially structured variables, such as microsite resource availability, localized biotic interactions (e.g., predation or competition), or microscale habitat features. Importantly, the failure of the db-RDA model in earlier analyses aligns with this interpretation: the dominant community patterns in oak forests were driven not by the measured environmental variables but by spatially structured processes. Interestingly, this spatial signal disappeared in the molecular OTU data, possibly due to the trophic complexity of the oak system. Metabarcoding captures DNA from multiple trophic levels, including prey in predator gut contents, introducing ecological "noise" that can obscure fine-scale spatial patterns of species occurrence. In contrast, the pine forest community exhibited a more deterministic structure, shaped primarily by environmental filtering. Variance partitioning revealed that environmental variables—alone or in combination with spatial structure—explained 18% of community variation. Notably, the largest explanatory fraction was the shared component ( $[c] = 12\%$ ), indicating that the environmental gradients themselves were spatially autocorrelated. Mantel correlograms supported this, detecting significant spatial autocorrelation in environmental variables at distances up to ~64 meters and a significant link between environmental distance and community structure at very fine scales (~1–5 m). This suggests that soil chemical properties vary in a predictable spatial pattern and that macrofauna directly respond to this fine-scale environmental mosaic. Unlike the oak system, the pine forest exhibited consistent results across both morphological and molecular datasets, reinforcing the interpretation of a simpler, more predictable community structure governed by abiotic filters.

Overall, the findings confirm the hypothesis. The oak forest is a complex, spatially governed system shaped by unmeasured and potentially biotic processes, while the pine forest reflects a more deterministic, chemically filtered system, where community composition tracks environmental gradients with spatial structure. Nevertheless, the high residual unexplained variance in both systems (>78%) highlights the importance of stochasticity and unmeasured ecological variables in shaping soil macrofaunal communities.

## 4.5 Identifying Bioindicator Taxa for Soil Health Monitoring

This study aimed to identify macroinvertebrate taxa strongly associated with environmental gradients and/or spatial patterns that could serve as reliable bioindicators of soil health. It was hypothesized that certain groups, such as Araneae, Coleoptera, Isopoda, and Gastropoda, would exhibit significant associations with specific soil properties and thus reflect broader ecosystem status. In the oak forest, indicator species analysis of morphological data revealed the clearest candidates. Isopoda and Diplopoda emerged as highly significant indicators, consistent with their ecological role as key detritivores. These groups are known to thrive in high-pH, calcium-rich soils, conditions typical of well-functioning temperate broadleaf systems. Their presence thus reliably reflects active decomposition and nutrient cycling. In particular, Isopoda showed significant spatial autocorrelation (Moran's I), suggesting the formation of ecologically meaningful patches, potentially linked to microsites of organic matter accumulation and favourable microclimates. These characteristics make Isopoda abundance a strong, interpretable indicator of functional soil health hotspots. Molecular data provided complementary insights. A general linear model linked Myriapoda OTU abundance to Total Organic Carbon (TOC), indicating that finer-scale molecular signals also reflect key resource-driven processes. However, the complexity of the oak system, with its spatial and biotic heterogeneity, complicates a straightforward bioindicator framework. In contrast, the pine forest, characterized by more uniform and acidic soil conditions, yielded clearer and more consistent indicator taxa. The standout candidate was Archaeognatha, which was identified as a significant indicator by both morphological and molecular methods. Its strong spatial clustering reinforces its ecological relevance, suggesting that its presence reflects specific, non-random environmental filters, likely tied to low pH and nutrient-poor conditions typical of coniferous systems. As such, Archaeognatha emerges as a robust and context-specific indicator of chemical soil stress.

### *A Context-Sensitive Bioindicator Toolkit*

These findings support the hypothesis, but also highlight the importance of ecosystem context and monitoring objectives when selecting bioindicators. In the oak forest, functional group indicators like Isopoda and Diplopoda offer practical value for tracking decomposer activity and nutrient cycling, process-oriented metrics relevant to soil functioning. In the pine forest, the strength and consistency of abiotic filtering yield more straightforward taxon-environment associations, with Archaeognatha acting as an effective stress indicator under acidic conditions.

Ultimately, the results suggest that a combined approach, linking morphological assessment of functional groups with molecular detection of cryptic taxa, may offer the most holistic and scalable strategy for soil health monitoring. While morphology provides interpretable abundance trends, molecular tools enhance taxonomic resolution and reveal hidden patterns, especially in less tractable systems. Together, they support the development of bioindicator frameworks tailored to specific ecosystem types and management goals.

## 5 Conclusion

This study demonstrates the value of macrofaunal communities as sensitive indicators of soil variability across forest types. By comparing oak and pine forest ecosystems in Sabugal, Portugal, and integrating both morphological and molecular identification methods, the research provides evidence that sampling strategies and community composition metrics must be adapted to the spatial heterogeneity and environmental complexity of each ecosystem.

Stratified sampling using a k-means design proved to be more efficient in the heterogeneous oak forest, enhancing biodiversity detection and reducing intra-site variance, whereas a random design was better suited to the homogeneous pine forest. Soil chemical analyses further confirmed the greater environmental variability in oak stands, validating the need for context-specific sampling frameworks.

Moreover, the study showed that while DNA metabarcoding expands taxonomic detection and captures elusive (cryptic) diversity, it must be calibrated against morphological data to ensure ecological interpretation and semi-quantitative validity. Together, these findings support the integration of both morphological and molecular tools into future soil health monitoring protocols and underline the importance of tailoring sampling strategies to local conditions.

## **6 Future Research Directions and Recommendations**

Within the framework and findings of this study, I propose a set of future directions and recommendations structured along a three-tiered approach encompassing methodological advancements, ecological research priorities, and policy-driven applications. These recommendations aim to strengthen the operational value, ecological relevance, and strategic integration of macrofauna-based assessments into soil health monitoring systems at both national and European scales.

### **Methodological Recommendations:**

**Tailored Sampling Designs:** Soil monitoring frameworks, including those under the EU Soil Monitoring Law, should adopt flexible sampling strategies, using stratified designs in heterogeneous systems like oak forests and simpler random designs in uniform areas such as pine plantations.

**Integration of Identification Methods:** Combining morphological and DNA metabarcoding approaches provides a more complete picture of biodiversity. Investment in reference libraries and standardizing protocols is essential.

**Advancing Semi-Quantitative Molecular Metrics:** Future work should refine the interpretation of relative read abundance (RRA) to support semi-quantitative assessments of macrofaunal biomass and functional relevance.

### **Ecological Research Directions:**

**Trait-Based and Functional Approaches:** Move beyond species counts to include traits, biomass, and abundance for better links between biodiversity and ecosystem services.

**Temporal Monitoring and Longitudinal Studies:** Implement long-term studies to assess macrofaunal dynamics under climate change and land-use shifts.

**Development of Bioindicator Taxa:** Prioritize taxa that reliably reflect soil conditions (e.g., Araneae, Isopoda, Coleoptera) for use as bioindicators.

### **Policy and Application:**

**Integration into European Monitoring Systems:** Macrofaunal and molecular data should be incorporated into LUCAS and EU soil health frameworks to reflect biological functioning.

**Development of Standardized Operational Protocols:** Harmonized sampling and processing protocols are needed for consistency across projects and countries.

By embracing these recommendations, future research and policy development can work in concert to build a comprehensive, scalable, and ecologically grounded framework for forest soil health assessment. This integration is essential for meeting EU soil health targets, enhancing ecosystem resilience, and securing the long-term provision of soil-based ecosystem services in forested landscapes.

## References

- Amori, G., Chiozza, F., & Rondinini, C. (2021). The global mammal assessment: A new and updated baseline for conservation. *Mammal Review*, 51(4), 455-460.
- Anderson, J. M., & Ingram, J. S. I. (1993). *Tropical soil biology and fertility: a handbook of methods*. CAB international.
- Augusto, L., Ranger, J., Binkley, D., & Rothe, A. (2002). Impact of several common tree species of temperate America and Europe on soil fertility. *Annals of Forest Science*, 59(3), 233-254.
- Ballabio, C., Panagos, P., & Montanarella, L. (2016). Mapping topsoil physical properties at European scale using the LUCAS database. *Geoderma*, 261, 110–123.
- Bardgett, R. D., & van der Putten, W. H. (2014). Belowground biodiversity and ecosystem functioning. *Nature*, 515(7528), 505–511.
- Baselga, A. (2010). Partitioning the turnover and nestedness components of beta diversity. *Global Ecology and Biogeography*, 19(1), 134-143.
- Bispo, A., Cluzeau, D., Creamer, R., Dombos, M., Graefe, U., Krogh, PH., Sousa, JP., Peres, G., Rutgers, M., Winding, A., & Römbke, J. (2009). Indicators for Monitoring Soil Biodiversity. *Integrated Environmental Assessment and Management*, 5(4), 717.
- Bourlat, S. J., Juliusdottir, T., Lowe, C. J., Freeman, R., Aronowicz, J., Kirschner, M., Lander, E. S., Thorndyke, M., Nakano, H., Kohn, A. B., Heyland, A., Moroz, L. L., Copley, R. R., & Telford, M. J. (2006). Deuterostome phylogeny reveals monophyletic chordates and the new phylum Xenoturbellida. *Nature*, 444(7115), 85–88.
- Briones, M. J. I. (2014). Soil fauna and soil functions: A jigsaw puzzle. *Frontiers in Environmental Science*, 2.
- Brokerhoff, E. G., Barbaro, L., Castagneyrol, B., Forrester, D. I., Gardiner, B., González-Olabarria, J. R., Lyver, P. O., Meurisse, N., Oxbrough, A., Taki, H., Thompson, I. D., Van Der Plas, F., & Jactel, H. (2017). Forest biodiversity, ecosystem functioning and the provision of ecosystem services. *Biodiversity and Conservation*, 26(13), 3005–3035.
- Broothaerts, N., Panagos, P., & Jones, A. (2024). *A proposal for soil health indicators at EU-level*. Publications Office of the European Union.

Brown, G.G., Silva, E.D., Thomazini, M.J., Niva, C.C., Decaëns, T., Cunha, L.F., Nadolny, H.S., Demetrio, W.C., Santos, A., Ferreira, T. and Maia, L.S. (2018). The role of soil fauna in soil health and delivery of ecosystem services (pp. 197-241).

Brussaard, L. (2012). Ecosystem services provided by the soil biota. In D. H. Wall (Ed.), *Soil Ecology and Ecosystem Services* (pp. 45–58). Oxford University Press.

Brus, D. J. (2019). *Sampling for digital soil mapping: A tutorial supported by R scripts*. GlobalSoilMap.

Brus, D.J., Kempen, B. and Heuvelink, G.B.M. (2011). Sampling for validation of digital soil maps. *European Journal of Soil Science*, 62(3), pp.394-407.

Bünemann, E. K., Bongiorno, G., Bai, Z., Creamer, R. E., De Deyn, G., de Goede, R., Fleskens, L., Geissen, V., Kuyper, T. W., Mäder, P., Pulleman, M., Sukkel, W., van Groenigen, J. W., & Brussaard, L. (2018). Soil quality – A critical review. *Soil Biology and Biochemistry*, 120, 105–125.

Cameron, E. K., Martins, I. S., Lavelle, P., Mathieu, J., Tedersoo, L., Gottschall, F., Guerra, C. A., Hines, J., Patoine, G., Siebert, J., Winter, M., Cesarz, S., Delgado-Baquerizo, M., Ferlian, O., Fierer, N., Kreft, H., Lovejoy, T. E., Montanarella, L., Orgiazzi, A., ... Eisenhauer, N. (2018). Global gaps in soil biodiversity data. *Nature Ecology & Evolution*, 2(7), 1042–1043.

Catford, J. A., Wilson, J. R. U., Pyšek, P., Hulme, P. E., & Duncan, R. P. (2022). Addressing context dependence in ecology. *Trends in Ecology & Evolution*, 37 (2), 158-170.

Cavander-Bares, J., Kozak, K. H., Fine, P. V., & Kembel, S. W. (2009). The merging of community ecology and phylogenetic biology. *Ecology Letters*, 12(7), 693-715.[\[3\]](#)

CMS, Câmara Municipal do Sabugal. (2018). *Primeira Revisão do Plano Diretor Municipal – Volume 4: Estudos Setoriais de Caracterização*. Sabugal: Município do Sabugal.

Coleman, D. C., Geisen, S., & Wall, D. H. (2024). Soil fauna: Occurrence, biodiversity, and roles in ecosystem function. In *Soil Microbiology, Ecology and Biochemistry* (pp. 131–159). Elsevier.

Creamer, R.E., Barel, J.M., Bongiorno, G. and Zwetsloot, M.J. (2022). The life of soils: Integrating the who and how of multifunctionality. *Soil Biology and Biochemistry*, 166, p.108561.

Cysneiros, L. F. D. (2023). *EVALUATING SOIL MACROFAUNA USING MORPHOLOGICAL AND DNA APPROACHES ALONG A GRADIENT OF FARMING INTENSIFICATION* (Master's thesis, University of Coimbra).

Decaëns, T. (2010). Macroecological patterns in soil communities. *Global Ecology and Biogeography*, 19(3), 287-302.

Decaëns, T., Jiménez, J. J., Gioia, C., Measey, G. J., & Lavelle, P. (2006). The values of soil animals for conservation biology. *European Journal of Soil Biology*, 42, S23–S38.

Elbrecht, V., & Leese, F. (2015). Can DNA-based ecosystem assessments quantify species abundance? Testing primer bias and biomass–sequence relationships. *Methods in Ecology and Evolution*, 6(9), 1040–1050.

European Commission. (2002). *Towards a Thematic Strategy for Soil Protection*.

European Environment Agency. (2023). *Soil monitoring in Europe: Indicators and thresholds for soil quality assessments*. Publications Office.

FAO. (2015). *Status of the world's soil resources: Main report*. FAO : ITPS.

FAO. (2020). *State of knowledge of soil biodiversity – Status, challenges and potentialities*. FAO.

Fernandez-Ugalde, O., et al. (2022). *LUCAS 2022 Soil Module sampling instructions and guidelines*. Publications Office of the European Union.

Ganault, P., Nahmani, J., Hättenschwiler, S., Gillespie, L.M., David, J.F., Henneron, L., Iorio, E., Mazzia, C., Muys, B., Pasquet, A. and Prada-Salcedo, L.D. (2021). Relative importance of tree species richness, tree functional type, and microenvironment for soil macrofauna communities in European forests. *Oecologia*, 196(2), pp.455-468.

Gonzalez, G., & Seastedt, T. R. (2001). Soil fauna and plant litter decomposition in tropical and subalpine forests. *Ecology*, 82(4), 955-964.

Gongalsky, K. B. (2021). Soil macrofauna: Study problems and perspectives. *Soil Biology and Biochemistry*, 159, 108281.

Griffiths, B. S., Römbke, J., Schmelz, R. M., Scheffczyk, A., Faber, J. H., Bloem, J., Pérès, G., Cluzeau, D., Chabbi, A., Suhadolc, M., Sousa, J. P., Martins Da Silva, P., Carvalho, F., Mendes, S., Morais, P., Francisco, R., Pereira, C., Bonkowski, M., Geisen, S., ... Stone, D. (2016). Selecting cost effective and policy-relevant biological indicators for European monitoring of soil biodiversity and ecosystem function. *Ecological Indicators*, 69, 213–223.

Guerra, C. A., Bardgett, R. D., Caon, L., Crowther, T. W., Delgado-Baquerizo, M., Montanarella, L., Navarro, L. M., Orgiazzi, A., Singh, B. K., Tedersoo, L., Vargas-Rojas, R., Briones, M. J. I., Buscot, F., Cameron, E. K., Cesár, S., Chatzinotas, A., Cowan, D. A., Djukic, I., Van Den Hoogen, J., ... Eisenhauer, N. (2021). Tracking, targeting, and conserving soil biodiversity. *Science*, 371(6526), 239–241.

Hajibabaei, M., Porter, T.M., Wright, M. and Rudar, J. (2019). COI metabarcoding primer choice affects richness and recovery of indicator taxa in freshwater systems. *PLoS One*, 14(9), p.e0220953.

Hättenschwiler, S., Tiunov, A. V., & Scheu, S. (2005). Biodiversity and litter decomposition in terrestrial ecosystems. *Annual Review of Ecology, Evolution, and Systematics*, 36, 191-218.

Hebert, P.D., Cywinska, A., Ball, S.L. and DeWaard, J.R. (2003). Biological identifications through DNA barcodes. *Proceedings of the Royal Society of London. Series B: Biological Sciences*, 270(1512), pp.313-321.

Hoffman, F. M., Kumar, J., Mills, R. T., & Hargrove, W. W. (2013). Representativeness-based sampling network design for the State of Alaska. *Landscape Ecology*, 28, 1567-1586.

Hogg, I.D. and Hebert, P.D. (2004). Biological identification of springtails (Hexapoda: Collembola) from the Canadian Arctic, using mitochondrial DNA barcodes. *Canadian Journal of Zoology*, 82(5), pp.749-754.

Illumina. (2013). *16S Metagenomic Sequencing Library Preparation*. Illumina, Inc.

Karlen, D. L., Veum, K. S., Sudduth, K. A., Obrycki, J. F., & Nunes, M. R. (2019). Soil health assessment: Past accomplishments, current activities, and future opportunities. *Soil and Tillage Research*, 195, 104365.

Kibblewhite, M. G., Ritz, K., & Swift, M. J. (2008). Soil health in agricultural systems. *Philosophical Transactions of the Royal Society B: Biological Sciences*, 363(1492), 685–701.

Köppen, W. (1936). Das geographische System der Klimate. In W. Köppen & R. Geiger (Eds.), *Handbuch der Klimatologie* (Vol. 1, Part C). Gebrüder Borntraeger.

Korobushkin, D. I., Pronina, N. A., Saifutdinov, R. A., Guseva, P. A., Tsurikov, S. M., & Dudova, K. V. (2025). Taxonomic Diversity and Abundance of Soil Macrofauna in Temperate Forests Under Different Types of Forest Management: A Case Study in European Russia. *Diversity*, 17(3), 216.

Kraft, N. J., et al. (2015). Disentangling the drivers of  $\beta$  diversity along latitudinal and elevational gradients. *Science*, 349(6251), 957-961.

Lavelle, P., Decaëns, T., Aubert, M., Barot, S., Blouin, M., Bureau, F., Margerie, P., Mora, P. and Rossi, J.P. (2006). Soil invertebrates and ecosystem services. *European journal of soil biology*, 42, pp.S3-S15.

Lehmann, J., Bossio, D. A., Kögel-Knabner, I., & Rillig, M. C. (2020). The concept and future prospects of soil health. *Nature Reviews Earth & Environment*, 1(10), 544–553.

Leibold, M. A., et al. (2004). The metacommunity concept: a framework for multi-scale community ecology. *Ecology Letters*, 7(7), 601-613.

Löbl, I., Klausnitzer, B., Hartmann, M. and Krell, F.T. (2023). The silent extinction of species and taxonomists—An appeal to science policymakers and legislators. *Diversity*, 15(10), p.1053.

Mamabolo, E., Pryke, J. S., & Gaigher, R. (2024). Soil macrofauna are important bioindicators of soil quality in agroecosystems under different management. *Ecological Indicators*, 167, 112723.

OHHLER (One Health High-Level Expert Panel), Adisasmitho, W. B., Almuhairi, S., Behravesh, C. B., Bilivogui, P., Bukachi, S. A., ... & Zhou, L. (2022). One Health: A new definition for a sustainable and healthy future. *PLoS pathogens*, 18(6), e1010537.

Orgiazzi, A., et al. (2018). LUCAS Soil, the largest expandable soil dataset for Europe: A review. *European Journal of Soil Science*, 69(1), 140–153.

Orgiazzi, A., Dunbar, M.B., Panagos, P., de Groot, G.A. and Lemanceau, P. (2015). Soil biodiversity and DNA barcodes: opportunities and challenges. *Soil Biology and Biochemistry*, 80, pp.244-250.

Orgiazzi, A., Panagos, P., Yigini, Y., Dunbar, M. B., Gardi, C., Montanarella, L., & Ballabio, C. (2016). A knowledge-based approach to estimating the magnitude and spatial patterns of potential threats to soil biodiversity. *Science of The Total Environment*, 545–546, 11–20.

Porter, T.M. and Hajibabaei, M. (2018). Scaling up: A guide to high-throughput genomic approaches for biodiversity analysis. *Molecular ecology*, 27(2), pp.313-338.

Pulleman, M., Creamer, R., Hamer, U., Helder, J., Pelosi, C., Pérès, G., & Rutgers, M. (2012a). Soil biodiversity, biological indicators and soil ecosystem services—An overview of European approaches. *Current Opinion in Environmental Sustainability*, 4(5), 529–538.

Quigley, M., & Madge, D. (1988). *Land Invertebrates*. Basil Blackwell Ltd, Oxford, UK

Rinot, O., Levy, G. J., Steinberger, Y., Svoray, T., & Eshel, G. (2019). Soil health assessment: A critical review of current methodologies and a proposed new approach. *Science of The Total Environment*, 648, 1484–1491.

Rousseau, L., Fonte, S.J., Tellez, O., van der Hoek, R. and Lavelle, P. (2013). Soil macrofauna as indicators of soil quality and land use impacts in smallholder agroecosystems of western Nicaragua. *Ecological indicators*, 27, pp.71-82.

Scheu, S., & Setälä, H. (2002). Multitrophic interactions in decomposer food webs. In *Multitrophic level interactions* (pp. 223-264). Cambridge University Press.

Schweitzer, J. A., Madritch, M. D., Felker-Quinn, E., & Bailey, J. K. (2012). From genes to ecosystems: Plant genetics as a link between above- and belowground processes. In D. H. Wall, R. D. Bardgett, V. Behan-Pelletier, J. E. Herrick, T. H. Jones, K. Ritz, J. Six, D. R. Strong, & W. H. van der Putten (Eds.), *Soil ecology and ecosystem services* (pp. 82–99). Oxford University Press.

Shelton, A.O., Gold, Z.J., Jensen, A.J., D' Agnese, E., Andruszkiewicz Allan, E., Van Cise, A., Gallego, R., Ramón-Laca, A., Garber-Yonts, M., Parsons, K. and Kelly, R.P. (2023). Toward quantitative metabarcoding. *Ecology*, 104(2), p.e3906.

Smith, P., Poch, R. M., Lobb, D. A., Bhattacharyya, R., Alloush, G., Eudoxie, G. D., Anjos, L. H. C., Castellano, M., Ndzana, G. M., Chenu, C., Naidu, R., Vijayanathan, J., Muscolo, A. M., Studdert, G. A., Eugenio, N. R., Calzolari, M. C., Amuri, N., & Hallett, P. (2024). Status of the World's Soils. *Annual Review of Environment and Resources*, 49(1), 73–104.

Stolte, J., Tesfai, M., Øygarden, L., Kværnø, S., Keizer, J., Verheijen, F., Panagos, P., Ballabio, C., Hessel, R., & European Commission (Eds.). (2016). *Soil threats in Europe*. Publications Office.

Symanczik, S., et al. (2025). *Mycorrhizal Fungi as Natural Bio-Fertilizers: How to Produce and Use*. Research Institute of Organic Agriculture FiBL.

Taberlet, P., et al. (2012). Environmental DNA. *Molecular Ecology*, 21(8), 1789–1793.

Tóth, G., et al. (2013). *LUCAS topsoil survey: methodology, data and results*. Publications Office.

Van Breemen, N., & Buurman, P. (2002). *Soil formation*. Springer Science & Business Media.

van der Putten, W. H., Mudgal, S., Turbé, A., Lavelle, P., Benito, P., & Ruiz, N. (2010). *Soil biodiversity: Functions, threats and tools for policy makers. Final report*. Publications Office.

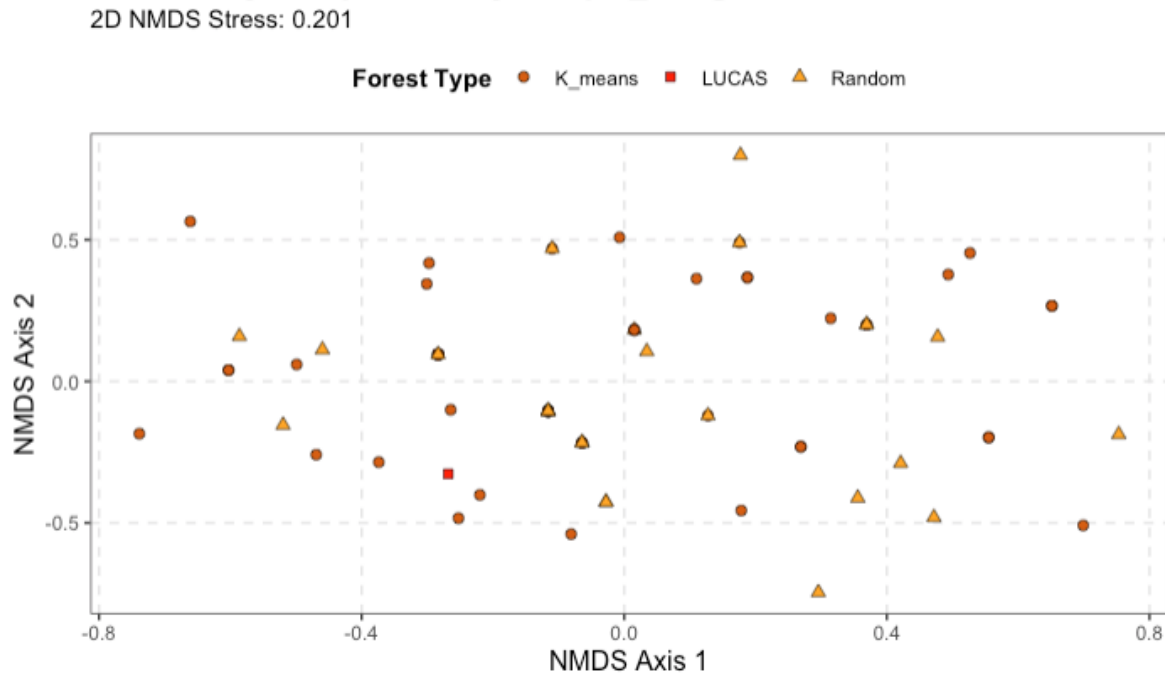
Vasconcellos, R. L. F., Segat, J. C., Bonfim, J. A., Baretta, D., & Cardoso, E. J. B. N. (2013). Soil macrofauna as an indicator of soil quality in an undisturbed riparian forest and recovering sites of different ages. *European Journal of Soil Biology*, 58, 105–112.

Wall, D. H., Nielsen, U. N., & Six, J. (2015). Soil biodiversity and human health. *Nature*, 528(7580), 69–76.

Wenglein, R., Lu, J., & Scheu, S. (2024). The influence of forest types including native and non-native tree species on soil macrofauna depends on site conditions. *Ecology and Evolution*, 14(9), e70311.

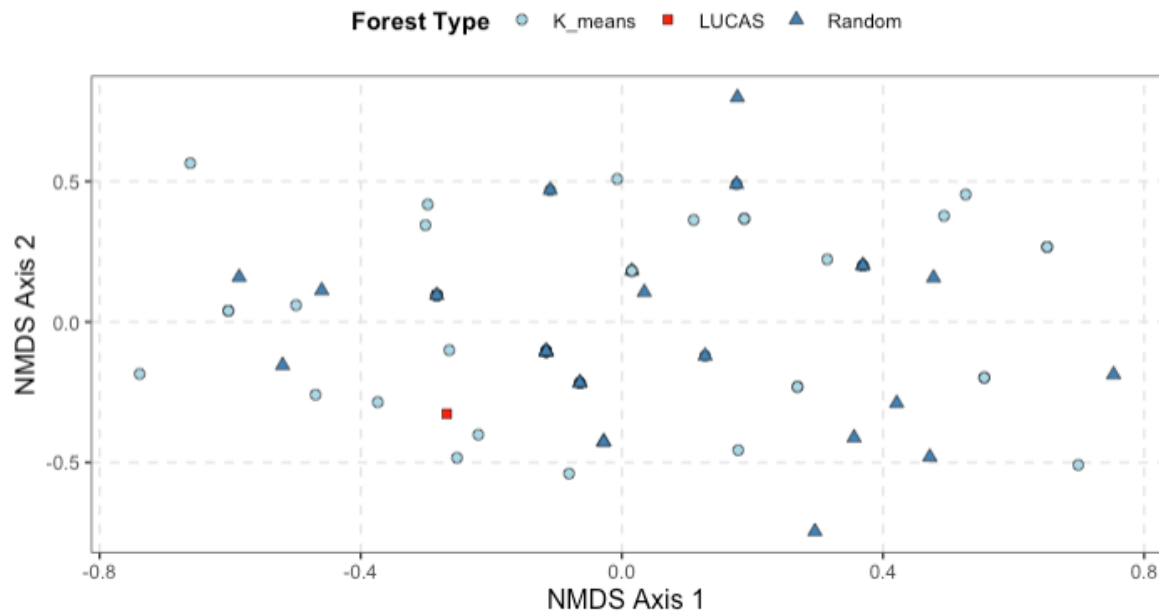
Wolters, V. (2001). Biodiversity of soil animals and its function. *European Journal of Soil Biology*, 37(4), 221–227

## Appendix

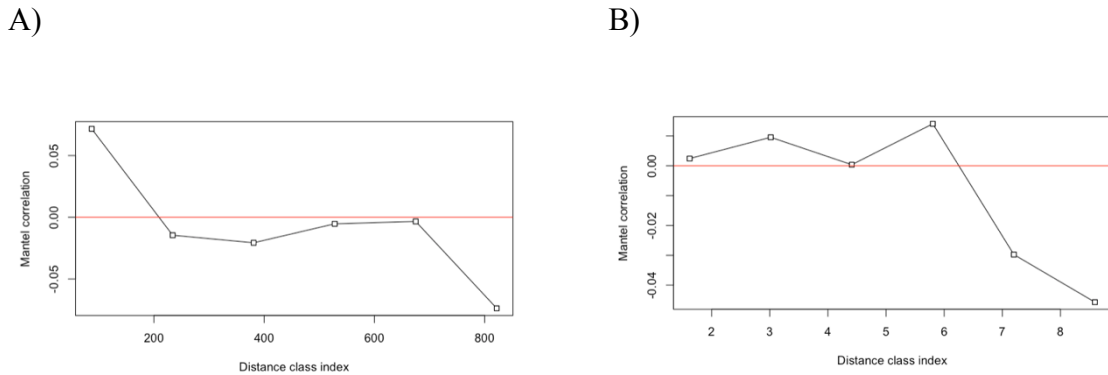


Supplementary Figure 1. Non-metric Multidimensional Scaling (NMDS) ordination of macrofaunal communities within the Oak forest system. Each point represents an individual sample, with shapes indicating the sampling design under which it was collected (K-means (dark orange circle), LUCAS (red square), or Random (orange triangle)). The analysis was based on a Jaccard dissimilarity matrix from presence-absence data. The ordination shows no clear separation or clustering of samples based on the sampling design, indicating that all three methods captured a similar spectrum of the Oak forest community. The stress value for the two-dimensional solution is 0.201.

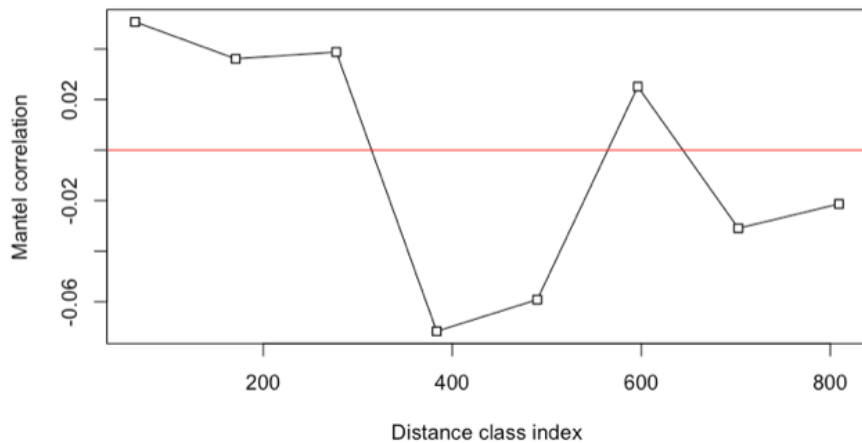
2D NMDS Stress: 0.201



Supplementary Figure 2: Non-metric Multidimensional Scaling (NMDS) ordination of community composition, showing samples grouped by sampling design. Each point represents an individual sample, with shapes indicating the strategy used to select its location (K-means (light blue circle), LUCAS (red square), or Random(steel blue triangle)). The ordination demonstrates a high degree of overlap between the sample groups, with no clear separation or clustering. This suggests that all three sampling designs captured a similar spectrum of the forest community. The stress value for the two-dimensional solution is 0.201.



Supplementary Figure 3: A )Mantel correlograms for the Oak forest molecular data, showing Spearman's correlation coefficient (Mantel r) is plotted against distance classes. (A) environmental spatial autocorrelation. (B) The community-environment relationship across spatial scales.



Supplementary Figure 4: Mantel correlograms for the Pine forest molecular data, showing Spearman's correlation coefficient (Mantel r) is plotted against distance classes of environment relationship across spatial scales .

Supplementary Table 1: descriptive statistics—mean (M), standard deviation (sd), and coefficient of variation (CV)—for a range of soil chemical properties measured in oak and pine forests. The variables include pH, phosphate (mg/100g), phosphorus (mg/kg), potassium oxide ( $K_2O$ ) (mg/100g), potassium (mg/kg), calcium, magnesium, exchangeable potassium, and manganese (all in cmolc/kg), as well as hydrogen ion concentration ( $H^+$ ) (cmolc/kg). Three sampling strategies: coupled k-means and random observations (all), k-means only, and random observations only. Mean and standard deviation are expressed in the units of each respective parameter, while the coefficient of variation (CV) is reported as a percentage, indicating relative variability around the mean. Notably, CV for pH is not computed due to the logarithmic nature of the pH scale, which lacks a true zero and renders CV

statistically inappropriate. Significant differences in variability across sampling methods, as assessed using Levene's test for homogeneity of variance, are indicated where  $p < 0.05$ .

Parameter		Oak			Pine			(oak-pine)
		Mean	SD	CV	Mean	SD	CV	
pH	all	4.307	0.141	*	4.248	0.103	*	0.116
	k_means	4.306	0.151	*	4.248	0.119	*	0.655
	random	4.318	0.128	*	4.238	0.063	*	<b>0.017</b>
	p-value (k_means - random)	0.793		<b>0.01</b>				
Phosphate	all	1.969	1.876	0.953	0.859	0.335	0.39	<b>0.003</b>
	k_means	1.752	1.301	0.742	0.756	0.32	0.424	<b>0.005</b>
	random	1.869	1.969	1.053	1.031	0.295	0.287	0.149
	p-value (k_means - random)	0.793		0.845				
Phosphorus	all	17.641	8.025	0.455	12.923	1.403	0.109	<b>0.003</b>
	k_means	16.72	5.587	0.334	12.48	1.358	0.109	<b>0.005</b>
	random	17.231	8.516	0.494	13.692	1.182	0.086	0.141
	p-value (k_means - random)	0.771		0.815				
Potassiumoxide	all	6.29	2.752	0.438	2.364	0.711	0.301	<b>0</b>
	k_means	6.416	2.936	0.458	2.296	0.782	0.341	<b>0</b>
	random	6.238	2.489	0.399	2.523	0.576	0.228	<b>0.012</b>
	p-value (k_means - random)	0.563		0.619				
Potassium	all	52.231	22.775	0.436	19.615	6.02	0.307	<b>0</b>
	k_means	53.32	24.349	0.457	19.04	6.624	0.348	<b>0</b>
	random	51.692	20.491	0.396	21	4.813	0.229	<b>0.015</b>
	p-value (k_means - random)	0.525		0.579				
TOC	all	3.988	1.326	0.332	8.172	1.832	0.224	0.066
	k_means	3.99	1.289	0.323	7.921	1.882	0.238	0.167
	random	3.932	1.483	0.377	8.771	1.685	0.192	0.606
	p-value (k_means - random)	0.803		0.723				
TN	all	0.257	0.082	0.318	0.434	0.086	0.198	0.973
	k_means	0.258	0.081	0.313	0.415	0.09	0.216	0.888
	random	0.251	0.088	0.352	0.476	0.065	0.138	0.383
	p-value (k_means - random)	0.846		0.422				
Calcium	all	0.842	0.714	0.848	0.586	0.273	0.467	<b>0.016</b>
	k_means	0.908	0.866	0.953	0.541	0.272	0.504	<b>0.016</b>
	random	0.715	0.298	0.418	0.686	0.266	0.387	0.534
	p-value (k_means - random)	0.097		0.876				

Magnesium	all	0.352	0.24	0.682	0.162	0.056	0.349	<b>0.001</b>
	k_means	0.372	0.283	0.762	0.157	0.061	0.391	<b>0.008</b>
	random	0.33	0.135	0.409	0.175	0.046	0.263	<b>0.026</b>
	p-value (k_means - random)		0.233			0.205		
Potassium_cmolc	all	0.17	0.07	0.409	0.056	0.02	0.36	<b>0</b>
	k_means	0.177	0.072	0.409	0.054	0.021	0.399	<b>0.001</b>
	random	0.162	0.064	0.395	0.063	0.018	0.278	<b>0.017</b>
	p-value (k_means - random)		0.637			0.844		
Sodium	all	0.04	0.026	0.652	0.092	0.048	0.52	0.095
	k_means	0.038	0.031	0.811	0.09	0.055	0.608	0.353
	random	0.043	0.014	0.334	0.098	0.035	0.356	0.065
	p-value (k_means - random)		0.254			0.744		
Aluminium	all	2.39	0.998	0.418	4.002	0.932	0.233	0.55
	k_means	2.442	1.121	0.459	3.83	1	0.261	0.673
	random	2.265	0.781	0.345	4.344	0.748	0.172	0.966
	p-value (k_means - random)		0.581			0.226		
Iron	all	0.06	0.079	1.315	0.11	0.051	0.467	0.771
	k_means	0.069	0.09	1.301	0.107	0.058	0.537	0.704
	random	0.045	0.053	1.181	0.119	0.038	0.317	0.804
	p-value (k_means - random)		0.384			0.08		
Manganese	all	0.142	0.095	0.669	0.016	0.009	0.543	<b>0</b>
	k_means	0.143	0.098	0.687	0.016	0.009	0.553	<b>0.002</b>
	random	0.143	0.097	0.678	0.016	0.009	0.538	<b>0.012</b>
	p-value (k_means - random)		0.98			0.722		
H_value	all	0.093	0.022	0.234	0.114	0.022	0.191	0.578
	k_means	0.094	0.023	0.243	0.113	0.026	0.227	0.168
	random	0.09	0.021	0.228	0.115	0.013	0.11	0.221
	p-value (k_means - random)		0.994			<b>0.007</b>		
CEC	all	4.091	1.199	0.293	5.139	1.166	0.227	0.601
	k_means	4.246	1.367	0.322	4.909	1.2	0.244	0.995
	random	3.791	0.819	0.216	5.618	1.024	0.182	0.47
	p-value (k_means - random)		0.233			0.434		

Supplementary Table 2: Results of the Mann-Whitney U test comparing the abundance of macrofauna taxonomic groups between T1 Oak forest and T2 Pine forest. P-values were adjusted for multiple comparisons using the Benjamini-Hochberg method.

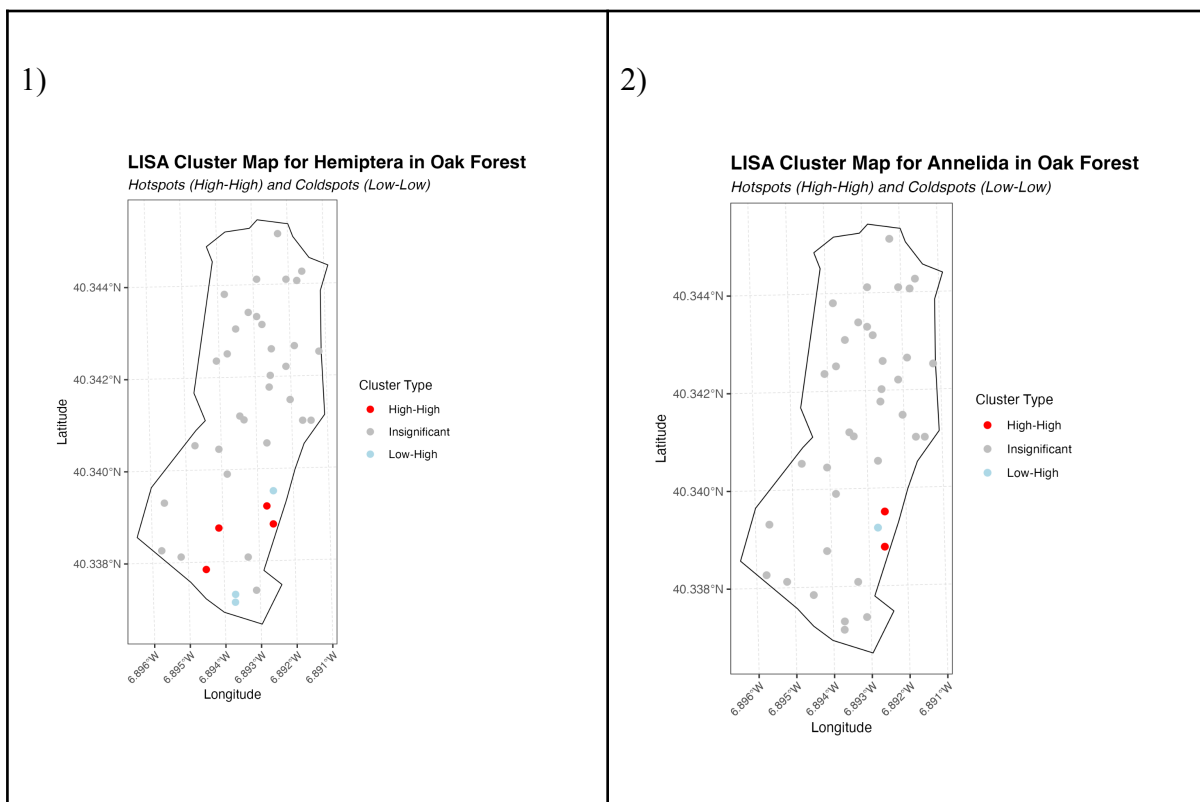
Taxa	n1 (Oak forest)	n2 (Pine forest)	statistic	p	p.adj	p.adj.signif
Annelida	39	39	780.0	0.57	0.66	ns
Araneae	39	39	1219.5	0.00	0.00	****
Archaeognatha	39	39	445.0	0.00	0.00	****
Blattodea	39	39	682.0	0.09	0.17	ns
Chilopoda	39	39	734.5	0.71	0.76	ns
Coleoptera	39	39	316.0	0.00	0.00	****
Diplopoda	39	39	1072.5	0.00	0.00	****
Gastropoda	39	39	577.0	0.03	0.07	ns
Hemiptera	39	39	688.0	0.46	0.57	ns
Hymenoptera	39	39	918.5	0.12	0.19	ns
Isopoda	39	39	916.5	0.01	0.02	*
Larvae	39	39	772.0	0.91	0.91	ns
Opiliones	39	39	721.5	0.16	0.24	ns
Orthoptera	39	39	799.5	0.31	0.43	ns
Pseudoscorpiones	39	39	819.0	0.08	0.17	ns

Supplementary Table 3: Results of the Mann-Whitney U test comparing the abundance of macrofauna taxonomic groups between T1 Oak forest and T2 Pine forest. P-values were adjusted for multiple comparisons using the Benjamini-Hochberg method.

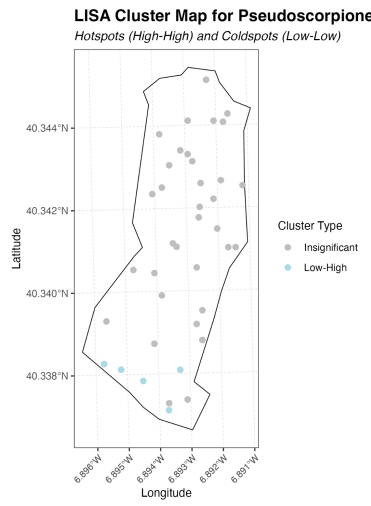
Variable	Test	Statistic	P_value
pH	T-test (equal var)	2.3	0.02
Phosphate	Wilcoxon test	1127.0	0.00
Phosphorus	Wilcoxon test	1122.5	0.00
Potassiumoxide	Wilcoxon test	1443.5	0.00
Potassium	Wilcoxon test	1442.5	0.00
TOC	T-test (equal var)	-11.6	0.00
TN	T-test (equal var)	-9.3	0.00
Calcium	Wilcoxon test	891.0	0.19
Magnesium	Wilcoxon test	1274.0	0.00
Potassium_cmolc	Wilcoxon test	1476.0	0.00
Sodium	Wilcoxon test	128.0	0.00
Aluminium	Wilcoxon test	168.5	0.00

Iron	Wilcoxon test	302.0	0.00
Manganese	Wilcoxon test	1521.0	0.00
H_value	Wilcoxon test	352.0	0.00
CEC	Wilcoxon test	373.0	0.00

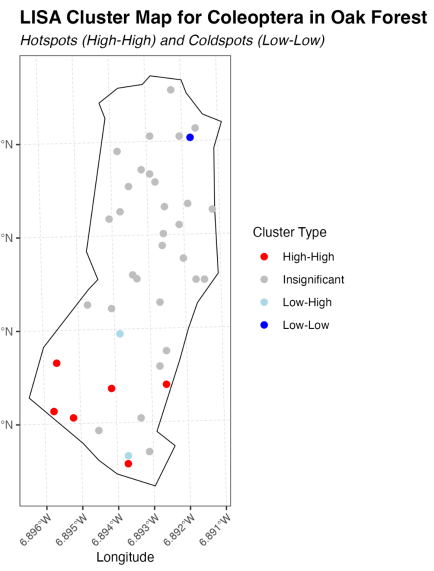
Supplementary Figure 5: Local Moran's I (LISA) cluster map of indicator taxa distribution in the Oak (1-5) and Pine (6-10) forest system. The map displays the results of the Local Indicators of Spatial Association analysis for the count abundance of key indicator species (e.g., Isopoda). Each point represents a sample location, colored according to its significant spatial cluster type. High-High clusters (red) indicate hotspots where a sample with high abundance is surrounded by neighbors also having high abundance. Low-Low clusters (blue) indicate coldspots where a sample with low abundance is surrounded by neighbors also having low abundance. High-Low (light blue) and Low-High (pink) spots represent spatial outliers, where a high-value sample is surrounded by low-value neighbors, or vice-versa. Non-significant locations are shown in grey. The analysis reveals the specific locations of statistically significant patches and outliers, providing insight into the fine-scale spatial structure of indicator taxa within the forest.



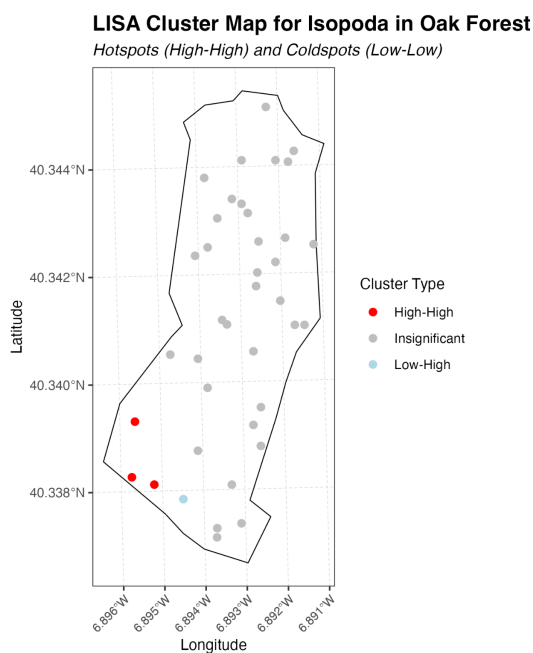
3)



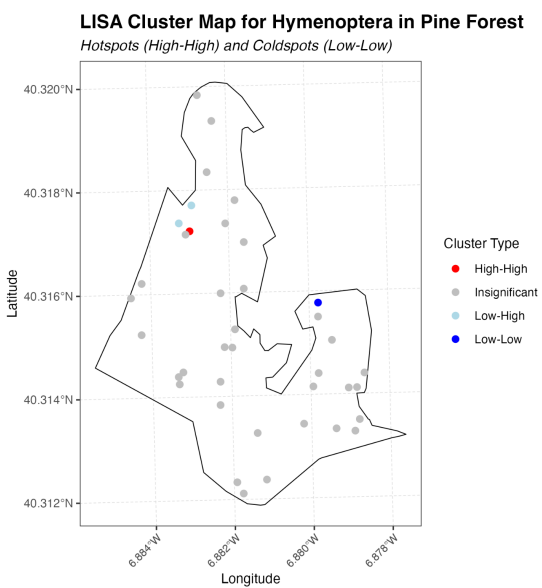
4)



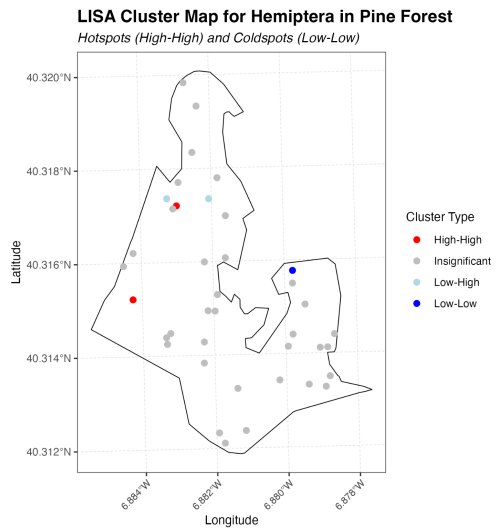
5)



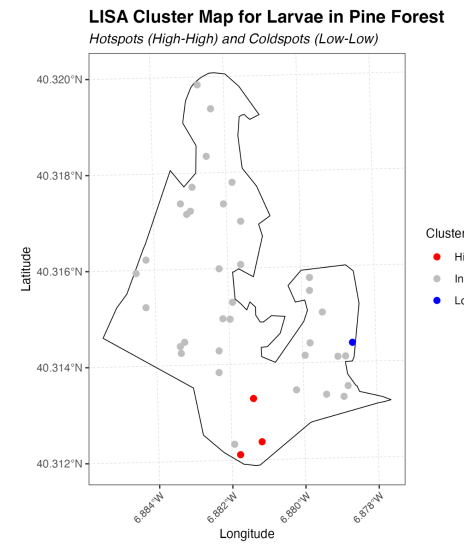
6)



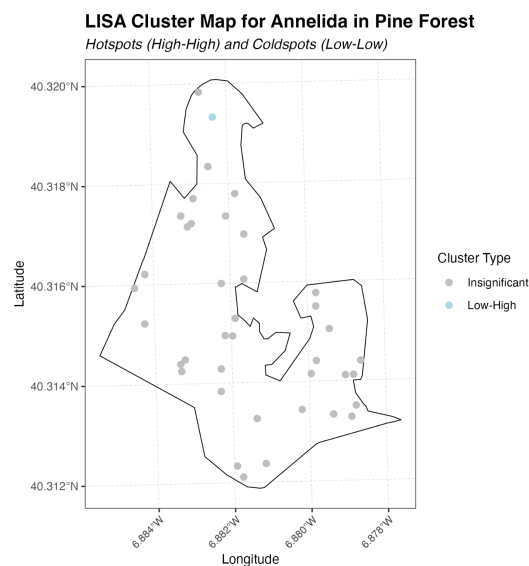
7)



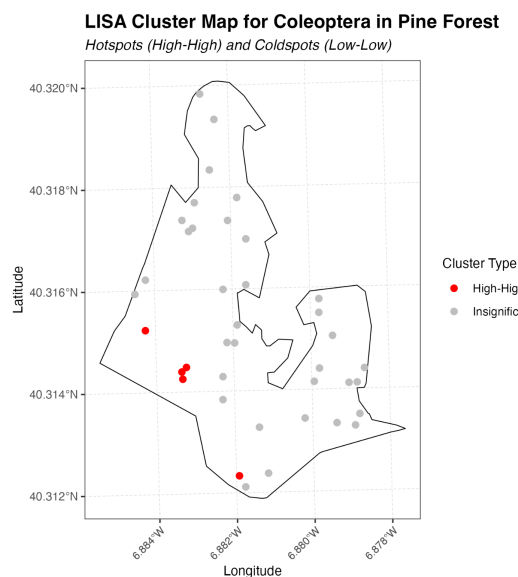
8)



9)



10)



Supplementary Figure 6: Spatial clustering of indicator taxa (OTU occurrence) in the Oak and Pine forest system identified by Local Moran's I (LISA) analysis. The map illustrates the spatial distribution of key indicator species (e.g., Archaeognatha) based on their abundance. Each point is a sample location, and its color signifies its role in a significant spatial pattern. High-High clusters (red)

represent significant hotspots of high abundance, while Low-Low clusters (blue) represent significant coldspots of low abundance. Spatial outliers (High-Low and Low-High) are also shown, indicating locations that differ significantly from their neighbors. Samples not part of any significant cluster are shown in grey. This analysis pinpoints the exact locations of non-random aggregations, highlighting the specific areas within the Pine forest that are particularly suitable or unsuitable for the indicator taxon.

